

CORONALLY ADVANCED FLAP WITH OR WITHOUT CONNECTIVE TISSUE GRAFT FOR THE TREATMENT OF SINGLE MAXILLARY GINGIVAL RECESSION WITH NON-CARIOUS CERVICAL LESION. A RANDOMIZED CONTROLLED CLINICAL TRIAL

Luigi Barbato¹, Elena Bendinelli¹, Tommaso Giuntoli¹, Michele La Marca¹, Lorenzo Landini¹, Filippo Selvaggi¹, Sandro Cincinelli¹, Jana Mervelt¹, Michele Nieri¹ and Francesco Cairo¹

¹ Research Unit in Periodontology and Periodontal Medicine, Department of Department of Experimental and Clinical Medicine, University of Florence, Florence, Italy

Key words: aesthetics, root coverage, gingival recession, coronally advanced flap, connective tissue graft, multiple gingival recessions.

Conflict of interest: The authors have stated explicitly that there are no conflicts of interest in connection with this article

Source of Funding: The study was self-funded by the authors and their institution

Running title: Root coverage and NCCL

Clinical Relevance

Scientific rationale for the study

The treatment of single recession with previously restored NCCL is poorly investigated in RCT.

Principal findings

Both CAF+CTG and CAF alone were similarly effective to obtain complete root coverage after 12 months. An interaction between gingival thickness at baseline with amount of recession reduction and final RES was reported.

Practical implications

Caution is suggested in an excessive use of CTG when treating Rec with baseline KT >0.8 mm, since the CAF alone promotes optimal amount of root coverage and better RES score compared with bilaminar technique.

Abstract

Introduzione: In questo studio è stata valutata l'efficacia clinica del lembo spostato coronalmente (CAF) associato o meno a innesto di tessuto connettivo (CTG) per il trattamento di recessioni single mascellari con abrasioni cervicali non cariose. **Materiali e Metodi:** Trenta pazienti con recessione mascellare singola e giunzione amelo-cementizia ricostruita sono stati randomizzati in uno dei due gruppi. Un misuratore, in cieco rispetto al trattamento, ha rilevato: copertura radicolare completa (CRC), quantità di riduzione della recessione (RecRed), tessuto cheratinizzato (KT), spessore gengivale (GT), soddisfazione del paziente e il Root coverage Esthetic Score (RES). **Risultati:** A 12 mesi non ci sono state differenze statisticamente significative per il CRC mentre il gruppo CAF+CTG ha mostrato maggiore guadagno di KT ($p<0.0001$) ed aumento di GT ($p<0.0001$). Il tipo di trattamento e il GT hanno mostrato un'interazione statisticamente significativa. In particolare per GT iniziale ≤ 0.84 mm il gruppo CAF+CTG ha mostrato maggiore RecRed mentre per GT >0.84 mm i risultati erano migliori nel gruppo CAF. Inoltre il gruppo CAF ha raggiunto migliore valore di RES quando il GT iniziale era >0.82 mm. **Conclusioni:** Entrambe le procedure sono efficaci per la copertura di recessioni single con abrasioni dello smalto ricostruite. L'utilizzo dell'innesto di connettivo associato al lembo spostato coronalmente dovrebbe essere limitato al solo caso di fenotipo sottile.

Abstract

Background: The aim of this study was to assess the clinical efficacy of coronally advanced flap (CAF) with or without connective tissue graft (CTG) for the treatment of single maxillary gingival recession with restored non-carious cervical lesion

Material and Methods: Thirty patients with single gingival recessions and previously restored non-carious cervical lesions were randomly allocated to the two groups. A blind examiner evaluated complete root coverage (CRC), recession reduction (RecRed), keratinized tissue (KT) gain, increase in gingival thickness (GT), patient satisfaction and root coverage esthetic score (RES).

Results: No significant difference in term of CRC was reported after 12 months. CAF+CTG was associated with greater KT gain ($p<0.0001$) and GT increase ($p<0.0001$) than CAF alone. An interaction between treatment and baseline GT and type of treatment was reported suggesting that when baseline GT was ≤ 0.84 mm adding CTG led to higher RecRed, while for values >0.84 mm the use of CAF alone was associated with better outcomes. Similarly, CAF alone provided better final RES score for baseline GT >0.82 mm.

Conclusion: Both procedures were similarly effective for root coverage at single recession with previously restored CEJ. Adding a CTG under CAF should be scheduled only when recession with thin periodontal phenotype is treated.

Introduction

Successful outcome of a root-coverage procedure is a stable gingival margin (GM) coronal to the cemento–enamel junction (CEJ) and soft tissue integration with adjacent tissue (Cairo et al., 2009). Very often root coverage procedures may be complicated by the presence of non-carious cervical lesion (NCCL) involving the CEJ area (Pini-Prato et al., 2010), leading to difficult soft tissue management during surgery or poor clinical and esthetic outcomes after healing (Cairo et al., 2009)

Some clinical proposals to manage NCCL have been suggested, combining possible partial (Cairo and Pini Prato, 2010; Zucchelli et al., 2014) or complete restoration (Santamaria et al., 2009) of the defect area in association with coronally advanced flap (CAF) with or without connective tissue graft (CTG). Furthermore, some clinical features as interdental papilla height (Zucchelli et al., 2006) and CEJ levels at adjacent and/or homologues teeth (Cairo & Pini Prato 2010) have been considered proper references to reconstruct the CEJ area. A recent Randomized Clinical Trial (RCT) showed also that restoration of NCCL in conjunction with root coverage was associated with better esthetic outcomes and dentin

hypersensitivity reduction than surgery alone (Santamaria et al. 2018)

The aim of this RCT is to compare CAF with or without CTG for the treatment of single maxillary gingival recession with previously restored NCCL.

Material and Methods

Participants

The present study is a parallel, randomized single-center clinical trial on the treatment of single recession at maxillary arch associated with non-carious cervical lesion (NCCL), according to the CONSORT statement (<http://www.consort-statement.org/>). Two different treatment modalities were compared: the Coronally Advanced Flap (CAF) plus Connective Tissue Graft (CAF+CTG, test group) and the CAF alone (CAF, control group). The flowchart of the study is presented in figure 1.

The study protocol was approved by the University Ethical Board (Ref. 981/14b). Informed consent was obtained from all the subjects included in the study. The study was conducted according to the principles outlined in the Declaration of Helsinki on experimentation involving human subjects, as revised in 2000.

Participants satisfying the following entry criteria were recruited:

- Age ≥ 18 years
- No systemic diseases or pregnancy.
- Self-reported smoking ≤ 10 cigarettes/day.
- Full-mouth plaque score (FMPS) and full-mouth bleeding score (FMBS) $\leq 10\%$ (measured at four sites per tooth).
- Presence of single RT1 (Cairo et al. 2011) buccal gingival recessions ≥ 2 mm of depth located in the anterior area of the upper jaw (central and lateral incisors, canine, first and second premolars, first molar) and associated with aesthetic complains and or dental sensitivity.
- Presence of NCCL associated with recession
- No history of mucogingival or periodontal surgery at experimental sites.

Exclusion criteria were:

- Prosthetic crown at experimental teeth
- Gingival recessions presenting minimal amount (< 1 mm) of apico-coronal keratinized tissue (KT) extension apical to recession area.

All NCCL at experimental teeth were previously treated with a composite filling to reconstruct the CEJ area before surgery. Anatomic landmarks at adjacent or contra-lateral teeth were used to identify the correct CEJ position in cases with abrasion; care was taken to limit the extension of the restorative material within 1mm apical to the ideal CEJ level (Cairo and Pini Prato, 2010). Each patient (experimental unit) contributed with a single recession.

Interventions/Operator/Investigators

All surgical procedures were performed by a single expert clinician (F.C.) with more than 15 years of experience in periodontal plastic surgery. A blinded examiner assessed all the clinical and aesthetic outcomes of treatments and attended a preliminary calibration session reporting intra-class correlation coefficient of 0.87 (CI 95% 0.82; 0.91).

Clinical measurements

The following measurements were taken at baseline for each treated tooth before restorative procedure using a periodontal probe (PCP UNC 15, Hu-Friedy)

Before restoration of CEJ, the following parameter was collected

- GM-NCCLc: the distance between the gingival margin and the most coronal level of NCCL

After NCCL restoration, the following measurements were also collected

- Rec 0: Recession depth at the mid buccal site measured from restored CEJ level to the gingival margin
- PD 0: Probing depth at the mid buccal site
- CAL 0: Clinical Attachment Level was calculated as Rec 0+PD 0
- IM-CEJr 0: Distance from incisal margin (IM) to the restored CEJ level.
- IM-GM 0: Distance from gingival margin (GM) to incisal margin (IM).
- IM-GMJ 0: Distance from incisal margin to mucogingival junction (MGJ)
- KT 0: Keratinized Tissue measured from the gingival margin to the MGJ at the mid buccal point.
- GT 0: Gingival thickness at baseline was measured 1.5 mm apical to the gingival margin using an injection needle, perpendicular to the tissue surface, and a silicon stop over the gingival surface (Cairo et al., 2016a). The silicon disk stop was placed in tight contact with the soft tissue surface and fixed with a drop of cyanoacrylic adhesive. After needle removal, the distance between needle tip and the silicon stop was estimated using a digital caliper with 0.01mm of accuracy.
- Sens 0: experimental tooth for which the patient reported dental hypersensitivity
- Sens VAS: Dental hypersensitivity tested using the air spray and quantified by the patients on a visual analogic scale (VAS) 0-100.

All variations of the position of the gingival margin were monitored at 3-month, 6-month and 1-year follow-ups.

Intra-operative measurements

The following measurements were taken during the surgical procedure at each experimental tooth.

- CEJr-BC: distance between restored cement enamel junction and bone crest after flap elevation
- IM-GM1: distance between incisal margin and gingival margin after suture

In addition, chair-time of the surgical procedure was measured from the end of local anesthesia until the completion of the sutures.

Clinical measurements to monitor early healing (day 10 and day 14)

At suture removal (10 days after surgery) and at the 2-week visit, the following measures were evaluated: Rec, IM-GM, IM-GMJ and KT. In addition, data on possible soft tissue complications (necrosis, edema, bleeding), general discomfort and pain (VAS) were also collected.

Demographic data and patient questionnaires (Baseline, end of surgery, day 10, day 14, 1 year)

At baseline, age, gender, smoking habits, number of cigarettes/day and presence root sensitivity (VAS from 0 to 100) were registered. After 10 and 14 days, data on post-operative pain and possible side effects or complications were registered. Patient discomfort was measured by VAS.

At the 1-year follow-up, patient reports on aesthetic satisfaction (VAS) and dental hypersensitivity (VAS) were collected. In case of drop out, the reason related was registered.

Pre-treatment procedures

Patients received oral hygiene instructions (roll technique) with a soft-bristled toothbrush to correct wrong habits related to the etiology of the recession at least 2 months before surgery.

Treatment procedures

The test group received CAF+CTG (Fig. 2) while the control group was treated with CAF alone (Fig. 3). After local anesthesia, two oblique, divergent releasing incisions extending beyond the mucogingival junction (MGJ) were performed. An intra-sulcular incision was performed at the buccal aspect of the involved tooth. Care was taken to raise split-thickness surgical papillae. A full-thickness flap until the exposure of 2-3 mm of buccal bone crest was then elevated using a small periosteal elevator. Subsequently, a partial-thickness flap was raised beyond the MGJ, eliminating any residual tension to achieve a passive coronal displacement of the flap. The papillae adjacent to the involved tooth were then de-epithelialized. A gentle root debridement was performed using a sharp curette up to 1 mm from the bone crest. The randomization sealed and opaque envelope was opened at this time and the operator was instructed whether or not to apply a CTG under the flap. In the test group only a 1mm-thick CTG was harvested and stabilized with periosteal sutures in the dehiscence area with the coronal border immediately apical to the restored CEJ level. The flap was then coronally displaced 1–2 mm above the CEJ in both test and control groups.

Post-surgical instructions

Patients were instructed to avoid mechanical trauma and tooth brushing for 2 weeks and to intermittently apply an ice bag for the first 4-5 hours. Patients received ibuprofen 600 mg at the end of the surgical procedure and were instructed to take another compulsory tablet 6 hours later. Additional doses were suggested in cases of need. Chlorhexidine mouth-risings (0.12%) were recommended twice daily for 1min. Smokers were reminded to quit smoking in the first 2 weeks after surgery. Ten days after surgery, sutures were removed and prophylaxis dental paste was applied using a rubber cup at teeth in the surgical area. Two weeks after surgery, patients were instructed to resume mechanical tooth-cleaning using a soft post-surgical toothbrush. Patients were recalled at 1, 2, 3, 6, 9 and 12 months after surgery for professional oral hygiene procedures and for collection clinical measurements when scheduled. The use of soft toothbrush was maintained until the 3-month follow-up, when a medium-bristle toothbrush was recommended.

Sample size

The sample dimension was calculated using $\alpha = 0.05$ and the power $(1-\beta)$ of 80%. For the variability, the value of standard deviation of 0.46 mm for recession reduction obtained in a previous article (Pini Prato et al., 2005) was used considering Rec T0 as covariate. The minimum clinically significant value

considered is 0.5 mm. On the basis of these data, the needed number of patients to be enrolled in this study was 12 for the test group (CAF+CTG) and 12 for the control group (CAF). However, the number of patients was increased of 20% for each arm considering the possibility of dropouts.

Randomization/Allocation concealment/Masking of examiners

Each experimental subject was randomly assigned to one of the two treatment regimens (CAF+CTG and CAF). The treatment assignment was noted in a specific form kept by the study registrar (M.N., statistician). Allocation concealment was performed by opaque sealed envelopes, sequentially numbered. The statistician generated the allocation sequence by means of a computer-generated random list and instructed a different subject to assign a sealed envelope containing the treatments. The opaque envelope was opened after flap elevation and treatment assignment communicated to the operator. Blinding of examiner was maintained throughout all experimental procedures.

Statistical analysis

Statistical analysis was performed using JMP 13.0 SAS Institute Inc. Descriptive statistics were performed using mean \pm standard deviation for quantitative variables and frequency and percentage for qualitative variables. The primary outcomes variables were the presence of CRC and RecRed, Secondary variables included RES values, KT, surgical-time, intake of anti-inflammatory tablets, post-operative discomfort (VAS) and final aesthetic satisfaction (VAS).

Linear models in order to investigate factors influencing some outcomes variables (RecRed, KT gain, esthetic VAS and RES) were performed. The explicative variables were treatment (T), the value at baseline (for RecRed and KT gain), gingival thickness at baseline and the interaction between treatment and baseline thickness. The interaction was maintained in the model only when significant. For CRC, the Fisher Exact test was performed. All the analyses were defined a priori.

Results

Experimental population, patients and defects characteristics at baseline

An original sample of 38 patients showing single gingival recession associated with NCCL at upper arch and satisfying the entry criteria were identified; 8 of 38 declined to follow the experimental procedures. A total of 30 patients were enrolled: 14 patients were treated in the test group (CAF+CTG) and 16 in the control group (CAF).

In the CAF+CTG group, 10 out of 14 were females (71%), and the mean age was 37.7 ± 9.4 years [Minimum: 27; Maximum: 63]; 4 patients were smokers. Six treated teeth were canines (43%), 7 premolars (50%) and 1 first molar (7%). The baseline buccal recession (Rec 0) was 3.4 ± 0.6 mm [2; 4]. In the CAF group, twelve out of 16 were females (75%), and the mean age was 40.5 ± 10.3 years [Minimum: 26; Maximum: 53]. Two patients were smokers. One treated tooth was incisor (6%), 7 canines (44%) and 8 premolars (50%). The baseline buccal recession (Rec 0) was 3.2 ± 0.5 mm [2; 4]. Details of baseline data are presented in table 1. There was no clinical difference at baseline between the two groups.

Evaluation of the surgical procedure and post-operative period

The mean duration of the surgical procedure was 55.4 ± 5.3 minutes for the test group and 38.4 ± 3.3 minutes for the control group ($p < 0.0001$). After 10 days, patients from the CAF group reported an intake of 2.6 ± 0.9 anti-inflammatory tablets and 4.0 ± 0.8 for the CAF+CTG group (difference 1.4; 95%CI from 0.7 to 2.0; $p = 0.0001$). There was no significant difference in term of post-surgical discomfort VAS values between the two groups (29.4 ± 12.2 for CAF+CTG vs 24.5 ± 11.1 for CAF, difference 4.9; 95%CI from -3.8 to 13.6; $p = 0.2561$). Furthermore, patients allocated in the test group

reported greater number of days with post-surgical discomfort (2.6 ± 0.5 for CAF+CTG vs 1.4 ± 0.6 for CAF, difference 1.2 days; 95%CI from 0.8 to 1.6; $p < 0.0001$). At the 2-week evaluation no significant side effect was detected apart from 6 cases of swelling (3 cases for each group).

Clinical outcomes

All patients attended all follow-up visits and no significant complication was reported. All NCCL restorations were stable at the last follow-up. At the final visit all patients were satisfied, with 90.9 ± 10.7 mean VAS value in the test group 95.4 ± 6.0 and in the control group. The difference was not significant (-4.6 ; 95% CI from -11.0 to 1.8 ; $P = 0.1531$).

Details of the clinical outcomes at 3, 6 and 12 months are presented in table 1. At the final follow-up, 10 out of 14 sites (71%) in the test group and 8 out of 16 in the control group (50%) showed CRC with no significant difference between treatments (RR= 1.43 [from 0.79 to 2.58]; $p = 0.2839$). Furthermore, the additional use of CTG yielded to greater final GT (difference between treatments 0.52 mm [95%CI from 0.41 to 0.63] $p < 0.0001$) than CAF alone.

Linear models to investigate factors influencing the outcomes variables (RecRed, KT gain RES and esthetic VAS) were also performed. For the outcome variable RecRed (table 2), an interaction between the treatment and baseline gingival thickness was reported ($p = 0.0014$), suggesting that for values of $GT \leq 0.84$ mm add of CTG was associated with higher final RecRed, while for values > 0.84 mm the use of CAF alone was associated with better outcomes. A similar model was also performed for KTgain For this outcome variable the interaction term was not significant. The treatment modality (CAF+CTG) was associated with higher benefit in term of KT gain (difference between treatments 1.4 mm [95%CI from 1.0 to 1.8] $p < 0.0001$). Considering final RES score, linear model demonstrated an interaction between the treatment and GT0: for GT value ≤ 0.82 mm add of CTG was associated with higher RES scores, while for values > 0.82 mm the use of CAF alone was associated with better aesthetic outcomes rated by the blind examiner (table 3). Considering the Esthetic VAS linear model demonstrated an interaction between the treatment and GT0: for GT value ≤ 0.76 mm add of CTG was associated with higher esthetic VAS scores, while for values > 0.82 mm the use of CAF alone was associated with better aesthetic outcomes.

Discussion

Partial or total CEJ destruction and associated enamel/root discrepancy may lead to surgical difficulties in proper flap/graft management with possible unsuccessful clinical and aesthetic outcomes of root coverage procedures (Cairo, 2017). An epidemiological study on 1,010 gingival recessions retrieved from 353 patients showed that 39% of gingival recession were associated with dental surface defects at CEJ level (Pini-Prato et al., 2010). Combined restorative and muco-gingival procedures have been suggested as a proper treatment modality for Rec associated with NCCL, leading to high patient satisfaction and optimal esthetic outcomes (Cairo and Pini-Prato, 2010; Zucchelli et al., 2011; Tonetti et al., 2014).

The present RCT was aimed to compare the use of CAF with or without CTG for the treatment of single Rec at the upper jaw with previously restored CEJ level. After 12 months, both procedures were similarly effective to obtain complete root coverage with no significant difference between test and control groups. Linear models to investigate factors influencing final amount of RedRed demonstrated an interesting interaction between baseline GT and type of treatment, suggesting that for Rec with $GT \leq 0.84$ mm the use of CTG under CAF yielded to higher RecRed, while for $GT > 0.84$ the flap alone was

associated with better outcomes. Even if a large body of evidence suggests that the bilaminar procedure should be considered the gold standard for root coverage (Cairo et al., 2008; Cortellini et al., 2009; Cairo et al., 2014), the present finding seems to indicate the use CTG only at REC with thin periodontal phenotype (Jepsen et al., 2018; Cortellini and Bissada, 2018). In addition, outcomes of the present study support the conclusions of previous clinical trials about the importance of baseline GT when performing CAF at both single (Baldi et al., 1999; Hwang and Wang, 2006) and multiple recession defects (Cairo et al., 2016b).

In this study, a significant interaction between the type of treatment and final aesthetic outcomes in term of RES score was also detected, showing that for baseline GT value ≤ 0.82 mm CAF+CTG provided higher RES scores, while for values >0.82 mm the use of CAF alone was associated with better aesthetic outcomes. This finding seems to suggest caution in promoting an excessive thickening of well-represented baseline KT, since impairments of soft tissue texture, unpleasant changes in color and alteration in gingival margin/muco-gingival junction positions may occur, hindering the original soft tissue characteristics and the final aesthetic evaluation (Cairo et al., 2016b). On the other hand, when gingival recessions are associated with very thin KT the addition of a CTG improves both clinical and aesthetic outcomes compared with CAF alone.

The present investigation showed that the addition of a CTG under CAF was associated with a significant increase in both apico-coronal KT (mean difference 1.4 mm, $p<0.0001$) and 1-year GT (mean difference 0.52 mm, $p<0.0001$) also at gingival recessions with restored CEJ. This observation supports the hypothesis that adding soft tissue graft is a predictable method to change the gingival phenotype (Cortellini and Bissada, 2018) supporting a more predictable stability of the gingival margin in the long term (Pini-Prato et al., 2010; Cairo et al., 2015). The present study also confirmed that CAF alone does not seem to be able in promoting significant KT changes compared with baseline conditions.

A significant heterogeneity exists in literature regarding the possible restorative management of NCCL in conjunction with root coverage procedures, including the elimination of the enamel defect by planning the residual CEJ (Holbrook T and Ochsenbein, 1983) and the use of resin-modified glass-ionomer restoration to completely restore the root defect under the graft/flap (Santamaria et al., 2009). In the present trial, a well-defined procedure to restore the CEJ and the coronal portion of the clinical crown of the tooth with resin-composite material was applied, assessing reference points at adjacent and/or homologues teeth and limiting the apical extension of the restoration ~ 0.5 -1mm below the level of ideal CEJ. Any root abrasion apical to this level was left unrestored. At the 1-year follow-up, all restorations were retained and well preserved; the associated gingival tissues presented with minimal probing depths and no BoP, thus showing that a composite reconstruction of NCCL limited to an area around the ideal allocation of the CEJ is compatible with periodontal health (Cairo & Pini-Prato, 2010).

This study confirmed that use of CTG was associated with longer surgical time (~ 17 minutes, $p<0.0001$) and higher morbidity with greater anti-inflammatory tablets consumption ($p=0.0001$) and greater number of days with post-surgical discomfort (~ 1.2 day, $p=0.0001$) than CAF alone (Cortellini et al., 2009; Cairo et al., 2012). Conversely, there was no significant difference in term of VAS values for post-surgical discomfort between groups at the time of suture removal (day 10). This finding seems to differ to that described in RCTs evaluating the treatment of multiple recessions defects (Cairo et al., 2016a; Tonetti et al., 2018): a possible reason could be related with graft dimension that may be significant higher when harvesting for multiple defects. Finally, this study confirmed that periodontal plastic surgery is well-accepted by patients as they reported to be very satisfied by procedures with no significant difference between test and control groups.

Within the limit of this study, the following conclusions can be drawn:

- Both procedures were associated with similar probability to obtain CRC at single Rec with

restored NCCL

- Higher post-operative morbidity was reported for CAF+CTG group
- CAF + CTG overall is more effective than CAF alone in recessions with thin periodontal phenotype (<0.8 mm) and use of CTG might be selectively limited to these cases
- The use of CAF alone provided better aesthetic outcomes rated by RES score in recessions with well represented KT (>0.8 mm), thus suggesting caution in an excessive thickening of baseline KT.

References

- BALDI, C., PINI-PRATO, G., PAGLIARO, U., NIERI, M., SALETTA, D., MUZZI, L. & CORTELLINI, P. 1999. Coronally advanced flap procedure for root coverage. Is flap thickness a relevant predictor to achieve root coverage? A 19-case series. *J Periodontol* **70**, 1077–1084.
- CAIRO, F., ROTUNDO, R., MILLER, P. D. & PINI PRATO, G. P. 2009. Root coverage esthetic score: a system to evaluate the esthetic outcome of the treatment of gingival recession through evaluation of clinical cases. *J Periodontol*, **80**, 705-10.
- CAIRO, F., PINI-PRATO, G.P. 2010. A technique to identify and reconstruct the cement-enamel junction level using combined periodontal and restorative treatment of gingival recession. A prospective clinical study. *Int J Periodontics Restorative Dent*, **30**: 573–581.
- CAIRO, F., NIERI, M., CINCINELLI, S., MERVELT, J. & PAGLIARO, U. 2011. The interproximal clinical attachment level to classify gingival recessions and predict root coverage outcomes: an explorative and reliability study. *J Clin Periodontol*, **38**, 661-6.
- CAIRO, F., CORTELLINI, P., TONETTI, M., NIERI, M., MERVELT, J., CINCINELLI, S. & PINI-PRATO, G. 2012. Coronally advanced flap with and without connective tissue graft for the treatment of single maxillary gingival recession with loss of inter-dental attachment. A randomized controlled clinical trial. *J Clin Periodontol* **39**, 760–768.
- CAIRO, F., NIERI, M. & PAGLIARO, U. 2014. Efficacy of periodontal plastic surgery procedures in the treatment of localized facial gingival recessions. A systematic review. *J Clin Periodontol*, **41** Suppl 15, S44-62.
- CAIRO, F., CORTELLINI, P., TONETTI, M., NIERI, M., MERVELT, J., PAGAVINO, G. & PINI-PRATO, G. (2015) Stability of root coverage outcomes at single maxillary gingival recession with loss of interdental attachment: 3-year extension results from a randomized, controlled, clinical trial. *J Clin Periodontol* **42**, 575–581.
- CAIRO, F., CORTELLINI, P., PILLONI, A., NIERI, M., CINCINELLI, S., AMUNNI, F., PAGAVINO, G. & TONETTI, M. S. 2016a Clinical efficacy of coronally advanced flap with or without connective tissue graft for the treatment of multiple adjacent gingival recessions in the aesthetic area: a randomized controlled clinical trial. *J Clin Periodontol*, **43**, 849- 56.
- CAIRO, F., PAGLIARO, U., BUTI, J., BACCINI, M., GRAZIANI, F., TONELLI, P., PAGAVINO, G. & TONETTI, M. S. 2016b. Root coverage procedures improve patient aesthetics. A systematic review and Bayesian network meta-analysis. *J Clin Periodontol*, **43**, 965- 975.
- CAIRO F. 2017. Periodontal plastic surgery of gingival recessions at single and multiple teeth. *Periodontol* 2000. **75**(1):296-316.
- CORTELLINI, P., TONETTI, M., BALDI, C., FRANCETTI, L., RASPERINI, G., ROTUNDO, R., NIERI, M., FRANCESCHI, D., LABRIOLA, A. & PINI-PRATO, G. P. 2009. Does placement of a connective tissue graft improve the outcomes of coronally advanced flap for coverage of single gingival recessions in upper anterior teeth? A multi-centre, randomized, double-blind, clinical trial. *J Clin Periodontol* **36**, 68–79.
- CORTELLINI, P. & BISSADA, N. F. 2018. Muco-gingival conditions in the natural dentition: Narrative review, case definitions, and diagnostic considerations. *J Periodontol*, **89** Suppl 1, S204-S213.
- HOLBROOK, T., OCHSENBEIN, C. 1983. Complete coverage of the denuded root surface with a one-stage gingival graft. *Int J Periodontics Restorative Dent* **3**:8–27.
- HWANG, D. & WANG, H. L. (2006) Flap thickness as a predictor of root coverage: a systematic review. *J Periodontol* **77**, 1625– 1634.
- JEPSEN, S., CATON, J.G., ALBANDAR, J.M., BISSADA, N.F., BOUCHARD, P., CORTELLINI, P., DEMIREL, K., DE SANCTIS, M., ERCOLI, C., FAN, J., GEURS, N.C., HUGHES, F.J., JIN, L., KANTARCI, A., LALLA, E., MADIANOS, P.N., MATTHEWS, D., MCGUIRE, M.K., MILLS, M.P., PRESHAW, P.M.,

- REYNOLDS, M.A., SCULEAN, A., SUSIN, C., WEST, N.X., YAMAZAKI, K. 2018. Periodontal manifestations of systemic diseases and developmental and acquired conditions: Consensus report of workgroup 3 of the 2017 World Workshop on the Classification of Periodontal and Peri-Implant Diseases and Conditions. *J Clin Periodontol*, **45** (Suppl 20),S219-S229.
- PINI PRATO, G. P., BALDI, C., NIERI, M., FRANCESCHI, D., CORTELLINI, P., CLAUSER, C., ROTUNDO, R. & MUZZI, L. 2005. Coronally advanced flap: the post-surgical position of the gingival margin is an important factor for achieving complete root coverage. *J Periodontol*, **76**, 713–722.
 - PINI-PRATO, G., FRANCESCHI, D., CAIRO, F., NIERI, M. & ROTUNDO, R. 2010. Classification of dental surface defects in areas of gingival recession. *J Periodontol*, **81**(6):885-90.
 - PINI-PRATO, G., CAIRO, F., NIERI, M., FRANCESCHI, D., ROTUNDO, R. & CORTELLINI, P. (2010) Coronally advanced flap versus connective tissue graft in the treatment of multiple gingival recessions: a split-mouth study with a 5-year follow-up. *J Clin Periodontol* **37**, 644–650.
 - SANTAMARIA, M.P., DA SILVA FEITOSA, D., NOCITI, F.H. JR, CASATI, M.Z., SALLUM, A.W. & SALLUM, E.A. 2009. Cervical restoration and the amount of soft tissue coverage achieved by coronally advanced flap: a 2-year follow-up randomized-controlled clinical trial. *J Clin Periodontol*. **36**(5):434-41.
 - SANTAMARIA, M.P., SILVEIRA, C.A., MATHIAS, I.F., NEVES, F.L.D.S., DOS SANTOS, L.M., JARDINI, MAN., TATAKIS, D.N., SALLUM, E.A. & BRESCIANI, E. 2018. Treatment of single maxillary gingival recession associated with non-carious cervical lesion: Randomized clinical trial comparing connective tissue graft alone to graft plus partial restoration. *J Clin Periodontol*. Apr 22.
 - TONETTI, M. S., JEPSEN, S. & WORKING GROUP 2 OF THE EUROPEAN WORKSHOP ON PERIODONTOLOGY. 2014. Clinical efficacy of periodontal plastic surgery procedures: consensus report of Group 2 of the 10th European Workshop on Periodontology. *J Clin Periodontol* 41(Suppl. 15), S36–S43.
 - TONETTI, M. S., CORTELLINI, P., PELLEGRINI, G., NIERI, M., BONACCINI, D., ALLEGRI, M., BOUCHARD, P., CAIRO, F., CONFORTI, G., FOURMOUSIS, I., GRAZIANI, F., GUERRERO, A., HALBEN, J., MALET, J., RASPERINI, G., TOPOLL, H., WACHTEL, H., WALLKAMM, B., ZABALEGUI, I. & ZUHR, O. 2018. Xenogenic collagen matrix or autologous connective tissue graft as adjunct to coronally advanced flaps for coverage of multiple adjacent gingival recession: Randomized trial assessing non-inferiority in root coverage and superiority in oral health-related quality of life. *J Clin Periodontol*, **45**, 78-88.
 - ZUCHELLI, G., TESTORI, T., DE SANCTIS, M. 2006. Clinical and anatomical factors limiting treatment outcomes of gingival recession: a new method to predetermine the line of root coverage. *J Periodontol* **77**: 714–721.
 - ZUCHELLI, G., GORI, G., MELE, M., STEFANINI, M., MAZZOTTI, C., MARZADORI, M., MONTEBUGNOLI, L. & DE SANCTIS, M. 2011. Non-carious cervical lesions associated with gingival recessions: a decision-making process. *J Periodontol*, **82**: 1713– 1724.

Corresponding Author

Dr. Francesco Cairo

E-mail: cairofrancesco@virgilio.it

Table 1: Baseline data and mean clinical outcomes at 6 and 12 months.

Variable	CAF (baseline) N=16	CAF+CTG (baseline) N=14	CAF (6 months) N=16	CAF+CTG (6months) N=14	CAF (12 months) N=16	CAF+CTG (12 months) N=14	p-value
Rec (mm)	3.2 ± 0.5	3.4 ± 0.6	0.3 ± 0.5	0.1 ± 0.3	0.5 ± 0.5	0.3 ± 0.5	-
RecRed (mm)	-	-	-	-	2.7 ± 0.6	3.1 ± 0.7	-
IM-MGJ (mm)	15.6 ± 1.7	15.9 ± 1.9	13.5 ± 0.8	14.5 ± 1.0	10.3 ± 0.8	10.2 ± 1.1	-
CRC (n/%)	-	-	-	-	8 (50%)	10 (71%)	0.2839
PD (mm)	1.1 ± 0.3	1.1 ± 0.3	1.1 ± 0.3	1.2 ± 0.4	1.2 ± 0.4	1.1 ± 0.3	-
KT (mm)	3.1 ± 0.5	2.9 ± 1.1	3.3 ± 0.5	4.6 ± 0.6	3.3 ± 0.7	4.6 ± 0.5	-
KT Gain (mm)	-	-	-	-	0.2 ± 0.7	1.7 ± 0.7	<0.0001*
GT (mm)	0.80 ± 0.09	0.78 ± 0.12	-	-	0.86 ± 0.16	1.38 ± 0.09	<0.0001*
Sens (n /%)	9 (56%)	9 (64%)	1 (6%)	0 (0%)	4 (25%)	2 (14%)	0.6567
Sens VAS (0-100)	24.9 ± 28.7	29.1 ± 29.6	1.4 ± 5.5	0.0 ± 0.0	3.6 ± 7.3	1.9 ± 4.9	0.4505
RES (0-10)	-	-	-	-	7.7 ± 1.8	8.3 ± 1.8	0.3652

Legend:

CAF= Coronally Advanced Flap; CAF+CTG= Coronally Advanced Flap plus Connective Tissue Graft; Rec Red= Recession Reduction; CRC= Complete Root Coverage; IM-MGJ= Distance from muco-gingival junction (MGJ) to incisal margin; PD = probing depth; KT = width of keratinized tissue; KT Gain = Gain in width of keratinized tissue; GT = Gingival Thickness; Sens= Number of patient/tooth with hypersensitivity; Sens VAS= tooth hypersensitivity measured by Visual Analogue Scale; RES= Root coverage Esthetic Score.

Table 2: Linear model to investigate factors influencing RecRed at 12 months

Term	Estimate	Std. Error	P-value
Intercept	-2.82	1.07	
Treatment (CAF+CTG vs CAF)	4.72	1.25	0.0009
Rec 0	0.83	0.14	<0.0001
GT 0	3.61	1.25	0.0078
Interaction (Treatment x GT 0)	-5.66	1.57	0.0014

Legend:

Rec 0= Buccal Recession at the baseline; GT 0= Gingival Thickness Baseline; CTG= Coronally Advanced Flap plus Connective Tissue Graft; CAF= Coronally Advanced Flap; Interaction (Treatment x GT 0)= interaction between treatment and gingival thickness at baseline.

Table 3: Linear model to investigate factors influencing RES score at 12 months.

Term	Estimate	Std. Error	P-value
Intercept	-3.05	3.49	
Treatment (CAF+CTG vs CAF)	18.21	4.37	0.0003
GT 0	13.50	4.37	0.0047
Interaction (Treatment x GT 0)	-22.29	5.49	0.0004

Legend:

GT 0= Gingival Thickness Baseline; CAF+CTG= Coronally Advanced Flap plus Connective Tissue Graft; Interaction (Rand x GT 0)= interaction between treatment and gingival thickness at baseline.

Figure 1

CONSORT Flow Chart of the study

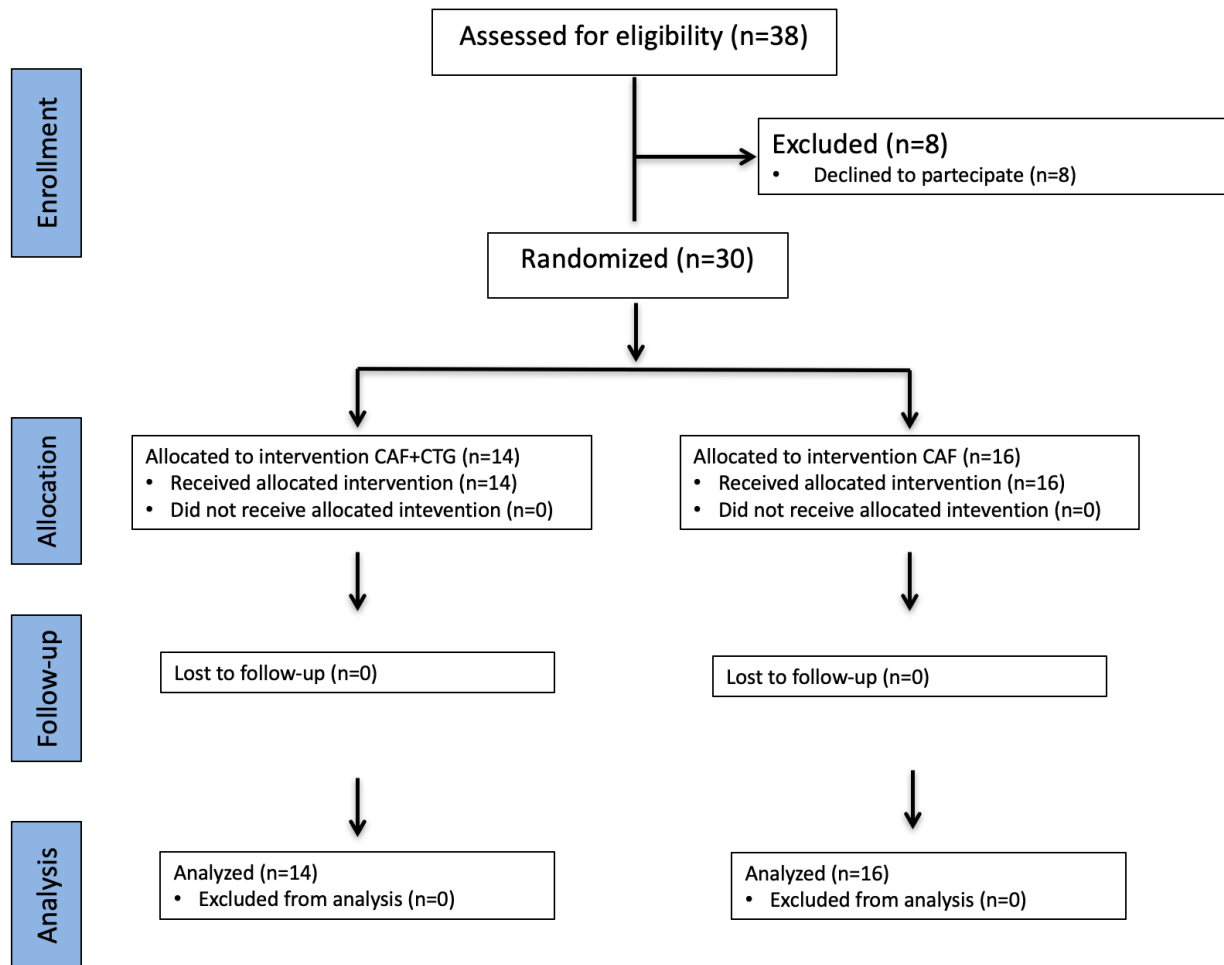


Figure 2

Patient allocated in the test group. (a) Baseline gingival recessions at upper first premolar associated with NCCL. (b) Restored CEJ level before surgery (c) Flap elevation (d) Connective tissue graft (CTG) was secured at the dehiscence area. (e) The flap is sutured. (f) Final healing at the 1-year follow-up with complete root coverage.

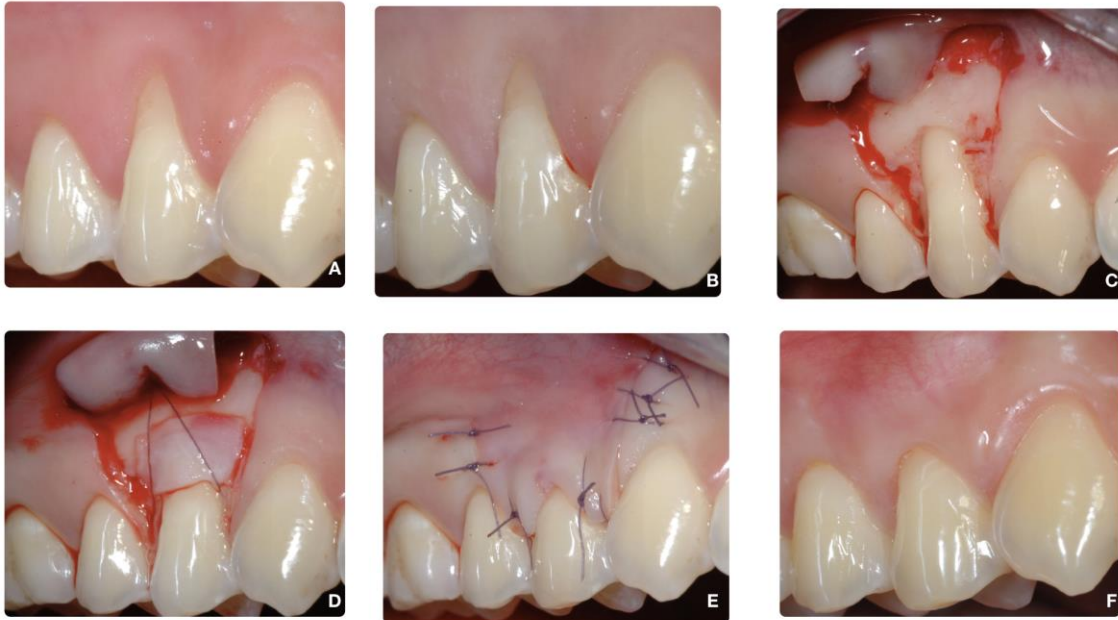


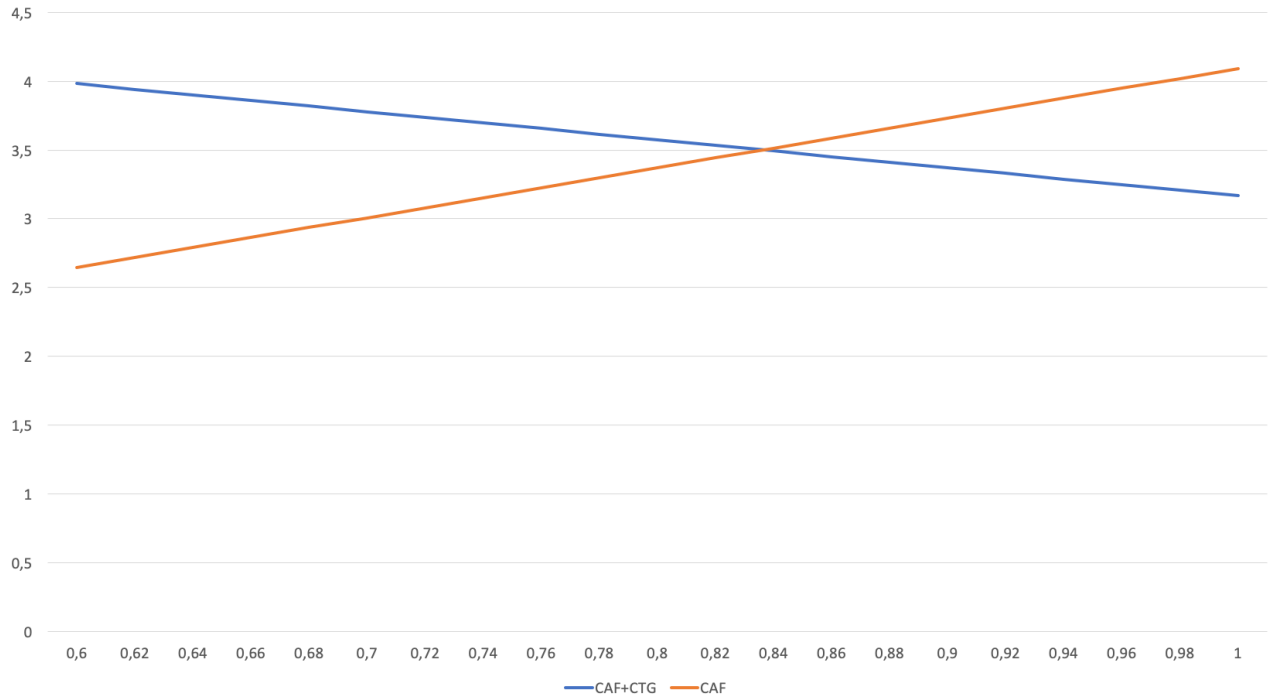
Figure 3

Patient allocated in the control group. (a) Baseline gingival recessions at upper first premolar associated with NCCL. (b) Restored CEJ level before surgery (c) The flap is sutured. (d) Final healing at the 1-year follow-up with complete root coverage.



Figure 4

The explorative model considering the interaction between surgical procedures and baseline gingival thickness (GT 0) is shown. The axis of abscissas is the GT 0 value in mm while ordinate axis is the final amount of recession reduction (RecRed) in mm. Considering a baseline Rec 0 = 4 mm, for value of thickness ≤ 0.84 mm adding CTG was associated with higher RecRed, while CTG seems to be not useful for value >0.84 mm since CAF alone was associated with higher RecRed.



THE EFFECT OF A SINGLE EXPOSURE TO A LOW DOSE BISPHOSPHONATE ON HUMAN MESENCHYMAL STEM CELLS ON A TITANIUM SURFACE (AN IN VITRO STUDY)

Mehta A, Owji N, Morden N, Alqhtani N, Buti J, D’Aiuto F, Knowles J.

University College London, Eastman Dental Institute, London. Great Britain

Abstract

Bisphosphonates have been shown to improve osseointegration however the effect of a single exposure versus a prolonged exposure to the drug remains unclear. This project aimed to investigate the effect of a single exposure to alendronate on the morphology and ultrastructure of human mesenchymal stem cells (hMSCs) compared to cells that had a continuous exposure for seven days.

Titanium discs with hMSCs were exposed to alendronate. The first group were exposed for seven days. The second group were exposed for 24-hours only, following which, the bisphosphonate-containing media was replaced with plain growth media. Morphological and ultrastructural changes were observed after 24-hours, three days and seven days using fluorescence imaging and scanning electron micrographs.

Following 24-hours’ exposure to alendronate, cells demonstrated increased morphological and ultrastructural changes compared to control cells. Over the seven-day period, these cells exhibited similar or even more morphological changes compared to cells that were exposed to the drug for up to seven days.

A single exposure to alendronate may have similar, if not enhanced effects on the morphological and ultrastructural changes of hMSCs on a titanium surface compared to cells that have been exposed to the drug for up seven continuous days.

Introduction

The global prevalence of tooth loss in 2010 was 2.3% representing 158 million people worldwide (Kassebaum et al., 2014). In the United Kingdom, the proportion of adults with twenty or less teeth were 13% in 2009 with the mean number of missing teeth found to be three (excluding third molars) (Steele et al., 2000, Bernabe and Sheiham, 2014). Tooth loss has been shown to affect patients’ quality of life (Nuttall et al., 2001) with negative effects on daily activities including patients’ ability to carry out basic functions such as eating and smiling (Adulyanon et al., 1997).

The challenge of restoring these spaces, improve masticatory function and aesthetic requirements whilst providing a prosthesis with long-term successful outcomes can be resolved by dental implants. Implant therapy relies on successful osseointegration, that is, “a direct structural and functional connection between ordered, living bone and the surface of a load-carrying implant” (Branemark 1959, Branemark, 1983). This process involves a series of cellular and extracellular biologic events which can be separated into three distinct stages; Osteogenesis, osteoconduction and osteoasaptation (Davies, 1998).

Many factors have been identified to enhance or inhibit osseointegration which are outlined in table 1 (Goutam et al., 2013).

Enhancement of osseointegration	Inhibition of osseointegration
Implant design, shape and diameter	Excessive implant mobility and micromotion
Titanium coating on Co-Cr metal implant	Nonsteroidal anti-inflammatory drugs especially selective COX-2 inhibitors
Laser treatment of Implant Surface	Warfarin and low molecular weight heparins
Human parathormone (1-34)	Inappropriate porosity of the porous coating of the implant
Bone source augment to socket	Osteoporosis, rheumatoid arthritis
Mechanical stability and loading conditions applied on the implant	Radiation therapy, smoking, advanced age, nutritional deficiency and renal insufficiency
Pharmacological agents such as simvastatin and bisphosphonates	Pharmacological agents such as cyclosporin A, methotrexate

Table 1: Factors affecting osseointegration of dental implants.

Extensive research has been conducted to enhance osseointegration and emerging evidence has begun to assess the use of bisphosphonates and mesenchymal stem cells to improve and accelerate the process. Mesenchymal stem cells are essential due to their ability to differentiate into cells that aid in regeneration (Hass et al., 2011, Kobolak et al., 2016). The quantity of mesenchymal stem cells is critical as it directly effects the number that can differentiate into osteoblasts for bone formation. Bisphosphonates have extensively been used to treat osteoporosis to reduce bone resorption, an essential aspect for bone healing (Drake et al., 2008b). Studies have shown significantly more bone formation around implants coated with bisphosphonates. Kajiwara and co-workers found a significant amount of new bone had formed around the bisphosphonate coated implants compared to the calcium coated and pure titanium implants in a rat model. Abtahi and co-workers investigated the effect of bisphosphonate coated titanium implants in a split-mouth study in sixteen patients (Abtahi et al., 2012). One implant was coated with a thin layer of two bisphosphonates (60% pamidronate and 40% ibandronate) and the other implant served as a control. A resonance frequency analyser measured implant stability to assess fixation. The results showed that bisphosphonate-coated implants had a larger increase in implant stability quotient (ISQ) values from baseline to six months compared to their paired controls, indicating that this local administration of bisphosphonates may improve the osseointegration process. The effect of low dose bisphosphonates on human mesenchymal stem cells and their osteogenic response to a

titanium surface has been investigated by Alqhtani and co-workers. In an *in-vitro* model, continuous systemic application of low dose bisphosphonates (alendronate and pamidronate, 100nM and 10nM), for up to 14 days, improved the activity and differentiation of human mesenchymal stem cells (Alqhtani et al., 2017). The data showed that bisphosphonates exerted a stimulatory effect on human mesenchymal stem cell osteogenic differentiation. The authors suggested that this increased osteogenic activity may enhance wound healing and accelerate the osseointegration process (Alqhtani et al., 2017). The study concluded that the application of low dose bisphosphonates, 1000 times less than a clinical dose, had a beneficial effect on hMSC proliferation and osteogenic differentiation on titanium surfaces.

The current literature shows that the systemic administration of low dose bisphosphonates has demonstrated an enhancement of hMSC activity, however, it is unclear if a single exposure to the drug will result in the same effect as a continuous exposure over a number of days. It is also unknown how long the effects can last for when the cells receive a single exposure to the drug for 24 hours only.

Therefore, the aim of this study was to determine the effect of a systemically administered low dose bisphosphonate, alendronate, on the morphology and ultrastructure of mesenchymal stem cells on titanium discs when cells are exposed to alendronate for 24 hours only compared to a continuous exposure for up to seven days.

Materials and Methods

This study observed the activity of human mesenchymal stem cells (hMSCs) on a titanium surface following the administration of different concentrations of a low dose bisphosphonate (alendronate) and comprised three variables: time, drug concentration and length of exposure to the drug. Observations were recorded at three intervals:

- One day (24 hours), which served as the baseline measurement
- Three days
- Seven days

Two different concentrations of alendronate (Sigma-Aldrich, Dorset, UK) were used: 100nM (T1) and 10nM (T2).

These were run in two parallel groups:

- **Group 1: hMSCs exposed to the drug continuously for up to seven days**
- **Group 2: hMSCs exposed to the drug for the first 24 hours only.**

After this, the alendronate containing media was replaced with plain growth media

- For each experimental condition there was also a control (C)

Samples stained for fluorescence imaging (using phalloidin or anti-vinculin antibody) were run in triplicate to preclude experimental bias and allow for sample failure. The hMSCs were tested for cell proliferation and examined with a fluorescence and scanning electron microscope.

Cell culture:

This study used hMSCs obtained from the Institute for Regenerative Medicine at the Texas A&M Health Science Centre College of Medicine, Texas, USA. The cells were isolated from the bone marrow (iliac crest) of a 22-year-old male donor. The hMSCs were isolated using density centrifugation, plated and then harvested at 60%-80% confluence.

Flow cytometry analysis demonstrated the cells ability to grow and differentiate into osteoblasts, adipocytes and chondrocytes. Cells as passage one (P1) were purchased and on arrival at the UCL Eastman Dental institute, London, UK, the cells were expanded and harvested as passage four (P4) for the use of this study.

Titanium disc preparation:

75 titanium discs (Strauman LTD, Switzerland), 15mm in diameter and 1mm in thickness were first polished to remove surface irregularities and roughness. This was followed by a sterilisation process which involved sonification in isopropanol, immersion in 0.1-N Nitric acid and exposure to ultra-violet light.

Cell sample preparation:

Cells were seeded onto the titanium discs in 24-well plates with the addition of either plain growth media (control), media containing 100nM alendronate (T1) or media containing 10nM alendronate (T2). The cells were placed in the incubator and observations were recorded after 24 hours, three and seven days. During the seven-day period, the media was replaced twice following several PBS washes. Group one received new media containing the appropriate concentration of alendronate and group two received plain media only. Summaries of the experimental protocol are explained in figures 1 and 2.

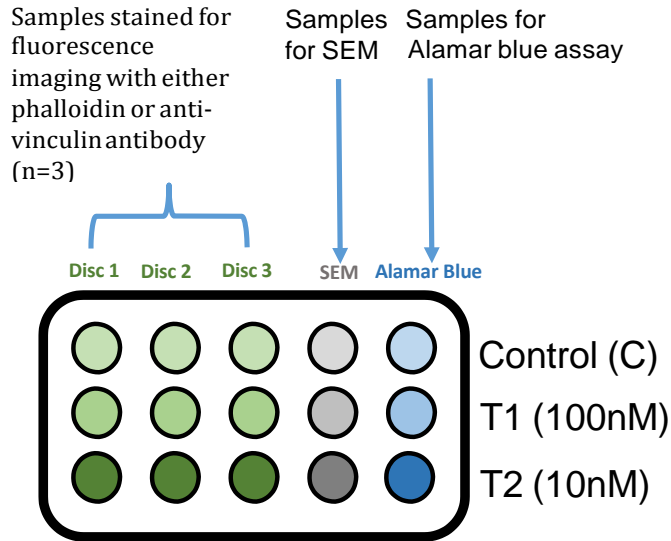
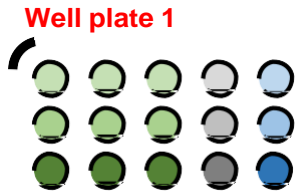


Figure 1: Set up of a well plate at the start of the experiment.

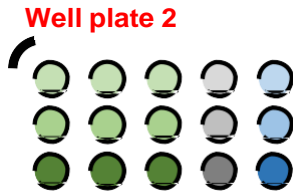
DAY 1
(24hours)



Well plate 1

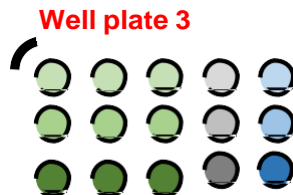
Group 1 and 2:
This well plate was observed after 24 hours of exposure to alendronate

DAY 3



Well plate 2

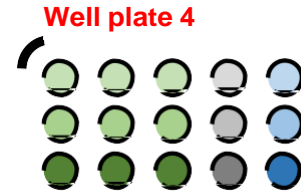
Group 1 (7-day exposure):
This well plate was observed after 3 days of exposure to alendronate



Well plate 3

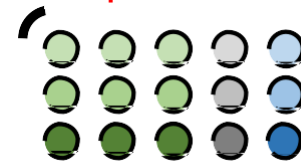
Group 2 (24-hour exposure):
This well plate was observed at day 3 after 24 hours of exposure to alendronate followed by 2 days exposure to plain growth media

DAY 7



Well plate 4

Group 1 (7-day exposure):
This well plate was observed after 7 days of exposure to alendronate



Well plate 5

Group 2 (24-hour exposure):
This well plate was observed at day 7 after 24 hours of exposure to alendronate followed 6 days exposure to plain growth media

Figure 2: Illustration of experimental protocol.

This experimental protocol was repeated twice; samples in ‘run one’ were stained with phalloidin and samples in ‘run two’ were stained with anti-vinculin antibody. Phalloidin, with a fluorescent marker, binds directly to the cytoskeleton allowing visualisation using fluorescence microscopy and staining with anti-vinculin antibody allowed visualisation of the adhesin vinculin. This assessed adhesion and attachment of the cells to the titanium surface.

Nuclear staining was performed using 4', 6- diamidino-2-phenylindole (DAPI) (Thermo Fisher, Hertfordshire, UK), a fluorescent stain that binds strongly to the DNA of the cells. All samples labelled for F-actin and vinculin were stained with DAPI.

The cell proliferation assay, Alamar blue, was used to measure proliferation of the hMSCs indicating cell viability. One sample in each group of the second run were assessed using the alamar blue protocol.

Imaging:

All discs were assessed using an inverted fluorescence microscope at 10 x magnification and 20 x magnification (Leica DM IRB Fluorescence Time Lapse Facility, Milton Keynes, UK). Image analysis was performed using ImageJ. Nuclei counts were performed on the fluorescence images, using Image-Pro Premium 9.2 (Media Cybernetics, Marlow, Buckinghamshire, UK). A stage micrometre of 0.1mm divisions was used to calibrate and calculate the area of each image. The nuclei were isolated from the background using the automated software. Where the software missed a nucleus, it was added manually and where two nuclei were counted as one, they were split manually. This provided a count of the number of cells per image. As this technique could be considered subjective, inter- and intra- examiner assessment were carried out on 10% of samples. There was consistent agreement between all the measurements taken for this assessment.

Cell morphology was analyzed using scanning electron microscopy (SEM) and examined using an SEM FEI XL30 FEG Scanning Electron Microscope (FEI, Eindhoven, Netherlands).

Statistical analysis:

Descriptive statistics were expressed as scatter graphs to display the nuclei counts for each image. The area of each image was 1.20mm² (1.27mm x 0.95mm). Bar graphs were used to show the fluorescence intensity levels detected for the alamar blue assay. Inferential analysis was conducted using a factorial experimental model to determine the impact of different factors on the percentage change in nuclei count over time compared to counts present at 24 hours (baseline). These factors included time, drug concentration and length of exposure to the drug. Possible interactions among terms were also explored. Factorial experiment analysis was performed using R Software.

Results

Cell morphology was assessed using two different staining methods and the nuclei were visualized with a fluorescent nuclear stain. SEM images were taken to further evaluate morphology and topography of the cells.

Day 1:

Control samples:

At 24 hours, fluorescence imaging showed cells had attached to the titanium surface and were beginning to spread with some evidence of elongation and alignment. The SEM samples also showed separate cells which were starting to elongate and align. The cell processes observed were extending from the cell body to the surface and were usually single and straight.

Test samples:

Cells exposed to 100nM alendronate in the growth medium (T1) and 10nM alendronate in the growth medium (T2) appeared more numerous on many of the discs compared to control discs. Samples stained with phalloidin showed multi-layers of cells, both disorganised and organised. The SEM images of the T1 and T2 samples shows ultrastructural differences when compared to the control. These cells showed an increase in cell processes in both test groups, in both runs. Numerous long cell processes that were notably undulating could be observed (figure 3).

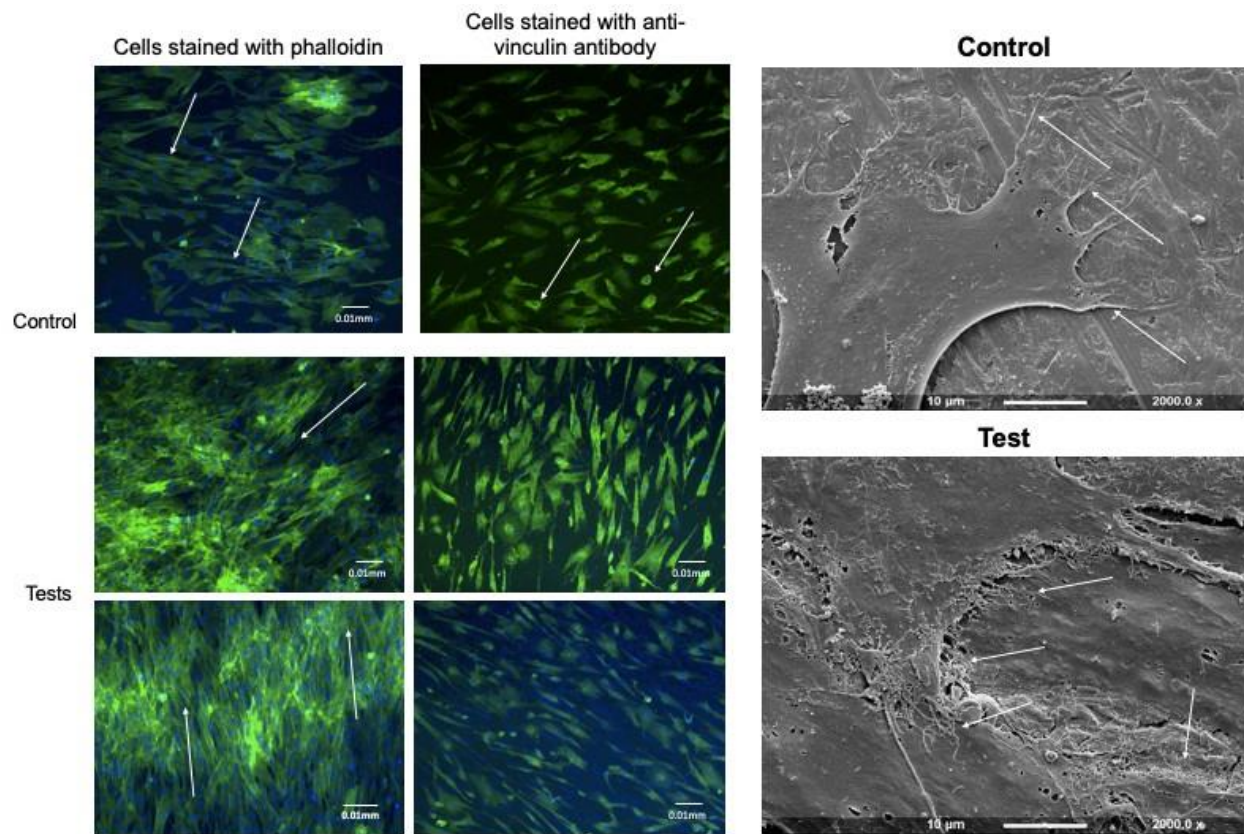


Figure 3: Fluorescence images show cells in the test group to be more numerous with evidence of elongation and alignment. The SEM images show cells in the test group to have an increase in cell processes that are notably undulating.

Day 3:

Control samples:

The cells of the controls could be seen to be more aligned in regions where they were numerous. No differences were observed in the images between group one and group two for both experimental runs within the control discs. The SEM assessment of control cells showed an increase in quantity of cells present on the titanium surface. Morphological features were similar to those observed on the control discs at 24 hours including cell processes appearing mostly straight.

Test samples:

All test samples stained with phalloidin demonstrated clear alignment with multi layers. Few differences could be observed between cells that were exposed to alendronate for 24 hours (group two) compared to cells that had been exposed to alendronate for three days (group one). Images from both groups displayed similar characteristics; elongation, alignment and spreading. SEM inspection of the test discs confirmed there were large areas of multi-layered, elongated and aligned cells. Multiple branching cell processes were also observed along the advancing front of many cells in both T1 and T2 groups. Cells exposed to the drug for 24 hours only were wider with more cell processes and more layers occupying the titanium surface (figure 4).

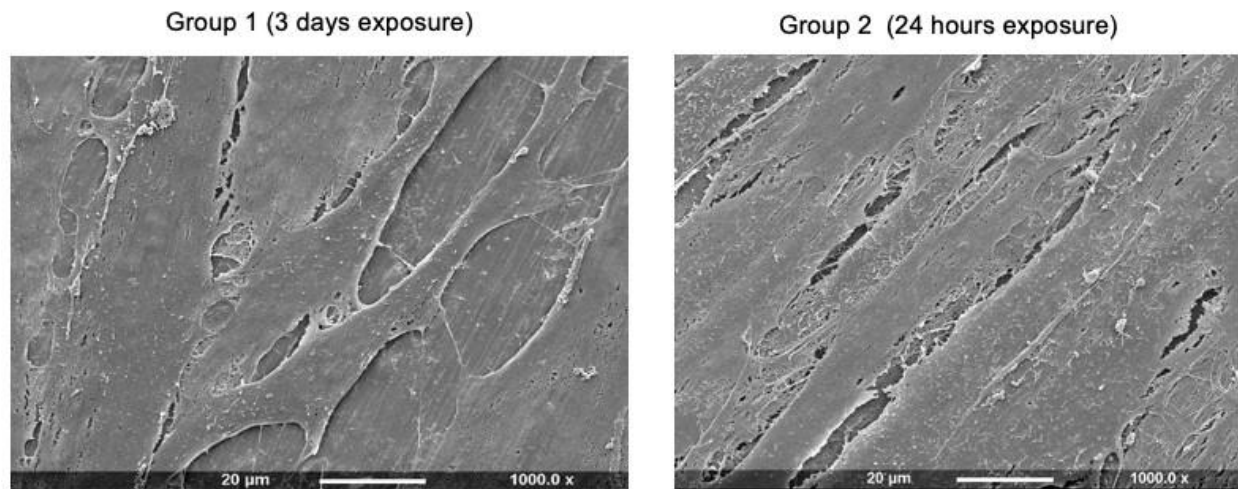


Figure 4: Results at Day 3. SEM images show cells exposed to the drug for 24 hours to be wider with more cell processes. More layers of cells are occupying the titanium surface.

Day 7:

Control samples:

By day 7 there was an increase in cells in all groups compared to their day one baseline images. Cells appeared greater in quantity, represented by higher numbers of blue stained nuclei and the arrangement and morphology of the cells were consistently aligned and elongated. These images were similar to the appearance of test samples that had been achieved by 24 hours and day three. The scanning electron micrograph supported these findings with evidence of multi-layer, aligned cells and a clear increase in cell processes.

Test samples:

For all treatments, the fluorescence images showed that the cells were numerous, confluent, elongated and aligned. Little differences could be observed between images from day seven cells that had been exposed to alendronate for only 24 hours (group two) and cells that had been exposed to alendronate for all seven days (group one). SEM images support the fluorescence images demonstrating multi-layered, elongated cells

with numerous cell processes. SEM images show the control samples to now have similar features to test samples (figure 5).

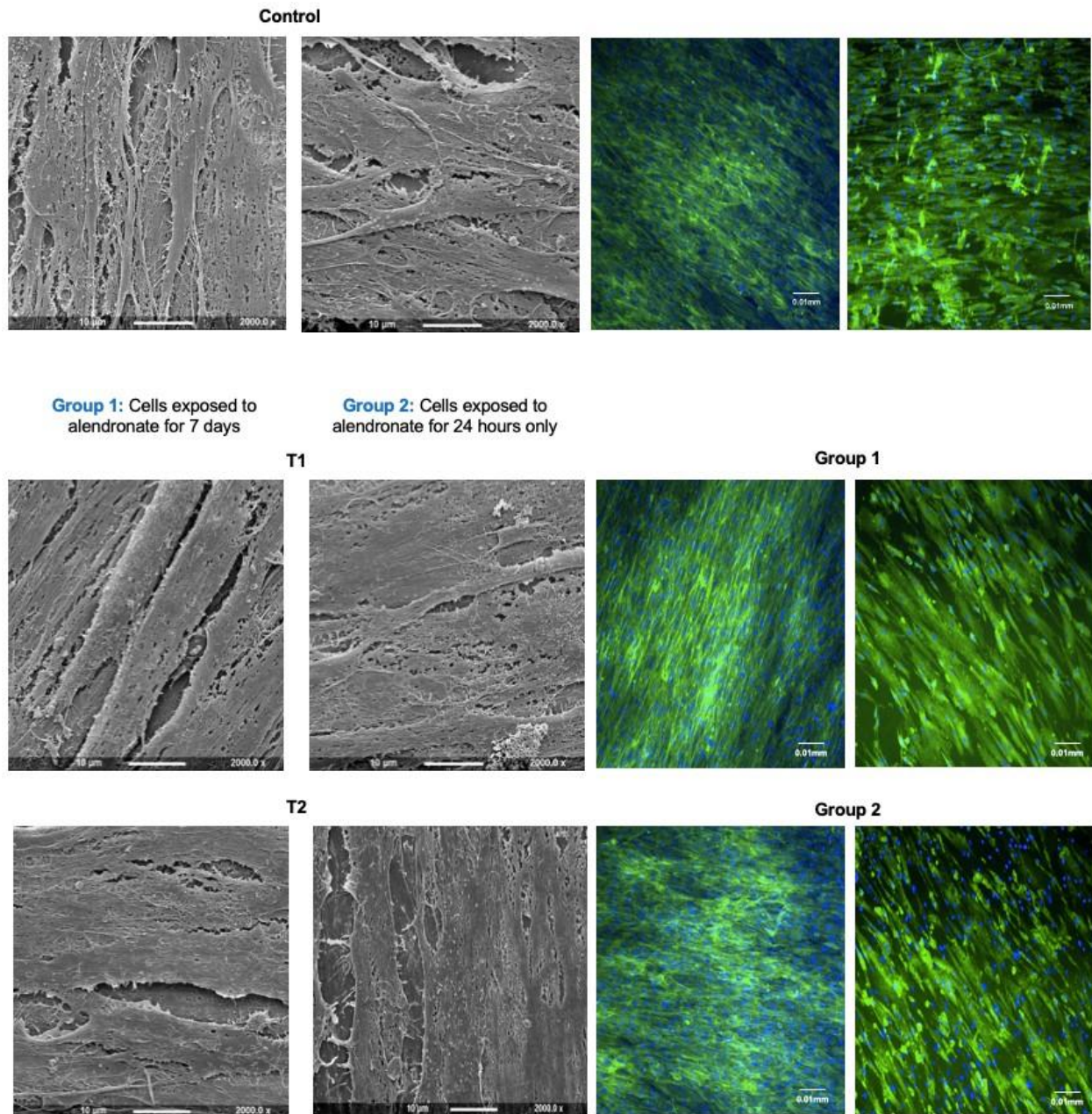


Figure 5: Results at Day 7. SEM and fluorescence images show control and test cells exhibiting similar morphological and ultrastructural features. All cells appear confluent, elongated and aligned. Cells exposed to alendronate for 24 hours show similar features to those exposed for seven days.

Results of the quantitative analysis:

All experimental models did not find a significant association between control or either test groups (T1 or T2) on the percentage change in number of nuclei compared to baseline counts.

Alamar blue assay:

The alamar blue assay was performed on one disc in group one and group two of the cells stained with anti-vinculin antibody (run two). Fluorescence intensities were recorded at 24 hours, at day three and at day seven. For cells that were exposed to the bisphosphonate for 24 hours only, fluorescence intensity decreased as the number of days increased. For cells that were exposed for seven continuous days, there was an initial reduction in fluorescence intensity between day one and day three. Following this, the fluorescence intensity increased by day seven.

Conclusions

Results from this study demonstrated positive morphological and ultrastructural changes on the hMSCs following exposure to alendronate. This was consistent with current evidence as described by Alqhtani and co-workers (Alqhtani et al., 2017).

At day three, the control samples increased in number and there was evidence of morphological changes within the cells, similar to those observed in test samples that had been established at 24 hours. These changes included multi-layering of cells, cell elongation and an extension of cell processes. The SEM images appeared to be similar, however cells which received 24 hour exposure, were greater in width and more extensively spread over the disc. The cells also exhibited more cell processes.

At day seven, similar observations were seen in the fluorescence images and scanning electron micrographs; there were no differences in morphological features from group one or group two experiments and if a difference was observed, it was in favour of cells exposed to alendronate for 24 hours only (group two). These results provide new information on how long structural changes can be observed following exposure to low doses of alendronate for up to seven days.

Nuclei counts varied over the seven days however there was an overall increase in cell count. By day seven, there were more cells compared to day one, and group two (cells exposed to alendronate for 24 hours only) had more cells than group one (cells exposed to alendronate for up to seven days). This data supports the morphological changes observed in the fluorescence and SEM images. The alamar blue proliferation assay indicated that as the number of days increased, cell viability decreased for most samples.

In this study, the beneficial effect of alendronate was predominantly observed during the first three days following exposure to the drug. This is an important finding which has advantageous clinical applications with regards to bone healing and osseointegration. Studies show that new bone formation can start as early as one week following implant placement (Berglundh et al., 2003a) and the most important time period in the process of osseointegration for hMSCs is approximately day four (Salvi et al., 2015a). Therefore, if activity of hMSCs can be enhanced or promoted during this crucial time period, it could lead to an acceleration in osseointegration. The findings of this research add to the limited knowledge base on bisphosphonates and osseointegration but highlight the benefit for their potential use.

Limitations:

Due to clustering of the cells on the disc, it was not possible to standardize selection of the area to be imaged per disc. Instead, the most densely populated area of the disc was selected. In order to reduce future bias, computer generated random co-ordinates could be formulated and these areas assessed with the use of a grid overlying the sample. Multiple co-ordinates can be selected to get a better representation of the disc which could improve the validity of the existing methodology for assessing cell morphology as well as nuclei counts.

Although assessment of morphologic features gives an indication of cell behaviour, imaging alone does not give information regarding changes in cell metabolic activity. The main limitation of the data collected regarding the Alamar blue proliferation assays was the limited sample size and hence no conclusions can be drawn. Future studies should assess cell viability, proliferation and ability to differentiate. The alamar blue assay should be used with a larger sample size, or alternative assays could be employed such as adenosine triphosphate (ATP) assay. Dead or dying cells contain little to no ATP and therefore this assay provides an accurate representation of live cells. The ability of cells to differentiate into mature osteoblasts is essential for successful osseointegration. Osteogenic factors could be introduced directly into the culture medium to encourage the hMSCs toward an osteogenic differentiation. The cells might then be assessed by testing for various differentiation markers such as intracellular alkaline phosphatase (ALP) and calcium deposition.

Within the limitations of this *in-vitro* study, the results suggest that a single exposure to alendronate for 24 hours may have a similar or more positive effect than cells exposed to the drug for seven days. Furthermore, these positive effects can last up to seven days.

Implications for research

Further *in vitro* studies are required to assess additional study outcomes including cell proliferation and differentiation measurements. Following identification of the ideal drug, dose and follow up period, an *in vivo* model can be tested.

Implications for clinical practice

A single exposure to the drug may be more beneficial in enhancing osseointegration than a 7-day course as it not only reduces the overall cost of treatment, but increases the likelihood of patient compliance to this adjunctive therapy.

Bibliography

1. ABTAHI, J., TENGVALL, P. & ASPENBERG, P. 2012a. A bisphosphonate-coating improves the fixation of metal implants in human bone. A randomized trial of dental implants. *Bone*, 50, 1148-1151.
2. ABTAHI, J., TENGVALL, P. & ASPENBERG, P. 2012b. A bisphosphonate-coating improves the fixation of metal implants in human bone. A randomized trial of dental implants. *Bone*, 50, 1148-51.
3. ADULYANON, S., VOORAPUKJARU, J. & SHEIHAM, A. 1996. Oral impacts affecting daily performance in a low dental disease Thai population. *Community Dent Oral Epidemiol*, 24, 385-9.
4. ALQHTANI, N. R., LOGAN, N. J., MEGHJI, S., LEESON, R. & BRETT, P. M. 2017. Lowdose effect of bisphosphonates on hMSCs osteogenic response to titanium surface in vitro. *Bone Rep*, 6, 64-69.

5. BERGLUNDH, T., ABRAHAMSSON, I., LANG, N. P. & LINDHE, J. 2003a. De novo alveolar bone formation adjacent to endosseous implants. *Clin Oral Implants Res*, 14, 251-62.
6. BERNABE, E. & SHEIHAM, A. 2014. Tooth loss in the United Kingdom--trends in social inequalities: an age-period-and-cohort analysis. *PLoS One*, 9, e104808.
7. BRANEMARK, P. I. 1959. Vital microscopy of bone marrow in rabbit. *Scand J Clin Lab Invest*, 11 Supp 38, 1-82.
8. BRANEMARK, P. I. 1983. Osseointegration and its experimental background. *J Prosthet Dent*, 50, 399-410.
9. DAVIES, J. E. 1998. Mechanisms of endosseous integration. *Int J Prosthodont*, 11, 391- 401.
10. DRAKE, M. T., CLARKE, B. L. & KHOSLA, S. 2008a. Bisphosphonates: Mechanism of action and role in clinical practice. *Mayo Clinic Proceedings*, 83, 1032-1045.
11. GOUTAM, M., CHANDU, G., MISHRA, S. K., SINGH, M. & TOMAR, B. S. 2013. Factors affecting Osseointegration: A Literature Review. *Journal of Orofacial Research*, 3, 197.
12. HASS, R., KASPER, C., BOHM, S. & JACOBS, R. 2011. Different populations and sources of human mesenchymal stem cells (MSC): A comparison of adult and neonatal tissue-derived MSC. *Cell Commun Signal*, 9, 12.
13. KAJIWARA, H., YAMAZA, T., YOSHINARI, M., GOTO, T., IYAMA, S., ATSUTA, I., KIDO, M. A. & TANAKA, T. 2005. The bisphosphonate pamidronate on the surface of titanium stimulates bone formation around tibial implants in rats. *Biomaterials*, 26, 581-7.
14. KASSEBAUM, N. J., BERNABE, E., DAHIYA, M., BHANDARI, B., MURRAY, C. J. &
15. MARCENES, W. 2014. Global Burden of Severe Tooth Loss: A Systematic Review and Meta-analysis. *J Dent Res*, 93, 20S-28S.
16. KOBOLAK, J., DINNYES, A., MEMIC, A., KHADEMHOSEINI, A. & MOBASHERI, A. 2016. Mesenchymal stem cells: Identification, phenotypic characterization, biological properties and potential for regenerative medicine through biomaterial micro-engineering of their niche. *Methods*, 99, 62-8.
17. NUTTALL, N., STEELE, J., PINE, C., WHITE, D. & PITTS, N. 2001. Adult dental healthsurvey: The impact of oral health on people in the UK in 1998. *British Dental Journal*, 190, 121.
18. SALVI, G. E., BOSSHARDT, D. D., LANG, N. P., ABRAHAMSSON, I., BERGLUNDH, T., LINDHE, J., IVANOVSKI, S. & DONOS, N. 2015a. Temporal sequence of hard and soft tissue healing around titanium dental implants. *Periodontology 2000*, 68, 135- 152.
19. STEELE, J. G., TREASURE, E., PITTS, N. B., MORRIS, J. & BRADNOCK, G. 2000. Total tooth loss in the United Kingdom in 1998 and implications for the future. *Br Dent J*, 189, 598-603.

Corresponding Author:

Dr Anjali Metha

E-mail: anjalibhimjiyani@gmail.com

CLINICAL OUTCOMES OF THE ENTIRE PAPILLA PRESERVATION TECHNIQUE WITH AND WITHOUT BIOMATERIALS IN THE TREATMENT OF ISOLATED INTRABONY DEFECTS: A RANDOMISED-CONTROLLED CLINICAL TRIAL

Serhat Aslan,¹ Nurcan Buduneli²

¹Private Office Dr. Serhat Aslan, İzmir, Turkey.

²Ege University, School of Dentistry, Department of Periodontology, İzmir, Turkey.

Running title: Entire papilla preservation technique with and without biomaterials

Key words: Clinical trial; Enamel matrix proteins; Guided tissue regeneration, periodontal; Microsurgery; Periodontal atrophy; Periodontitis; Surgical flaps; Treatment outcome

Conflict of Interest and Source of Funding Statement: The study was funded solely by the institution of the authors. The authors declare no conflicts of interest related with this study.

Abstract

Background: This randomised clinical trial compared the clinical efficacy of the entire papilla preservation technique (EPP) alone and in combination with enamel matrix proteins plus bovine-derived bone substitutes (EMD+BS) in the treatment of isolated interdental intrabony defects.

Material and methods: A total of 30 patients with one isolated deep intrabony defects were enrolled 15 of them were randomly assigned to EPP alone while the other 15 to EPP EMD+BS. Access to the intrabony defect for debridement was provided by a single vertical incision positioned in the buccal gingiva of the neighbouring interdental space. Following the elevation of a buccal flap, an interdental tunnel was prepared undermining the defect-associated papilla. Granulation tissue was removed and root surfaces were carefully debrided. In the EPP EMD+BS group, bone substitutes and EMD were applied. EPP group did not receive any regenerative biomaterials. Microsurgical suturing technique was used for optimal wound closure. Outcome measures included gain in clinical attachment level (CAL), probing depth (PD) reduction, and gingival recession (REC).

Results: Early healing phase was uneventful in all cases and 100% primary wound closure was maintained throughout the study period. Intragroup differences between baseline and 1-year were statistically significant in both groups in terms of CAL gain and PD reduction ($p \leq 0.001$), no statistically significant differences were detected in REC ($p > 0.05$). There were no statistically significant differences in mean \pm SD CAL gain (6.3 ± 2.5 mm *versus* 5.83 ± 1.12 mm), PD reduction (6.5 ± 2.65 mm *versus* 6.2 ± 1.33 mm), and increase in gingival recession (0.2 ± 0.25 mm *versus* 0.36 ± 0.54 mm) between the EPP EMD+BS and EPP groups.

Conclusions: EPP with and without regenerative biomaterials can provide significant amount of CAL gain and PD reduction, with negligible increase in gingival recession.

Within the limits of the present study, it can be concluded that addition of regenerative biomaterials do not improve the overall clinical outcomes.

Introduction

The ultimate end-point of treatment following the completion of initial periodontal therapy is accomplishing regeneration of the lost periodontal tissues. Various surgical techniques and biomaterials have been investigated to achieve periodontal regeneration since the very first inception of guided tissue regeneration (GTR) technique (Nyman et al. 1982). Barrier membranes in combination with bovine-derived bone substitutes, enamel matrix proteins (EMD), demineralized freeze-dried bone allografts have been used for the formation of new cementum, new periodontal ligament and new alveolar bone (Heijl 1997, Sculean et al. 1999, Camelo et al. 2001). Various factors such as plaque control, percentage of bleeding on probing, location and morphology of the defect, smoking habit, and exposure of the barrier membrane significantly influence the clinical outcomes following the implantation of these biomaterials (Tonetti et al. 1993, Machtei 1994, De Sanctis et al. 1996a, Kornman & Robertson 2000, Farina et al. 2013). Exposure of the applied biomaterials is the major issue in the field of regeneration, as this event may lead to contamination of the surgical site and jeopardizes wound stability. To overcome this clinical issue, different approaches have been proposed to provide an ideal environment for early as well as late wound stability. Instead of using GTR technique, researchers have focused on biologics such as EMD and this shift significantly decreased the incidence of early wound healing complication (Sanz et al. 2004). On the other hand, implementation of microsurgical technique and its principles into the regenerative periodontal surgery increased the rate of primary healing by minimizing the trauma to the soft tissues (Tibbets & Shanelec 1998, Cortellini & Tonetti 2001). Moreover, evolution of the surgical flap design improved early wound healing and stability that are critical factors for the clinical outcomes. Papilla preservation technique (Takei et al. 1985), modified papilla preservation technique (Cortellini et al. 1995), simplified papilla preservation technique (Cortellini et al. 1999), minimally invasive surgical approaches with papilla elevation (Cortellini & Tonetti 2007) or without palatal papilla elevation (Cortellini & Tonetti 2009, Trombelli et al. 2009) aim at preserving the interdental papillary complex and enhancing wound stability. All the aforementioned techniques, however, entail an incision over the defect-associated interdental papilla that may jeopardize the volume and complex vascular integrity of the interdental tissues.

Recently, a novel surgical approach, the “entire papilla preservation (EPP)” technique has been proposed for regenerative treatment of isolated deep intrabony defects (Aslan et al. 2017a). This novel concept provides an intact gingival chamber over the intrabony defect, with completely preserved interdental papilla. One-year prospective cohort study (Aslan et al. 2017b) with twelve isolated deep non-contained intrabony defects treated with EMD+bone substitutes, revealed 100% primary closure during all stages of wound healing and documented 6.83 mm of mean clinical attachment gain. However, the efficacy of this novel surgical concept when combined with biomaterials remains unclear. Therefore, the aim of the present randomised and controlled clinical trial was to investigate the clinical efficacy of “EPP” alone in comparison to EPP combined with regenerative biomaterials.

Material and Methods

Experimental design

The present study is designed as a single-centre, parallel group, and randomised, controlled clinical trial comparing the efficacy of two treatment modalities in 30 patients. The present paper is written according to the CONSORT statement for improving the quality of reports of parallel-group randomised trials. The study protocol was approved by the Institutional Review Board of School of Medicine, Ege University, İzmir, Turkey (protocol no. 15-4.1/10). A single defect was treated in each patient and all the experimental sites were accessed with the “EPP” technique (Aslan 2017a) and debrided carefully. EDTA gel was applied on the instrumented root surfaces. EMD+bone substitutes were applied in one group (EPP EMD+BS, 15 defects), while the other group (EPP, 15 defects) did not receive any regenerative biomaterials. The single vertical incision was sutured with single interrupted sutures. Patients were enrolled in a stringent maintenance programme with recalls on a weekly basis for the first month and then monthly controls for professional tooth cleaning for the 12 months postoperatively. Clinical periodontal parameters were recorded at baseline, which is 3 months after completion of initial periodontal therapy. Periodontal probing was avoided in the experimental site during the 12-month study period. Final clinical outcomes were recorded 12 months after the regenerative periodontal surgery.

Study population

Inclusion criteria were; being systemically healthy, having the clinical diagnosis of advanced periodontitis, willing to receive regenerative periodontal surgery after completion of non-surgical periodontal therapy and giving a written informed consent. Eligible patients had one isolated intrabony defect with probing depth (PD) ≥ 7 mm, clinical attachment level (CAL) ≥ 8 mm and at least 4 mm intrabony component involving predominantly the interproximal area of the affected tooth. Moreover, the patients had to exhibit full-mouth plaque score (FMPS) and full-mouth bleeding score $\leq 20\%$. Current smokers, patients with known systemic diseases such as diabetes and cardiovascular diseases or using medications that affect periodontal tissues, pregnant or lactating women were excluded from the study. Local exclusion criteria were; one-wall intrabony defects, defects that involve buccal and lingual sites, presence of inadequate endodontic treatment and/or restoration in the relevant teeth.

Surgical procedures

All surgical procedures were performed by one experienced periodontal surgeon (S.A.). The surgical site was anesthetized using articaine-epinephrine 1:100,000. Trans-papillary infiltration was avoided to prevent physical (needle penetration) and chemical (in terms of prolonged vasoconstriction) trauma to the gingival tissues. Bone sounding was performed following the onset of anesthesia.

The “Entire papilla preservation” technique is a tunnel-like approach of the defect-associated interdental papilla. An operating microscope (x6 to x21 magnification) was used to increase the visibility of the surgical site (Cortellini & Tonetti 2001). Following a buccal intra-crevicular incision, a bevelled vertical releasing incision was performed in the buccal gingiva of the neighbouring interdental space and extended just beyond the mucogingival line to provide appropriate mechanical access to the intrabony defect. A microsurgical periosteal elevator was used to elevate a buccal full-thickness muco-periosteal flap extending from the vertical incision to the defect-associated papilla. A specifically designed angled tunnel

elevator facilitated the interdental tunnel preparation under the papillary tissue. Utmost care was taken to elevate the interdental papilla in full-thickness manner up to the intact lingual bone crest. A microsurgical scissor was used to remove the granulation tissue from the inner aspect of the defect-associated interdental papilla. Excessive thinning of the papilla was avoided not to compromise the blood supply. The granulation tissue was removed with a mini-curette. Any residual subgingival plaque or calculus was gently removed from the exposed root surface with an ultrasonic scaler. The surgical area was thoroughly rinsed with sterile saline and root conditioning of the exposed surface was done applying 24% EDTA gel (Pref-Gel, Institut Straumann, AG, Basel, Switzerland) for 2 minutes to remove the smear layer. Then, the exposed root surface was rinsed with sterile saline just before opening the randomisation envelope and treatment was continued basing on the group assignment. In the EPP EMD+BS group, EMD (Emdogain, Institut Straumann, AG, Basel, Switzerland) was applied to the exposed root surface. Subsequently, a deproteinized bovine-derived bone substitute (Cerabone, Botiss Biomaterials GmbH, Berlin, Germany) was placed into the intrabony defect. Contamination with blood or saliva was prevented during biomaterial application. In the EPP group, the intrabony defect was left to fill with a blood clot, as a result of bleeding from the residual bone walls. No periosteal releasing incision was performed. Gentle pressure was applied to the surgical area using saline-wetted gauze for 1 min to readapt the mucoperiosteal flap. Microsurgical suturing technique with 6-0 or 7-0 monofilament suture materials was performed for optimal wound closure of the surgical area.

Post-surgical care

After the surgery, patients received 600 mg ibuprofen and were instructed to take a subsequent dose 8 hours later. If necessary, patients were advised to take additional tablet and to report. Systemic doxycycline (100 mg b.i.d.) was prescribed during the first post-operative week. The patients were asked to refrain from using mechanical oral hygiene measures for a period of 4-weeks. During this period, the patients were requested to rinse with 0.12% chlorhexidine digluconate mouthrinse for 1 min twice daily. The sutures were removed 2 weeks after the surgery. Each patient received professional tooth cleaning (performed by S.A.) during the monthly control appointments for the following 12 months.

Clinical parameters

Clinical periodontal parameters were recorded at baseline, which is 3 months after completion of initial periodontal therapy. Final clinical outcomes were recorded 12 months after the regenerative periodontal surgery. Clinical periodontal parameters were recorded at 4 sites (mesial, buccal, distal, and oral) of each tooth present except the third molars. All clinical measurements at baseline and also 1-year after the surgery were carried out by the same examiner blinded to the study group (N.B.). Before the study, the examiner was calibrated for the intra-examiner reproducibility and accuracy. Full-mouth plaque scores (FMPS) were recorded as the percentage of total surfaces exhibiting plaque (O'Leary 1972). Bleeding on probing (BOP) was assessed dichotomously (as present or absent) and BOP was deemed positive if it occurred within 15 seconds after periodontal probing. Full-mouth bleeding scores (FMBS) were then calculated (Cortellini 1993a). PD and recession of the gingival margin (REC) were rounded to the nearest 0.5 mm at the deepest location of the experimental interproximal site. CAL was calculated as the sum of PD and REC. Primary closure of the surgical sites was evaluated on a weekly basis for the first

month after the surgery. Any adverse effects such as haematoma, pain, discomfort, oedema, and additional painkiller intake were recorded.

Clinical characterization of the intrabony defects during the surgery

Defects were described as 1-,2-,3-wall or combination defects according to Papapanou et al. (2000). Depth of the intrabony component (INFRA) was measured as the distance between the crest of the marginal bone and the deepest location of the osseous defect, and width of the intrabony defect as the horizontal distance between the crest of the marginal bone and root surface.

Surgical and patient-centered outcomes

Operation time was measured with a chronograph, starting at delivery of local anaesthesia till the final suture. Primary closure of the surgical site was checked with magnification at the end of surgery and then weekly for 6 weeks. Presence of a discontinuity in the soft tissues was registered as wound failure. Patients were asked to fill the questionnaire at the end of the surgery to report about intraoperative pain and subjective opinion for the discomfort of the procedure. A visual analogue scale (VAS) of 100 mm long was used to evaluate the degree of discomfort (0=no pain/hardship; 100=unbearable pain/hardship). Patients were asked at week 1 for their experience with post-operative pain and discomfort using a standard questionnaire; pain intensity was quantified with a VAS essentially as described (Cortellini et al. 2001, Tonetti et al. 2002).

Data analysis

CAL gains, residual PD and REC change were the outcome variables. Data within each group were expressed as mean \pm standard deviation of 15 defects in 15 patients. All calculations were performed using the software IBM SPSS Statistics version 25.0. To assess normality, the Shapiro-Wilk test was applied. Repeated measures ANOVA (baseline and 1-year) and Independent samples Student t-test were used for normally distributed parameters. Wilcoxon's test for intragroup comparisons and Mann-Whitney U test for intergroup comparisons were used for parameters that were not normally distributed.

The level of significance used in the statistical analyses was set at 5% ($\alpha \leq 0.05$). Assuming a standard deviation in CAL gain of 1.0 mm, a sample size of 28 patients (14 patients per group) was estimated to have an 83% power to detect a difference of 1.0 mm in CAL gain between groups by using a parametric test with a 0.05 two-sided significance level (Trombelli et al. 2010).

Results

Experimental population and characteristics of surgical sites

Thirty patients were enrolled in this randomised-controlled clinical trial. The EPP alone was applied in 15 subjects (mean age 43.93 ± 12.85 years, range 21-63 years, 7 females). The EPP EMD+BS was applied in other 15 subjects (mean age 44.93 ± 13.06 years, range 22-60 years, 5 females). There was no drop-out throughout the study protocol and no missing data for the statistical analysis.

The two experimental groups were homogeneous and well-balanced, with no statistically significant differences according to age, gender, tooth type, severity, and morphology of the intrabony defects (Table 1). The experimental defects were mainly combination of 2-wall components (86% of defects for the EPP EMD+BS group; 93% of defects for the EPP group).

Post-surgical and early healing phase

The surgical time for EPP alone was rather short (55.07 ± 7.86 min, range 39-68 min). Slightly longer surgical time was required for EPP EMD+BS that accounted for 65.4 ± 10.94 min on average (range 50-93 min). The difference between the two groups was statistically significant ($p < 0.01$).

Primary closure of the defect-associated papilla and single vertical incision was obtained in all treated sites (100% primary closure rate), irrespective of regenerative biomaterial application or not. No adverse events (e.g. oedema or haematoma) were noted in any of the treated sites.

None of the subjects reported severe intraoperative pain or subjective feeling of hardship of the surgical procedure at the end of the intervention. On day-4, none of the patients reported any post-operative pain. A slight discomfort was reported by two patients (13.3%) of the EPP EMD+BS group (mean VAS 9.33 ± 9.03) and by one patient (6.7%) of the EPP group (mean VAS 8.33 ± 9.38). The difference between the two groups did not reach statistical significance ($p = 0.757$). The mean additional painkiller intake was 0.87 ± 0.74 tablets for the EPP EMD+BS group and 0.73 ± 0.88 tablets for the EPP group, without inter-group significant differences ($p = 0.296$).

Clinical outcomes at 1-year

Clinical characteristics at baseline and 1-year are shown in Table 2. Both groups presented with low levels of FMPS and FMBS, shallow residual probing depths, significant amounts of CAL gains and very limited increase in gingival recession.

CAL significantly decreased from baseline to 1-year for both groups; however, no statistically significant differences were found in CAL change between groups ($p = 0.983$). Eight EPP EMD+BS defects (53%) showed a gain ≥ 6 mm; five defects (33%) 5 mm; and two defects (14%) 4 mm. Seven EPP defects (47%) showed a gain ≥ 6 mm; five defects (33%) 3 to 4 mm; and three defect (20%) 4 mm.

PD significantly decreased from baseline to 1-year for both groups; however, no significant differences were found in PD reduction between the groups ($p = 0.866$). Five EPP EMD+BS defects (33%) showed residual PD of 2 mm, eight defects (53%) 3 mm; and two defects (14%) ≥ 4 mm. Three EPP defects (20%) showed residual PD of 2 mm, nine defects (60%) 3 mm; and three defects (20%) ≥ 4 mm.

REC increased from baseline to 1-year for both groups. No statistically significant differences were found in REC increase between the two groups ($p = 0.523$). No gingival recession occurred in nine of EPP EMD+BS defects (60%) and eight of EPP defects (53%).

Conclusions

Within the limits of the present study:

-EPP with and without regenerative biomaterials seems to provide ideal conditions during the early and late wound healing phases. However, the addition of the regenerative biomaterials did not improve the overall clinical outcomes, statistically. Long-term results are needed to confirm the stability of the present findings.

-Completely preserved interdental papilla revealed 100% primary closure in all treated sites. This phenomenon probably further enhanced the stability of the blood clot and no soft tissue complication or wound failure was observed.

-Patient-centered outcome measures clearly demonstrated the clinical applicability of the EPP, as a minimally invasive surgical approach.

-Based on the obtained results, it can be concluded that improvements in flap design and execution seem to be more efficient than the regenerative biomaterials when applied in appropriate intrabony defect configuration.

References

- Aslan S, Buduneli N, & Cortellini P. (2017a). Entire papilla preservation technique: A novel surgical approach for regenerative treatment of deep and wide intrabony defects. *International Journal of Periodontics & Restorative Dentistry*, 37, 227–233.
- Aslan S, Buduneli N, Cortellini P. (2017b). Entire papilla preservation technique in the regenerative treatment of deep intrabony defects: 1-Year results. *Journal of Clinical Periodontology*, 44:,926–932.
- Camelo M, Nevins ML, Lynch SE, Schenk RK, Simion M, Nevins M. (2001) Periodontal regeneration with an autogenous bone-Bio-Oss composite graft and a Bio-Gide membrane. *International Journal of Periodontics & Restorative Dentistry* **21**, 109-19.
- cort 93
- Cortellini, P., Pini-Prato, G. P. & Tonetti, M. S. (1993a) Periodontal regeneration of human infrabony defects I. Clinical Measures. *Journal of Periodontology*, 64, 254–260.
- Cortellini P, Prato GP, Tonetti MS. (1995) The modified papilla preservation technique. A new surgical approach for interproximal regenerative procedures. *Journal of Periodontology* **66**, 261-6.
- Cortellini P, Prato GP, Tonetti MS. (1999) The simplified papilla preservation flap. A novel surgical approach for the management of soft tissues in regenerative procedures. *International Journal of Periodontics & Restorative Dentistry* **19**, 589-99.
- Cortellini P, Tonetti MS. (2001) Microsurgical approach to periodontal regeneration. Initial evaluation in a case cohort. *Journal of Periodontology*, 72:559-69.
- Cortellini P, Tonetti MS. (2007a) A minimally invasive surgical technique (MIST) with enamel matrix derivative in the regenerative treatment of intrabony defects: a novel approach to limit morbidity. *J Clin Periodontol* **34**, 87-93
- Cortellini P, Tonetti MS. (2009) Improved wound stability with a modified minimally invasive surgical technique in the regenerative treatment of isolated interdental intrabony defects. *J Clin Periodontol* **36**, 157–163.
- De Sanctis M, Zucchelli G, Clauser C. (1996a) Bacterial colonization of bioabsorbable barrier material and periodontal regeneration. *J Clin Periodontol* **23**, 1039-46.
- Farina R, Simonelli A, Rizzi A, Pramstraller M, Cucchi A, Trombelli L. (2013) Early postoperative healing following buccal single flap approach to access intraosseous periodontal defects. *Clin Oral Investig* **17**, 1573-83.
- Heijl L. (1997) Periodontal regeneration with enamel matrix derivative in one human experimental defect. A case report. *J Clin Periodontol* **24**, 693-6.
- Kornman KS, Robertson PB. (2000) Fundamental principles affecting the outcomes of therapy for osseous lesions. *Periodontol 2000* **22**, 22-43.
- Machtei EE, Cho MI, Dunford R, Norderyd J, Zambon JJ, Genco RJ. (1994) Clinical, microbiological, and histological factors which influence the success of regenerative periodontal therapy. *Journal of Periodontology* **65**, 154-61.
- Nyman S, Lindhe J, Karring T, Rylander H. (1982) New attachment following surgical treatment of human periodontal disease. *J Clin Periodontol* **9**, 290-6.
- O’Leary, T. J., Drake, R. B., & Naylor, J. E. (1972). The plaque control record. *Journal of Periodontology*, 43, 38.
- Papapanou, P. N., & Tonetti, M. S. (2000). Diagnosis and epidemiology of periodontal osseous lesions. *Periodontology 2000*, 22, 8–21.
- Sanz M, Tonetti MS, Zabalegui I, Sicilia A, Blanco J, Rebelo H, et al. (2004) Treatment of intrabony defects with enamel matrix proteins or barrier membranes: results from a multicenter practice-based clinical trial. *Journal of Periodontology*, 75:726-33.

- Sculean A, Donos N, Windisch P, Brex M, Gera I, Reich E, Karring T. (1999) Healing of human intrabony defects following treatment with enamel matrix proteins or guided tissue regeneration. *J Periodontal Res* **34**, 310-22.
- Takei HH, Han TJ, Carranza FA Jr, Kenney EB, Lekovic V. (1985) Flap technique for periodontal bone implants. Papilla preservation technique. *Journal of Periodontology* **56**, 204-10.
- Tibbetts LS, Shanelec D. (1998) Periodontal microsurgery. *Dent Clin North Am* **42**, 339-59.
- Tonetti MS, Pini-Prato G, Cortellini P. (1993) Periodontal regeneration of human intrabony defects. IV. Determinants of healing response. *Journal of Periodontology* **64**, 934-40.
- Tonetti, M. S., Lang, N. P., Cortellini, P., Suvan, J. E., Adriaens, P., Dubravec, D., Wallkamm, B. (2002). Enamel matrix proteins in the regenerative therapy of deep intrabony defects. A multicenter randomized controlled clinical trial. *Journal of Clinical Periodontology*, **29**, 317–325.
- Trombelli L, Farina R, Franceschetti G, Calura G. (2009) Single-flap approach with buccal access in periodontal reconstructive procedures. *Journal of Periodontology* **80**, 353-60.
- Trombelli L, Simonelli A, Pramstraller M, Wikesjö UM, Farina R. (2010) Single flap approach with and without guided tissue regeneration and a hydroxyapatite biomaterial in the management of intraosseous periodontal defects. *Journal of Periodontology* **81**:1256-1263.

Corresponding Author:

Dr. Serhat Aslan

E-mail: dr.serhataaslan@gmail.com

Figure 1. Representative case treated with the entire papilla preservation technique (EPP group) without regenerative materials. (a) Ten mm preoperative probing depth at the distal side of the maxillary left lateral incisor. (b) Interdental tunnel preparation by undermining the defect-associated papilla. Note the elasticity of alveolar mucosa and full access to the defect area by the help of a single vertical incision. (c) Defect measurement with UNC-15 periodontal probe. (d) After the application of 24% EDTA gel, bleeding from residual bone walls. (e) Primary closure of surgical area following the blood clot formation using microsurgical knots and intact interdental papilla. (f) 14 days after the surgery. (g) Excellent wound healing and integrity of defect-associated interdental papilla. (h) The 1-year photograph shows a 3 mm of residual probing depth and a CAL gain of 7 mm. No gingival recession occurred (i) Baseline radiograph. (j) 1-year radiograph.



Table 1. Patient characteristics and clinical parameters measured at baseline.

	EPP EMD+BS (N=15)	EPP (N=15)	Significance (<i>p</i>)
Gender (female/ male)	5/ 10	7/ 8	0.456
Age (mean ± SD)	44.93 ± 13.06	43.93 ± 12.85	0.755
Tooth type (<i>incisor/ canine/ premolar/ molar</i>)	10/ 1/ 2 / 2	6/ 1/ 4/ 4	0.263
FMPS (%)	13.93 ± 2.31	13.13 ± 1.55	0.517
FMBS (%)	9.4 ± 1.95	10.2 ± 1.32	0.452
PD (mm)	9.33 ± 2.87	9.26 ± 1.65	0.409
CAL (mm)	11.66 ± 3.45	11.4 ± 2.17	0.690
REC (mm)	2.33 ± 1.23	2.13 ± 1.12	0.697
INFRA (mm)	6.63 ± 2.74	6.7 ± 1.62	0.329
Intrabony width (mm)	3.08 ± 0.81	3.04 ± 0.63	0.901
CEJ-BD (mm)	12.8 ± 3.5	12.48 ± 2.12	0.648
X-ray angle (deg.)	28.8 ± 8.76	29.33 ± 9.48	0.874
Main defect configuration (-1/ -2/ -3 wall)	0/ 13/ 2	0/ 14/ 1	1

FMPS, full-mouth plaque score; FMBS, full-mouth bleeding score; PD, probing depth; CAL, clinical attachment level; REC; gingival recession; INFRA, depth of the intrabony component of the defect; CEJ-BD, cemento-enamel junction and the bottom of the defect; Intrabony width, horizontal distance from the root surface to the alveolar bone crest.

Table 2. Clinical outcomes at baseline and 1-year after treatment.

Parameter	Baseline	1-year	Change	<i>p</i>
CAL				
EPP EMD+BS	11.66 ± 3.45	5.36 ± 1.85	6.3 ± 2.5	<0.001
EPP	11.4 ± 2.17	5.56 ± 1.74	5.83 ± 1.12	<0.001
<i>p</i>	0.690	0.6	0.983	
PD				
EPP EMD+BS	9.33 ± 2.87	2.83 ± 0.74	6.5 ± 2.65	<0.001
EPP	9.26 ± 1.65	3.06 ± 0.79	6.2 ± 1.33	<0.001
<i>p</i>	0.409	0.404	0.866	
REC				
EPP EMD+BS	2.33 ± 1.23	2.53 ± 1.36	-0.2 ± 0.25	0.14
EPP	2.13 ± 1.12	2.5 ± 1.4	-0.36 ± 0.54	0.14
<i>p</i>	0.697	0.932	0.523	

CAL, clinical attachment level; PD, probing depth; REC; gingival recession.

Table 3. Surgery-related outcomes.

	EPP EMD+BS(N=15)	EPP (N=15)	Significance (<i>p</i>)
Time	65.4 ± 10.94	55.07 ± 7.86	<0.01
Hardship (VAS)	18.33 ± 6.17	17.67 ± 5.62	0.812
Pain intensity (VAS)	9.33 ± 9.03	8.33 ± 9.38	0.757
Painkiller tablets (n)	0.87 ± 0.74	0.73 ± 0.88	0.296
Post-operative discomfort (n)	2 (13.3%)	1 (6.7%)	1
Post-operative pain (n)	1 (6.7%)	1 (6.7%)	1

Time, chair-time measured from delivery of anesthesia to completion of the surgical procedures, in minutes; Hardship, personal opinion of the patient for the hardship of the procedure, in 100 mm VAS scale; Painkillers, the number of pain killers taken in addition to the 2 compulsory ones delivered after the surgery; Post-operative discomfort and pain, as questioned at 1-week recall visit; the intensity of pain measured with VAS scale.

COMPARISON OF DIFFERENT CHEMICAL AND MECHANICAL DECONTAMINATION MODALITIES ON TITANIUM DENTAL IMPLANTS: MICROBIOLOGICAL AND BIOCOMPATIBILITY ANALYSES

Citterio F.^{1,§}, Zanotto E.^{2,§}, Pellegrini G.³, Annaratone L.⁴, Bertero L.⁴, Barbui A.M.², Dellavia C.³, Aimetti M¹

¹Università di Torino, C.I.R. Dental School, Department of Periodontology, Turin, Italy

² S.C. Microbiologia e Virologia U. AO Città della Salute e della Scienza di Torino, Turin, Italy

³ Dept. of Biomedical Surgical and Dental Sciences, Università degli Studi di Milano, Milan, Italy

⁴ Dipartimento di Scienze Mediche, Anatomia Patologica, Università degli Studi di Torino, Turin, Italy

§ contributed equally to this research

Abstract

The aim of this *in vitro* study was to evaluate the efficacy of chemical and mechanical methods used for decontamination of titanium dental implants previously infected with polymicrobial biofilms in a model simulating a peri-implant defect. Furthermore, the effect of each decontamination protocol on MG-63 cells morphology and adhesion to the treated implants was assessed. A polymicrobial biofilm has been grown on 40 implants. Before treatment the implants were placed into a model simulating a peri-implant defect. Implants were randomly assigned to 5 treatment groups: 1) no treatment, 2) air-abrasion without any powder, 3) air-abrasion with powder of erythritol, amorphous silica and 0.3% chlorhexidine (ESC), 4) a sulfonic/sulfuric acid solution alone (HBX), or 5) a combination of ESC and HBX (ESC+HBX). From 5 implants per group the remaining colonies were counted (as log₁₀CFU/mL) for each bacterial strain and for the total number of colonies. The remaining 3 implants per group and 3 non-contaminated implants were used to assess biocompatibility after treatment. A significant decontaminant effect was achieved using the HBX alone or in combination with ESC while no differences were shown between the groups receiving other treatments. Moreover treatments with HBX were able to reduce the contamination of the implants to a level that didn't interfere with MG-63 regrowth.

Introduction

The main cause of peri-implant diseases is bacteria (1,2). Therefore the treatment of these diseases is targeted on effective removal of the microbial biofilm (3). Peri-implant mucositis and incipient forms of peri-implantitis might be treated by non-surgical debridement. Anyway, more severe forms of peri-implantitis often require additional therapy, since the morphology of the fixture offers macroscopic and microscopic repair to bacterial cells harbored on the surface and the results of non-surgical treatment of such conditions is usually unpredictable.

A variety of chemical and/or mechanical methods have been tested for treatment of implant surface, but none was found to be superior to others (4). A recent systematic review (5) showed that air powder abrasion with glycine powder may result in better clinical outcome than other approaches, even if complete resolution of the disease was still unlikely. Air powder abrasion has shown some advantages in terms of biofilm removal in some *in vitro* experiments when compared to other treatment approaches (6). However, complete surface cleaning is not achievable irrespective of the surgical or non-surgical approach (7,8). For this reason a combination of mechanical and chemical methods has been claimed to provide

better results. In recent years, new approaches have been proposed to treat biofilm-induced diseases. A novel topical sulfonic/sulfuric acid (HBX) solution has been developed. The sulfate components strongly absorb water from vital organic biofilm components. The result is a coagulation of the entire biofilm matrix that i) destroys its attachment mechanisms to the underlying tissues, and ii) kills bacterial cells (12). Up to now, the use of HBX alone or in combination with air powder abrasion has shown promising results for the non-surgical treatment of acute periodontal abscesses and peri-implantitis (13,14,15).

Another important aspect of implant surface decontamination is the effect of treatment modalities on the surface topography and chemical composition that may impair the re-osseointegration. Sodium bicarbonate or a powder composed of erythritol, amorphous silica and 0.3% chlorhexidine (ESC) have been demonstrated effective to remove biofilm from rough implant surfaces without interfering with osteoblast growth over the previously contaminated titanium surface (9-11) whilst chemicals such as chlorhexidine (CHX) and citric acid (CA) has been proven to adversely affect cellular regrowth after treatment.

For these reasons, the aim of this study was the evaluation of the decontamination potential of HBX application followed by air-abrasion with ESC powder on previously biofilm-contaminated implants in terms of residual viable bacterial load measured in log₁₀CFU/ in comparison with the treatment with HBX alone, ESC alone, with air-abrasion without any powder and no treatment. Furthermore, the effect of each decontamination protocol on MG-63 cells morphology and adhesion to the treated implants was assessed.

Materials and Methods

Forty-three sterile dental implants (OSSEOTITE® CERTAIN™ IOS IMPLANT 4.00mm x 11.50 mm; BIOMET 3i LLC, Palm Beach Garden, FL, USA), were included into the study.

Implants contamination

A polymicrobial biofilm has been grown on 40 implants. In order to develop a vial polymicrobial biofilm *in vitro* the following bacteria have been obtained commercially and used:

- *Staphylococcus aureus* (ATCC25923)
- *Staphylococcus epidermidis* (ATCC49461)
- *Streptococcus anginosus* (ATCC33397)
- *Streptococcus salivarius* (ATCC13419)
- *Streptococcus mitis* (ATCC9811)
- *Fusobacterium nucleatum* (ATCC10953)
- *Capnocytophaga ochracea* (ATCC27872)

Whole unstimulated saliva was collected from 10 periodontally healthy volunteers. Subjects who used antibiotics in the previous two weeks have been excluded from the donors. Saliva has then been pooled, aliquoted and stored at -20°C.

Biofilm has been grown on 40 dental implants (BIOMET 3i LLC, Palm Beach Garden, FL, USA) in medium consisting of 60% of whole unstimulated saliva and 40% brain heart infusion (BHI). In brief, each bacterial strain has been separately cultured on CDC ANAEROBE +5% SB plates for 48h at 37°C in CO₂ (*S. aureus*, *S. epidermidis*, *S. anginosus*, *S. salivarius*, *S. mitis* e *C. ochracea*) or in anaerobic conditions (*F. nucleatum*). Then, a bacterial suspension 4 McF (1200 X 10⁶ CFU/ml) in BHI has been prepared. Saliva aliquots were defrosted and the bacteria contained in it were identified by mean of the MALDI-TOF (Matrix Assisted Laser Desorption Ionization – Time of Fly).

Forty dental implants have been then incubated in 3ml of defrosted pooled saliva in anaerobic conditions at room temperature for 4h, in order to promote the formation of the *acquired pellicle* (16). Next, saliva has been substituted with 1.8ml of defrosted pooled saliva, 1.2ml of BHI and 602ml of mixed bacterial suspension (86µl of suspension 4 McF per each strain) that has been removed and renewed 16h after. At 40h the implants have been washed and the culture medium renewed. Incubated dental implants had been repeatedly washed with sterile saline after 16h, 20h, 24h, 40h, 44h, 48h and 64h. Total time of anaerobic incubation was 64h at 37.0 °C.

Model of peri-implantitis defect

A model that simulated a crater-like peri-implant defect was created by the mean of an aluminum hemisphere of 1 cm of diameter inserted into dental impression material (EliteHD+ Putty Normal Set; Zermack, Badia Polesine Italy) contained into a squared plastic box. Implants were then placed into the model that simulated a peri-implant defect with a 5mm deep intrabony, crater-like component and a 5mm deep suprabony component.

Implants decontamination

Fourty contaminated implants were randomly assigned to five different groups including 4 decontaminating procedures and 1 control group by the use of a computer generated random sequence of numbers (SPSS 24.0; SPSS Inc., Chicago, IL, USA) :

- Group ESC: air powder abrasion with ESC alone (Air- Flow Master®, E.M.S. Electro Medical Systems GmbH, Munich, Germany; Air-Flow® Plus Sub+Supragingival, E.M.S. Electro Medical Systems GmbH, Munich, Germany);
- Group HBX: HBX alone (EPIEN MEDICAL, Saint Paul, MN, USA);
- Group HBX+ESC: combination of air powder abrasion with ESC and HBX;
- Group AW: using only a spray of air and water coming from the air abrasive device.
- Group C: no treatment

In groups ESC and HBX+ESC, air flow system was used on the dental unit and set at a static water pressure of 4.5 bar and a static air pressure of 6 bar for each specimen. Cleansing time was set at 120 seconds per implant with circumferential movements going all around the implant surface. Efforts were made in order to maintain the spray as perpendicular to the implant long axis as possible.

In groups EBX and HBX+ESC, HBX was applied for 20 seconds to the implant surface proceeding from the most apical part of the defect to the most coronal part of it with circular movements. When the treatment procedure was the combination of ESC and HBX, the latter was applied before the ESC. At the end of the treatment procedures all the implants, including those of group C, were gently rinsed for 60 seconds with sterile saline solution.

Microbiological tests

Quantification of viable bacterial cells

After decontamination, 5 implants per group were randomly selected and were placed into 15ml Falcon tubes. They were immersed in a 0.1% dithiothreitol solution (DTT), and vortexed for 15 minutes in order to remove the residual biofilm. Then implants were removed and the DTT solution has been centrifuged for 5 minutes at 2500 rpm. The supernatant has been eliminated and the resultant cell suspension was serially diluted (10-fold). 20µl of suspended bacteria were collected and aliquots of 10µl were plated in duplicates on blood agar plates supplemented with 5% defibrinated horse blood. Per each dilution two plates were incubated anaerobically (Gas Pak, Becton, Cockeysville, USA) and the conditions were controlled with affiliated indicator strips. Other two plates were incubated aerobically both at 37°C for 48h. The resulting colonies were counted (as CFU/mL) for each bacterial strain and for the total

number of colonies. *F. nucleatum*, and *Propionibacterium acnes*, which was present in the pooled saliva, were counted on plates in anaerobic conditions. The other bacterial species were counted on the plates in aerobiosis. Only plates containing between 25 to 250 colonies were considered valid (Tomasiewicz, Hotchkiss, Reinbold, Read, & Hartman, 1980). Counts were provided according to bacterial species and total bacterial counts. All counts were then transformed into the \log_{10} CFU/ml.

Identification of bacterial cells

The identification of the bacteria grown on culture plates has been performed using the MALDI-TOF.

Biocompatibility test

The remaining 3 implants per treatment group and the 3 non-contaminated/non-treated group (group NC) (total 18 implants) were used for the biocompatibility test.

Osteoblast-like Cells regrowth on treated implants

Immediately after treatment, osteoblast-like cells (osteosarcoma cells; MG-63; ATCC® CRL-1427™; LGC Standards, Wesel, Germany) were seeded onto the top of implants. Before cells were seeded, 1.3 ml of media was placed in each micro-plate well containing the implants. Then, 150 μ l of cell suspension, adjusted to 1.5×10^5 cells/ml, were pipetted in meandering pattern above prepared specimen. The cells were cultured in Dulbecco's Modified Eagle's medium (DMEM) with 10% Fetal Bovine Serum (FBS) without phenol red and any antibiotics (to allow concomitant biofilm re-growth) at 37°C in a humidified atmosphere with 5% CO₂ for 5 days, without media changing. Cells were cultivated in tissue culture flasks (Eppendorf Italia Srl, Milan, Italy) and were split at approximately 80% of confluence by trypsin (0.05%)/EDTA (0.02%) solution (Sigma-Aldrich, Milan, Italy), stopped with DMEM containing 20% FBS, to attain an adequate number of cells.

Influence of Decontamination on MG-63 growth

In order to assess the effect of each decontamination protocol on the MG-63 morphology and adhesion to implant surface, after incubation period, samples were fixed with 2.5% glutaraldehyde in buffered saline solution, dehydrated through a graded series of alcohol, dried and observed at Scanning Electron Microscope (SEM) for morphological assessments and Backscattered Electron Microscope (BES) for semi-quantitative analysis (Jeol Nikon JCM-6000P, at 15 kV). All implants were photographed by a blind operator (GP). For each implant, (a) one photo at low magnification (20x) was taken to describe cells distribution on implant surface; (b) 6 photos at a total magnification of 55x were taken in the area where cells had been seeded to perform semi-quantitative analysis; (c) high magnification photos (440x to 1500x) were taken on few randomly selected samples to assess the cellular morphology.

The percentage of implant surface covered by adherent cells was calculated by the same blind operator (GP) on 55x photos using an image analysis system (adobe, Photoshop CS5).

Statistical analysis

In order to assess the decontaminant effect of the different treatment methods the viable CFU/ml was determined per each identified bacterial species and per the total bacteria grown on culture plates from duplicate experiments to provide stringent estimates of reliable results of CFU/ml drawn from this specific methodology. Thereafter, CFU/ml was calculated and the results were converted in the log scale to obtain a normal distribution. Inter-group log reduction was provided. The results were statistically analyzed using SPSS 24.0 (SPSS Inc., Chicago, IL, USA). Kolmogorov-Smirnov test revealed normal distribution of data ($p > 0.005$) for all groups except for group ESC ($p < 0.005$). Levene's test revealed heterogeneity of variances ($p < 0.005$). Since the variance was not homogenous, Kruskal-Wallis test was run. In order to

investigate inter-group differences pair-wise comparisons were performed. P-value was set at 0.05. The influence of decontamination treatment on cellular adhesion was analyzed by descriptive statistics. The percentage of implant surface covered by MG-63 cells was computed for all samples (n=3) of each group, then mean and standard deviation were calculated for each group.

Results

Microbiological test - Quantification of viable bacterial cells

The effect of the five different decontamination methods on the viability of the implant-associated biofilm (\log_{10} CFU/ml) is shown in **Figure 1**.

The presentation of the results is according to the type of treatments and viable \log_{10} CFU/ml. Means, medians, standard deviations, minimum, and maximum of \log_{10} CFU/ml per the total bacterial counts are presented in **Table 1**. The Kruskal-Wallis test revealed that at least one group was different from the others ($p = 0.001$). Pair-wise comparisons showed that the use of HBX and the combination of HBX + ESC were superior to group C ($p = 0.012$ and $p = 0.037$ respectively) in reducing total bacterial counts. HBX performed also better than AW ($p = 0.018$). The differences between the HBX + ESC and AW were on the threshold of statistical significance ($p = 0.056$).

The percentage reduction of total viable \log_{10} CFU/ml is reported in **Table 2**.

The MALDI-TOF identified the following bacteria in the pooled defrosted saliva: *Pseudomonas aeruginosa*, *Serratia marcescens*, *Streptococcus parasanguinis*, *Streptococcus faecalis*, *Klebsiella Oxytoca*, *Granulicatella adiacens*, *P. acnes*, and *Micrococcus luteus*. Limit of detection (LOD) was $< 1.0 \times 10^2$ CFU/ml. Limit of quantification (LOQ) was set at $< 2.5 \times 10^3$ CFU/ml. Means, medians, standard deviations, minimum, and maximum of \log_{10} CFU/ml per single species are presented in **Table 3**.

The bacteria detected on all implants of group C were *S. epidermidis*, *S. anginosus*, *S. mitis*, *S. salivarius*, *P. aeruginosa*, *S. marcescens*, and *S. parasanguinis*. Changes in terms of \log_{10} CFU/ml are presented in **Figure 2**. Treatment HBX and HBX + ESC resulted in a shift of viable CFU/ml under the LOD on all the treated implant for *S. epidermidis*, *S. anginosus*, *S. salivarius*. *S. parasanguinis* was undetectable in all the implants receiving HBX or HBX + ESC either, except for 1 implant in the group HBX + ESC, however it was under the LOQ [estimated $2.40 \log_{10}$ (CFU/ml)]. *S. mitis*, *P. aeruginosa*, and *S. marcescens* were significantly reduced, but were still detectable on the majority of the implants despite always being below the LOQ. Estimated values have been reported anyways.

Biocompatibility test - Influence of Decontamination on MG-63 morphology and adhesion

At morphological analysis at SEM, in all groups cells appeared housed on the implant surface, with clear cytoplasmic extensions that allow the between cells connection as well as the adhesion to the rough surface. No functional orientation was observed in any group.

At analysis at BES, differences between groups were found on cellular distribution. In group C and AW pictures showed spread cells distributed mainly among implant threads. In group C bacterial aggregates were visible. In group ESC cells covered homogenously the implant surface but were not densely packed. In one specimen no cell was visible. In groups HBX, HBX+ESC and NC cells were more densely packed on the implant surface. However in one specimen of group HBX, few cells covered the implant surface (**Figure 3**). Semi-quantitative analysis revealed a trend toward an increasing percentage of implant surface covered by adherent cells from group C to group HBX+ESC and NC (**Table 4**).

Conclusions

In the present *in vitro* model treatment with HBX either alone or in combination with ESC provided a significant decontaminant effect on previously contaminated implants while no differences were shown between the groups receiving other treatments. Moreover, it was observed that the percentage of implant surface covered by adherent MG-63 cells after 5 days of incubation was influenced by the treatment method. In particular the percentage of surface covered by adherent cells showed progressive increase through groups C, AW, ESC, HBX, HBX+ESC, and NC.

In recent years, the most used antimicrobial agents have been CA, CHX and hydrogen peroxide (H₂O₂). A systematic review identified CA as the most effective agent against single-species or multi-species biofilms killing up to 99.9% of bacteria (17). CA also demonstrated some potentiality in the removal of single-species biofilm from titanium surfaces (17,18). However it often does not achieve complete removal with effectiveness equivalent to those of water and saline rinses. CHX has shown good and limited bactericidal effect against early and mature biofilms, respectively, but no cleaning properties *per se* (18,19,20). H₂O₂ has a moderate to good bactericidal effect, but no obvious cleaning properties (18,19,21). Interestingly in our research, we demonstrated that HBX is able to produce a significantly greater reduction of viable bacteria compared to group C (99.99% greater bacterial load reduction). In a previous paper it was reported that 40% CA followed by PBS rinses was unable to inactivate 12-hours old bacterial biofilms formed on smooth titanium discs intraorally in humans after submerging the discs in it for 1 minute (19), probably due to the glycocalyx which protects the bacteria. On the other hand, we demonstrated that HBX followed by saline rinses was able to completely suppress *S. epidermidis*, *S. anginosus*, *S. salivarius*, and *S. parasanguinis* and reduce significantly *S. mitis*, *P. aeruginosa*, *S. marcescens* and the total viable CFU/ml also when not combined with ESC. This could be explained by the anti-biofilm properties of HBX (12).

If we take into consideration that mechanical debridement with air abrasive devices has been proven to leave consistent amount of untouched implant surface in conditions simulating a surgical access (8) we can assume that disinfection of infected titanium surfaces by mechanical means only, might not be adequate. This is in agreement with previous studies (22,23), which concluded that mechanical debridement alone was insufficient for biofilm disruption or elimination due to the complex implant surface topographies, and claimed for a combination of mechanical and chemical modalities of implant surface decontamination. In our study implant surface decontamination with ESC alone didn't differ in terms of residual viable log₁₀CFU/ml from groups receiving no treatment. This is in contrast with the conclusions of a systematic review which found the *in vitro* cleaning efficacy of air-powder abrasive devices consistent (24). In general studies using sodium bicarbonate, glycine or ESC *in vitro* reported more than 84% removal of bacteria or bacterial products irrespective of the surface type (10,25,26). Conversely, in the present research ESC failed to reduce significantly the viable counts of bacteria on implant surfaces (72.44%), probably because the model of the peri-implant defect and the screw-shaped implants impeded the direct abrasion of the biofilm from the majority of the implants surface. In fact the studies reporting promising results for air-powder abrasive were in general performed either on titanium discs (10,11,25,27) or implants outside of peri-implantitis defect model (26) where the air abrasive could easily reach the whole titanium surface. However this is not the case during clinical practice, where accessibility is a major issue.

Interestingly, we found no differences in terms of residual viable log₁₀CFU/ml between AW and ESC. This is in contrast with the findings of two *in vitro* studies performed on titanium discs (27,28), which demonstrated that the use of an air abrasive device without

powder (only water) resulted in significantly less biofilm removal compared with the use of the same device with different powders. A possible explanation for this difference resides again in the limited accessibility for the powder to the implant surface due to the peri-implant defect model and/or the implant macrostructure.

Within the limitation of this study it has been demonstrated that different treatment modalities have different impacts on the MG-63 cells proliferation. Semi-quantitative analysis showed HBX alone or in combination with ESC may reduce the bacterial load to an extent, which may render the previously contaminated implant surfaces as biocompatible as the non-contaminated controls. Conversely, treatment with AW or ESC showed a percentage of covered implant surface which was lower. This is in line with the results obtained in the first part of the experiment, where it was demonstrated that neither AW or ESC were able to significantly reduce the bacterial load on contaminated implants. Schwarz et al. (29) previously observed that the plaque removal efficacy of various mechanical methods used for the treatment of peri-implantitis failed to predict the biologic response of decontaminated titanium surfaces and did not restore their biocompatibility. This may be partially in contrast with the findings of the present study in which it may be observed that the detoxification potential of the treatment modalities is directly related to the cellular growth close to the implants.

We observed that HBX didn't prevent osteoblast-like cells to recolonize the implant surface. This is different from previous reports on other chemical decontaminants such as CHX or CA. Kotsakis et al. (30) showed that CA and CHX has cytotoxic activity, and cellular growth was inhibited in the CHX group compared to non contaminated controls. CA has been demonstrated to possess a transient inhibitory effect of on osteoblastic cell proliferation that last for approximately 5 days (31). In the present study it was observed that in the groups that received HBX cellular morphology was not altered and may be related to no or limited cytotoxic activity by HBX. This is further confirmed by the tests for cytotoxicity using the ISO Agarose Overlay with L-929 Mouse Fibroblast Cells method performed with HBX when it was considered to be non-toxic under the conditions of that test.

In conclusion, within the specific conditions and limitations of this *in vitro* study, it has been demonstrated that, despite the limited accessibility due to the model simulating the peri-implant Class Ie defect, a significant decontaminant effect on the moderately rough implants involved in this study was achieved using the sulfonic/sulfuric acid solution in gel while no differences were shown between the groups receiving other treatments. Moreover treatment with HBX and the combination treatment with HBX and ESC were able to reduce the contamination of the implants to a level that didn't interfere with MG-63 cells growth on the decontaminated implants. These findings prompt further investigations on dental implants decontamination using chemical decontamination. Combination of physical and chemical therapy may provide more predictable results in the future.

Bibliography

1. Lindhe J, Meyle J, Group D of European Workshop on Periodontology. Peri-implant diseases: Consensus Report of the Sixth European Workshop on Periodontology. Blackwell Publishing Ltd; 2008. pp. 282–5.
2. Pontoriero R, Tonelli MP, Carnevale G, Mombelli A, Nyman SR, Lang NP. Experimentally induced peri-implant mucositis. A clinical study in humans. *Clinical Oral Implants Research*. 1994 Dec;5(4):254–9.
3. Figuro E, Graziani F, Sanz I, Herrera D, Sanz M. Management of peri-implant mucositis and peri-implantitis. *Periodontology 2000*. 2014 Oct;66(1):255–73.
4. Claffey N, Clarke E, Polyzois I, Renvert S. Surgical treatment of peri-implantitis. *J Clin Periodontol*. Blackwell Publishing Ltd; 2008 Sep;35(8 Suppl):316–32.

5. Schwarz F, Becker K, Renvert S. Efficacy of air polishing for the non-surgical treatment of peri-implant diseases: a systematic review. *J Clin Periodontol.* 2015 Oct 16;42(10):951–9.
6. Augthun M, Tinschert J, Huber A. In vitro studies on the effect of cleaning methods on different implant surfaces. *Journal of Periodontology.* 1998 Aug;69(8):857–64.
7. Ronay V, Merlini A, Attin T, Schmidlin PR, Sahrman P. In vitro cleaning potential of three implant debridement methods. Simulation of the non-surgical approach. *Clinical Oral Implants Research.* 2016 Jan 22;:n/a–n/a.
8. Sahrman P, Ronay V, Hofer D, Attin T, Jung RE, Schmidlin PR. In vitro cleaning potential of three different implant debridement methods. *Clinical Oral Implants Research.* 2015 Mar;26(3):314–9.
9. Louropoulou A, Slot DE, Van der Weijden F. Influence of mechanical instruments on the biocompatibility of titanium dental implants surfaces: a systematic review. *Clinical Oral Implants Research.* 2014 Mar 19;26(7):841–50.
10. Schwarz F, Ferrari D, Popovski K, Hartig B, Becker J. Influence of different air-abrasive powders on cell viability at biologically contaminated titanium dental implants surfaces. *J Biomed Mater Res Part B Appl Biomater.* Wiley Subscription Services, Inc., A Wiley Company; 2009 Jan;88(1):83–91.
11. Matthes R, Duske K, Kebede TG, Pink C, Schlüter R, Woedtke von T, et al. Osteoblast growth, after cleaning of biofilm-covered titanium discs with air-polishing and cold plasma. *J Clin Periodontol.* 5 ed. 2017 Jun;44(6):672–80.
12. Bracke J, Basara M. EPIEN Medical Technical Bulletin. The Global Opportunity for HYBENX® Technology to Reduce Pathogenic Biofilm. 2015 Dec pp. 1–4.
13. Pini-Prato G, Magnani C, Rotundo R. Nonsurgical Treatment of Peri-implantitis Using the Biofilm Decontamination Approach: A Case Report Study. *The International journal of ...* 2015.
14. Pini Prato G, Magnani C, Rotundo R. Treatment of Acute Periodontal Abscesses Using the Biofilm Decontamination Approach: A Case Report Study. *Int J Periodontics Restorative Dent.* 2016 Jan;36(1):55–63.
15. Lombardo G, Signoretto C, Corrocher G. A topical desiccant agent in association with ultrasonic debridement in the initial treatment of chronic periodontitis: a clinical and microbiological study. *The new ...* 2015.
16. Leonhardt A, Olsson J, Dahlén G. Bacterial colonization on titanium, hydroxyapatite, and amalgam surfaces in vivo. *Journal of Dental Research.* 1995 Sep;74(9):1607–12.
17. Ntrouka VI, Slot DE, Louropoulou A, Van der Weijden F. The effect of chemotherapeutic agents on contaminated titanium surfaces: a systematic review. *Clinical Oral Implants Research.* Blackwell Publishing Ltd; 2011 Jul;22(7):681–90.
18. Ntrouka V, Hoogenkamp M, Zaura E, Van der Weijden F. The effect of chemotherapeutic agents on titanium-adherent biofilms. *Clinical Oral Implants Research.* Blackwell Publishing Ltd; 2011 Nov;22(11):1227–34.
19. Gosau M, Hahnel S, Schwarz F, Gerlach T, Reichert TE, Bürgers R. Effect of six different peri-implantitis disinfection methods on in vivo human oral biofilm. *Clinical Oral Implants Research.* Blackwell Publishing Ltd; 2010 Aug;21(8):866–72.
20. Dostie S, Alkadi LT, Owen G, Bi J, Shen Y, Haapasalo M, et al. Chemotherapeutic decontamination of dental implants colonized by mature multispecies oral biofilm. *J Clin Periodontol.* 2017 Mar 6;44(4):403–9.
21. Mouhyi J, Sennerby L, Wennerberg A, Louette P, Dourov N, Van Reck J. Re-establishment of the atomic composition and the oxide structure of contaminated titanium surfaces by means of carbon dioxide laser and hydrogen peroxide: an in vitro study. *Clin Implant Dent Relat Res.* 2000;2(4):190–202.

22. Karring ES, Stavropoulos A, Ellegaard B, Karring T. Treatment of peri-implantitis by the Vector system. *Clinical Oral Implants Research*. 2005 Jun;16(3):288–93.
23. Schwarz F, Sculean A, Romanos G, Herten M, Horn N, Scherbaum W, et al. Influence of different treatment approaches on the removal of early plaque biofilms and the viability of SAOS2 osteoblasts grown on titanium implants. *Clin Oral Investig*. Springer-Verlag; 2005 Jun;9(2):111–7.
24. Louropoulou A, Slot DE, Weijden F. The effects of mechanical instruments on contaminated titanium dental implant surfaces: a systematic review. *Clinical Oral Implants Research*. 2013 Jul 8;25(10):1149–60.
25. Nemer Vieira LF, Lopes de Chaves e Mello Dias EC, Cardoso ES, Machado SJ, Pereira da Silva C, Vidigal GM Jr. Effectiveness of Implant Surface Decontamination Using a High-Pressure Sodium Bicarbonate Protocol. *Implant Dent*. 2012 Oct;21(5):390–3.
26. Dennison DK, Huerzeler MB, Quinones C, Caffesse RG. Contaminated implant surfaces: an in vitro comparison of implant surface coating and treatment modalities for decontamination. *Journal of Periodontology*. 1994 Oct;65(10):942–8.
27. Drago L, Del Fabbro M, Bortolin M, Vassena C, De Vecchi E, Taschieri S. Biofilm removal and antimicrobial activity of two different air-polishing powders: an in vitro study. *Journal of Periodontology*. American Academy of Periodontology; 2014 Nov;85(11):e363–9.
28. Tastepe CS, Liu Y, Visscher CM, Wismeijer D. Cleaning and modification of intraorally contaminated titanium discs with calcium phosphate powder abrasive treatment. *Clinical Oral Implants Research*. 2013 Nov;24(11):1238–46.
29. Schwarz F, Nuesry E, Bieling K, Herten M, Becker J. Influence of an erbium, chromium-doped yttrium, scandium, gallium, and garnet (Er,Cr:YSGG) laser on the reestablishment of the biocompatibility of contaminated titanium implant surfaces. *Journal of Periodontology*. 2006 Nov;77(11):1820–7.
30. Kotsakis GA, Barbosa CLJ, Lill K, Chen R, Rudney L, Aparicio C. Antimicrobial Agents Used in the Treatment of Peri-Implantitis Alter the Physicochemistry and Cytocompatibility of Titanium Surfaces. *Journal of Periodontology*. 2016 Jul; 87(7):809-19
31. Guimarães LF, Fidalgo TKDS, Menezes GC, Primo LG, Costa e Silva-Filho F. Effects of citric acid on cultured human osteoblastic cells. *Oral Surg Oral Med Oral Pathol Oral Radiol Endod*. 2010 Nov;110(5):665–9.

Corresponding Author:

Dr Filippo Citterio

E-mail: filippocitterio89@gmail.com

Figure 1. Total viable log₁₀(CFU/ml) in the five treatment groups.

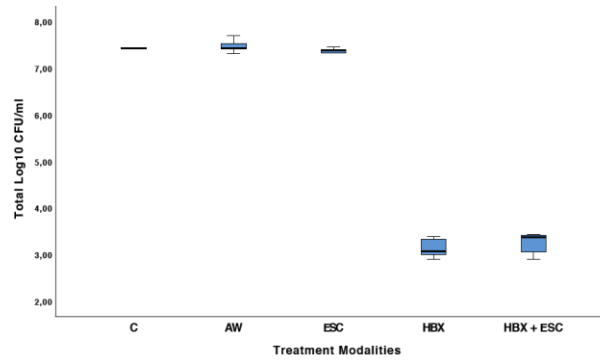


Figure 2. Changes in terms of log₁₀ CFU/ml of *S. epidermidis*, *S. anginosus*, *S. mitis*, *S. salivarius*, *P. aeruginosa*, *S. marcescens*, and *S. parasanguinis* in the five treatment groups.

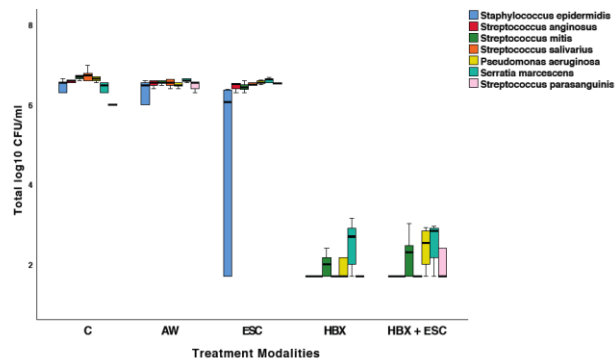


Figure 3. 55x microphotographs of the implants from different experimental groups

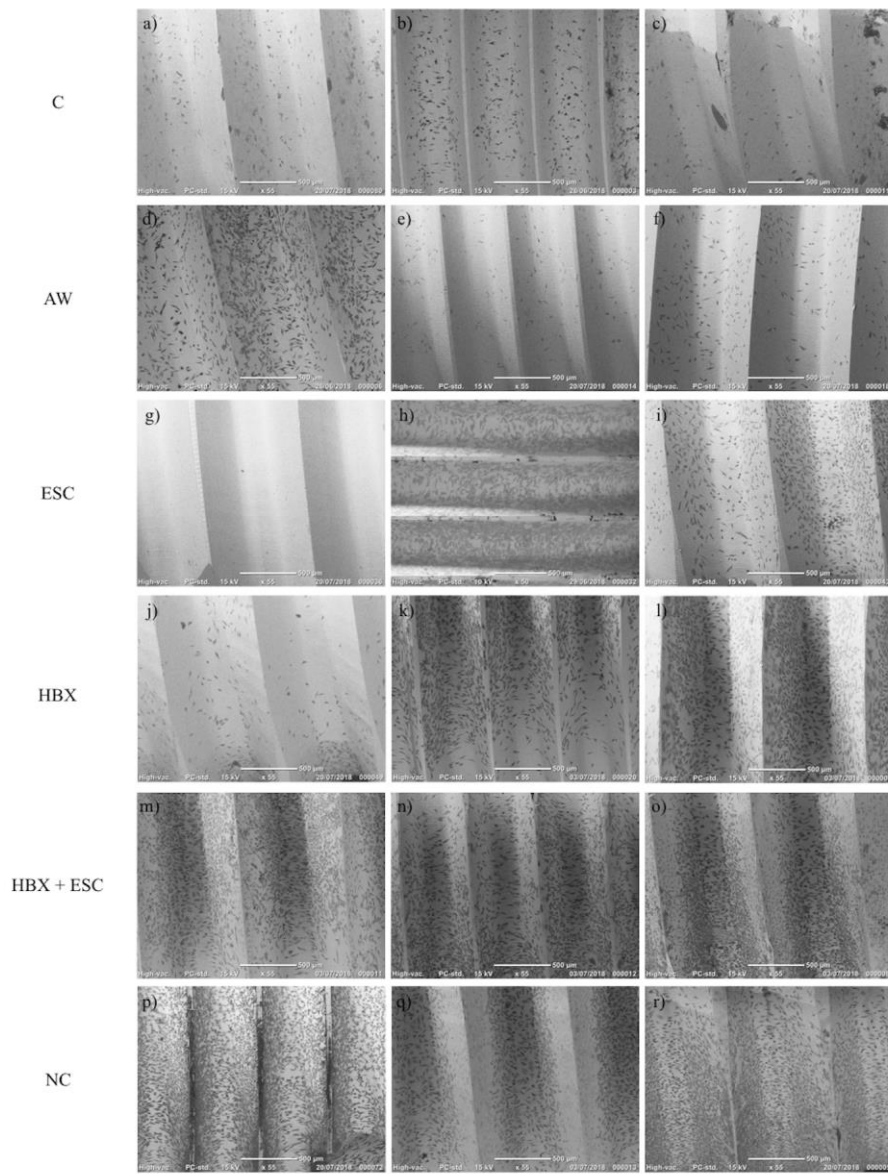


Table 1 - Mean, median, standard deviation, minimum, and maximum of total viable log₁₀(CFU/ml) in the five treatment modalities

Treatment modality	Mean	Median	St. Dev.	Min	Max
C ^{a,c}	7.48	7.43	.12	7.41	7.69
AW ^b	7.48	7.43	.15	7.31	7.70
ESC	7.34	7.38	.10	7.18	7.45
HBX ^{a,b}	3.14	3.08	.21	2,90	3.39
HBX + ESC ^c	3.23	3.38	.24	2.90	3.43

^a, p = 0.012; ^b, p = 0.018; ^c, p = 0.037

Table 2 – Logarithmic reduction and percentage reduction of total viable log₁₀(CFU/ml) in the treatment modalities compared to group C

Treatment modality	Log reduction	Percentage (%)
C	-	-
AW	0	0
ESC	0.14	72.44
HBX	4.34	99.99
HBX + ESC	4.25	99.99

Table 3

Table 3 – Mean \pm standard deviation viable \log_{10} (CFU/ml) in the five treatment modalities for each bacterial species.

Bacterial Species	C	AW	ESC	HBX	HBX + ESC
<i>S. aureus</i>	4.28 \pm 2.37	3.54 \pm 2.52	2.62 \pm 2.06	< 2.00	< 2.00
<i>S. epidermidis</i>	6.47 \pm 0.16 ^a	5.46 \pm 2.12	4.44 \pm 2.50	< 2.00 ^a	< 2.00 ^a
<i>S. anginosus</i>	6.61 \pm 1.00 ^b	6.53 \pm 0.08 ^c	6.46 \pm 0.11	< 2.00 ^{b;c}	< 2.00 ^{b;c}
<i>S. mitis/oralis</i>	6.72 \pm 0.13 ^{b;e}	6.63 \pm 0.20 ^d	6.44 \pm 0.11	1.99 \pm 0.30 ^{b;d}	2.24 \pm 0.56 ^e
<i>S. salivarius</i>	6.74 \pm 0.15 ^f	6.60 \pm 0.22	6.47 \pm 0.19	< 2.00 ^f	< 2.00 ^f
<i>F. nucleatum</i>	2.59 \pm 2.00	3.55 \pm 2.54	2.64 \pm 2.10	< 2.00	< 2.00
<i>C. ochracea</i>	2.62 \pm 2.06	2.62 \pm 2.06	< 2.00	< 2.00	< 2.00
<i>P. aeruginosa</i>	6.71 \pm 0.20 ^{b;h}	6.56 \pm 0.20	6.56 \pm 0.05 ^g	2.03 \pm 0.53 ^{b;g}	2.40 \pm 0.54 ^h
<i>S. marcescens</i>	6.62 \pm 0.27	6.66 \pm 0.14 ^{j;k}	6.57 \pm 0.12 ⁱ	2.49 \pm 0.62 ^{ij}	2.52 \pm 0.56 ^k
<i>S. parasanguinis</i>	6.08 \pm 0.18	6.55 \pm 0.25 ^{l;m}	6.59 \pm 0.14 ^{f;n}	< 2.00 ^{f;l}	1.98 \pm 0.38 ^{m;n}
<i>S. faecalis</i>	2.56 \pm 1.92	3.48 \pm 2.44	< 2.00	< 2.00	< 2.00
<i>K. oxytoca</i>	2.56 \pm 1.92	3.48 \pm 2.44	< 2.00	< 2.00	< 2.00
<i>G. adiacens</i>	< 2.00	3.45 \pm 2.40	< 2.00	< 2.00	< 2.00
<i>P. acnes</i>	< 2.00	< 2.00	< 2.00	< 2.00	< 2.00
<i>M. luteus</i>	< 2.00	2.56 \pm 1.92	< 2.00	< 2.00	< 2.00

^a, p = 0.019; ^b, p = 0.003; ^c, p = 0.047; ^d, p = 0.039; ^e, p = 0.008; ^f, p = 0.004; ^g, p = 0.044; ^h, p = 0.017; ⁱ, p = 0.045; ^j, p = 0.019; ^k, p = 0.022; ^l, p = 0.006; ^m, p = 0.029; ⁿ, p = 0.020.

Table 4

Table 4 - Mean and standard deviation of the percentage of implant surface covered by MG-63 cells in the 5 different treatment groups and in the non-contaminated implants

Treatment Modality	Mean	St.Dev
C	7,41%	4,75%
AW	12,41%	4,38%
ESC	24,11%	6,72%
HBX	33,55%	11,33%
HBX + ESC	51,69%	9,55%
NC	60,13%	9,34%

THE EFFECT OF IMMEDIATE IMPLANT PLACEMENT ON ALVEOLAR RIDGE PRESERVATION: RADIOGRAPHIC RESULTS OF A RANDOMIZED CONTROLLED CLINICAL TRIAL COMPARING THESE TWO TREATMENT MODALITIES AND NATURAL HEALING AFTER TOOTH EXTRACTION

Clementini Marco ⁽¹⁾, **Agostinelli Agnese** ⁽¹⁾, **Castelluzzo Walter** ⁽¹⁾, **Cugnata Federica** ⁽²⁾,
Vignoletti Fabio ⁽¹⁾, **de Sanctis Massimo** ⁽¹⁾

(1) Department of Periodontology, Università Vita-Salute San Raffaele, Milan, Italy

(2) University Centre of Statistics for Biomedical Sciences (CUSBS), Università Vita-Salute San Raffaele, Milan, Italy

Keywords: tooth extraction; alveolar ridge preservation; immediate implant placement; radiographic changes; CBCT

Conflict of interest and source of funding statement

The authors report no conflict of interests related to the study. The project (14-034) was supported by a grant from the Osteology Foundation, Switzerland.

Acknowledgements

The authors would like to thank Dr. Lucrezia Paterno' Holtzman for review of the English language.

ClinicalTrials.gov ID: NCT03422458

ABSTRACT

Aim: to radiographically evaluate the effect of simultaneous implant placement plus alveolar ridge preservation (ARP) as compared to ARP or spontaneous healing (SH) on vertical and horizontal bone dimensional changes after 4 months of healing.

Materials and methods: thirty patients requiring extraction of one upper or lower single-rooted tooth or premolar were randomly assigned to: immediate implant placement +ARP (IMPL/DBBM/CM), ARP (DBBM/CM) or SH. Cone Beam Computer Tomography (CBCT) scans, performed before tooth extraction and after 4 months, were superimposed in order to assess: changes in ridge height at the buccal and lingual aspect; changes in ridge width at three levels (1mm, 3mm, 5mm)

Results: No statistically significant differences between the groups were observed for the vertical bone resorption on the buccal and the lingual side, while significant differences were found between SH group (-3.37 ± 1.55 mm.; $-43.2 \pm 25.1\%$) and both DBBM/CM (-1.56 ± 0.76 mm.; $-19.2 \pm 9.1\%$) and IMPL/DBBM/CM (-1.29 ± 0.38 mm. ; $-14.9 \pm 4.9 \%$) group in the horizontal dimension at the most coronal aspect.

Conclusion: a preservation technique, with or without immediate implant placement, reduces the horizontal bone morphological changes that occur, mostly in the coronal portion of the buccal bone plate following tooth extraction, when compared to spontaneous healing.

CLINICAL RELEVANCE

Scientific rationale for the study: no human study has ever compared simultaneous implant placement+ARP to ARP alone and to spontaneous healing. Hence, the question that remains unanswered is whether simultaneous implant placement+ARP may influence bone modelling and remodelling as compared to ARP or to spontaneous healing.

Principal findings: in the horizontal dimension at the most coronal aspect minor dimensional changes were observed in DBBM/CM and IMPL/DBBM/CM groups compared to major changes observed in SH group

Practical implications: immediate implant placement in post-extraction sites plus an ARP technique may be a viable option, to reduce hard tissue morphological changes and treatment time.

INTRODUCTION

It is well known that following the loss of a tooth, severe hard and soft-tissue alterations may take place at the affected site (Pietrokovski & Massler, 1967; Schropp et al., 2003), resulting in a subsequent reduction of both vertical and horizontal ridge dimensions (Araujo & Lindhe, 2005; Discepoli et al., 2013; Van der Weijden et al., 2009; Tan et al., 2012). In many occasions, these bone dimensional changes do not allow either appropriate pontic fabrication or correct placement of endosseous implants.

Over the past 20 years, several surgical procedures, grouped under the term of “alveolar ridge preservation” (ARP), have been introduced, aiming to maintain the existing soft and hard tissues as well as a stable ridge volume, to simplify subsequent treatment procedures and optimize functional and esthetic outcomes (Hämmerle et al., 2012). A recent controlled clinical study (Jung et al., 2013) with a 6 month follow-up evaluated different techniques for ARP. The authors concluded that the application of a demineralized bovine bone mineral (DBBM) with 10% collagen into an extraction socket, covered either with a collagen matrix or an autogenous soft tissue graft, resulted in less vertical and horizontal changes compared with spontaneous healing or the use of b-tricalcium phosphate particles alone without primary closure. Moreover, a conspicuous number of systematic reviews on this topic have confirmed the efficacy of ARP in preventing post-extraction dimensional changes of the alveolar ridge (Ten Heggler et al., 2011; Vignoletti et al., 2012; Horvath et al., 2012; Vittorini Orgeas et al., 2013; Mardas et al., 2010; MacBeth et al., 2017, Avila-Ortiz et al., 2019). However, when ARP techniques are performed before implant placement, this treatment modality requires a minimum of three to six months before implant insertion (De Risi et al., 2015, Avila-Ortiz et al., 2019), prolonging treatment time and needing a second surgical procedure for implant insertion.

Immediate implant placement (IIP) in fresh extraction sockets was introduced, in order to reduce exposure of patients to surgery and may limit physiological bone resorption (Schulte & Heimk, 1976, Lazzara et al. 1989). However, IIP may not always provide successful clinical outcomes (Lang et al., 2012, Tonetti et al., 2017) and it is well known nowadays that this surgical protocol fail to prevent the horizontal and vertical ridge alterations (Vignoletti & Sanz, 2014, Vignoletti et al., 2012; Araujo et al., 2005). This may result in impaired esthetics (Evans & Chen, 2008, Tonetti et al., 2017) such as marginal soft tissues recessions, especially when affecting the buccal side of maxillary sites in patients with a high smile line (Cosyn et al., 2012,).

In order to improve the aesthetic outcomes and attenuate the bone dimensional changes several techniques have been proposed, such as flapless protocols, immediate provisionalization, connective tissue grafting, GBR techniques or filling of the gap with a bone replacement graft (Chen & Buser, 2014). Although no consensus exists on the efficacy of regenerative techniques at the time of immediate implant placement (Clementini et al., 2015), results from a very recent clinical trial demonstrated that placing a bone replacement graft in the marginal gap between the implant and the buccal bone plate significantly reduced (approximately 0.5 mm) the horizontal dimensional changes of the buccal bone after IIP in fresh extraction sockets. (Sanz et al., 2017).

The body of evidence on the treatment of extraction sockets indicates that ARP is an effective technique to reduce the physiological bone dimensional changes that occur after tooth extraction when compared to spontaneous healing (Avila-Ortiz et al., 2019). Nevertheless, very limited human evidence is available comparing immediate implant placement to spontaneous healing. Data from pre-clinical studies demonstrated that both horizontal and vertical buccal bone resorption occurs after immediate implant placement when compared to spontaneous healing (Araujo et al., 2005), and these morphological changes seems to be more pronounced with immediate implant placement

(Discepoli et al., 2015). On the other hand, it is clinically well known that immediate implant placement alone fails to prevent the physiologic resorption of the bone crest (Botticelli et al., 2005, Clementini et al. 2015), however this process may be reduced to some extent through grafting the gap (Chen et al. 2007, Sanz et al., 2017, Clementini et al. 2015). Whether this reduction is similar to the reduction provided by ARP is still unknown, since up-to-date no human study has ever compared simultaneous implant placement+ARP to ARP alone and to spontaneous healing. Hence, the question that remains unanswered is whether simultaneous implant placement+ARP renders different results in term of radiographic bone changes as compared to ARP and spontaneous healing. Thus, the aim of this randomized controlled clinical trial was to evaluate the effect of simultaneous implant placement+ARP (test treatment) as compared to ARP (control treatment) or spontaneous healing (negative control) on bone dimensional changes after 4 months of healing post-extraction. The primary objective was to radiographically evaluate the horizontal dimensional changes in mm., whereas the secondary objective was to evaluate the horizontal dimensional changes in percentage and the vertical dimensional changes in mm. and percentage.

MATERIALS & METHODS

Study design

This study was a prospective controlled, randomized, clinical investigation according to the CONSORT statement (<http://www.consort-statement.org/>). All procedures and materials were approved by the local ethical committee (REF:14-034, 24/07/2015) and monitored following the Good Clinical Practice. The trial was registered at [http:// www.clinicaltrials.gov/](http://www.clinicaltrials.gov/) (REF: NCT03422458)

Sample size

To calculate the number of patients to be treated, summary statistics (mean and standard deviation) reported by Jung et al. (2013) were used for the variable HW-1C, respectively for the control group (mean=-3.3, sd=2) and DBBM-C/CM (mean=-1.2, sd=0.8). The effect size resulted equal to 1.4 and this value was used to determine the sample size based on a two independent sample Mann-Whitney test (two-tailed) with a significance level alpha set equal to 5% and power equal to 80%. GPower software, v. 3.1, was used. This resulted in 10 subjects for each group.

Population

Participants were selected on a consecutive basis among patients of the Dental Clinic at University Vita Salute San Raffaele, Milan, Italy between January 2016 and January 2018. Patients agreed to participate in the study by signing a written informed consent, in full accordance with the ethical principal of Declaration of Helsinki on experimentation involving human subjects, as revised in 2008.

Inclusion Criteria

- Adult patients (> 18 years old) requiring extraction (for caries, fracture, prosthetic reasons) of one upper or lower single rooted tooth (incisor, canine) or premolar.
- Presence of adjacent (mesial and/or distal) natural teeth.
- The presence of an intact extraction socket (evaluated after a flapped tooth extraction), with a coronal margin of the buccal bone crest that deviated ≤ 1 mm from the coronal margin of the lingual bone crest and ≤ 3 mm from the mesial and/or distal inter proximal bone crest (evaluated on the pre-operative CBCT).
- Systemically healthy patients not smoking more than 10 cigarettes/day.
- Patients with adequate oral hygiene (FMPS < 25%), and periodontal health (FMBS < 10% and absence of PPD > 4 mm with BoP) (Lang & Bartold, 2018).

Exclusion Criteria

- Uncontrolled diabetes (HbA1c>7), osteoporosis or any other systemic or local disease or condition that would compromise post-operative healing.

- Patients with a history of malignancy, radiotherapy, or chemotherapy for treatment of malignancy.
- Pregnant patient or intended to get pregnant or currently nursing.
- Patients taking medications or having treatments with an effect on healing in general (e.g. steroids, large doses of antiinflammatory drugs, bisphosphonates).

Randomization process and allocation concealment

Randomization was performed using a computer-generated list by someone not involved in other aspects of the study. Allocation concealment was performed by opaque continuously numbered sealed envelopes that were opened after tooth extraction and assessment of the integrity of the bone plates.

Treatment procedures

A full thickness envelope flap including the mesial and distal tooth was performed, and the tooth was extracted with great care to preserve the buccal bone plate and the surrounding soft and hard tissues. Granulation tissue was carefully removed with hand instruments and sterile saline rinses were performed. After assessment of the integrity of the bone plates, patients were randomly assigned to (**Figure 1**):

- Test group (IMPL/DBBM/CM): immediate implant placement, plus a collagenated bovine bone mineral grafted into the gap up to the buccal bone crest, sealed with a collagen porcine matrix at the soft tissue level.
- Control group (DBBM/CM): collagenated bovine bone mineral grafted into the socket up to the buccal bone crest, sealed with a collagen porcine matrix at the soft tissue level.
- Negative control group (SH): spontaneous healing.

More specifically, in IMPL/DBBM/CM group an immediate implant (TTi WINSIX®, Biosafin, Ancona, Italy) with prosthetically driven placement was performed positioning the platform 1 mm subcrestally respect to the most apical crest, in accordance with the guidelines described by the company. After implant placement and closure cap insertion, a bone substitute material (Geistlich Bio-Oss Collagen; Geistlich Pharma AG, 6110 Wolhusen, Switzerland) was placed in the gap formed between the implant surface and the hard tissue walls of the extraction socket. Grafting was performed to the level of the palatal and lingual bone crest. Subsequently, after flap replacement, the soft tissue borders were de-epithelialized and a collagen porcine matrix (Geistlich Mucograft Seal; Geistlich Pharma AG, 6110 Wolhusen, Switzerland) was adapted to seal the graft and the implant using single interrupted resorbable sutures.

In DBBM/CM group a bone substitute material (Geistlich Bio-Oss Collagen; Geistlich Pharma AG, 6110 Wolhusen, Switzerland) was placed in the extraction socket to the level of the palatal and lingual bone plate. Subsequently, after flap replacement, the soft tissue borders were de-epithelialized and a collagen matrix (Geistlich Mucograft Seal; Geistlich Pharma AG, 6110 Wolhusen, Switzerland) was adapted to seal the graft using single interrupted resorbable sutures. In SH group flap was repositioned with interrupted resorbable sutures and the coagulum within the socket was left for spontaneous healing.

Patients were instructed to rinse twice a day (starting the day after surgery) with 0.2% chlorhexidine and received antibiotics (Augmentin 1g) for 6 days and analgesic medication (Ibuprofen 600 mg) if needed. All patients were recalled at 7 days for suture removal. Patients then followed their individual maintenance program according to the individual periodontal and caries risk assessment. Four months post-extraction, all patients were recalled for a follow-up in order to schedule the following therapies.

Clinical measurements

Full-mouth plaque score (FMPS) (O’Leary, Drake, & Naylor, 1972), full-mouth bleeding score (FMBS) (Muhlemann & Son, 1971) and keratinized tissue height (KTH), measured from the most coronal extension of gingival margin to the mucogingival line, were recorded with a periodontal probe (PCP UNC 15, Hu-Friedy) at baseline and 4 months. Moreover, gingival thickness (GT) was assessed at baseline and 4 months, as described in Clementini et al. 2018. All clinical measurements were made by a single blinded calibrated examiner (A.A.).

Radiographic measurements

Before treatment procedures, a cone-beam computed tomography (CBCT) scan was performed using a 3D exam (NewTom VGi evo, QR S.r.l., Verona), following the producer's prescriptions: resolution of 0.2 mm, scan time: 15 s, exposure time: 1.8 s. After four months post-extraction, all selected patients underwent to a second CBCT scan with the same settings as described above.

To calculate CBCT measurements a similar approach as the one proposed by Jung et al. (2013) was adopted. Firstly, in the baseline data set the distance from the mesial and/or distal bone crest was calculated in the axial section, and subsequently the cross section was selected passing through the pulp canal of the involved tooth. The CBCT performed 4 months after tooth extraction was selected by the same procedure, considering the distance from the mesial and/or distal bone crest previously calculated. Then a computer-assisted (GeoGebra GmbH, Wolfauer Str 90, 4040 Linz, Austria) superimposition of the original DICOM (Digital Imaging and Communications in Medicine) data of the two CBCT scans was done in areas where no changes had taken place during the 4 months (e.g. the cranial base in the maxilla or the lower border and angle in the mandible respectively). Varying the degree of transparency of the sections, DICOM data of the two CBCT scans were manually checked in order to assure a perfect match. Finally the measurements were computed on the selected scans at baseline and at 4 months, by means of reference the following points and lines defined and drawn in the baseline image (**Figure 2**)

- Four reference points: the point representing the radiographic apex of the tooth (Apical Central Point, ACP) and the point representing the cusp of the tooth (Coronal Central Point, CCP). In cases where the crown of the tooth was missing or in cases of bicuspid, a segment was traced using 2 points (the most coronal and buccal point and the most coronal and lingual point of the tooth) and the centre of this segment was taken as the coronal reference point; two points representing respectively the most coronal buccal (Coronal Buccal Point, CBP) and the most coronal lingual (Coronal Lingual Point, CLP) portion of the buccal and lingual bone plates.
- Eleven reference lines, subsequently drawn, as follows: a vertical central line (VCL), in the center of the socket, which crosses the apical (ACP) and coronal (CCP) central reference points; a vertical buccal line (VBL) and a vertical lingual line (VLL), parallel to the VCL and crossing respectively the most coronal point of the buccal (CBP) and lingual (CLP) bone crest; the buccal bone crest line (BCL_B) and the lingual bone crest line (BCL_L) connecting respectively the most coronal point of the buccal (CBP) and lingual (CLP) bone crest and perpendicular to VCL; the horizontal lines, perpendicular to the VCL drawn in precedence at 1, 3, 5 mm and parallel to the straight lines passing through CBP (BCL_B) and CLP (BCL_L) . .

With respect to these reference points and lines, the following measurements were performed in mm.:

- thickness of the buccal and lingual bone plate at three levels (1 mm, 3mm and 5mm), only at baseline;
- vertical ridge height, measured at the buccal and lingual site, at baseline and 4 months;
- mid-buccal and mid-lingual horizontal ridge width, measured at 1 mm, 3 mm, 5 mm below respectively the CBP and CLP, at baseline and 4 months.

In addition, the following dimensional changes over time, based on the measurements performed at baseline and at 4 months, were assessed and expressed both in percentages and in mm:

- changes in ridge height at the buccal and lingual aspect;
- changes in ridge width at three levels (1mm, 3mm, 5mm) respectively of the whole ridge, from the middle of the ridge to the buccal bone crest and from the middle of the ridge to the lingual bone crest.

All superimpositions of CBCT images and measurements of morphological changes were made by a single calibrated examiner (W.C.), who superimposed and measured, 24 hours apart, baseline and 4 months CBCT images of 3 different cases not included in the study. Intraclass coefficient correlation (Bliese, 2000) was 0.9891839.

Data analysis

Descriptive statistics were provided for all the measures collected in the study. To test whether treatment groups were different, Kruskal-Wallis test, i.e., the non-parametric counterpart to standard ANOVA, followed by post-hoc analysis (Dunn's pairwise test and Bonferroni's adjustment of p-values), has been applied for comparison of differences between groups.

All the analyses were performed using R statistical software (R Development Core Team, 2016). In all the analyses, the significance threshold was set at 0.05.

RESULTS

The study population consisted of 32 subjects that were screened for participating in this clinical trial from 2015 to 2018. Of these patients, two were excluded due to a loss of buccal bone plate after tooth extraction. A total of 30 subjects were finally recruited, randomized and included in the clinical trial: 10 allocated to the SH group (negative control), 10 allocated to DBBM-CM group (control), 10 allocated to IMPL/DBBM-CM group (test), respectively. Hence, a total of 30 subjects were included in the analysis (**Figure 3**).

No significant differences between treatment groups were found at the baseline (**Table 1**) regarding age, gender, smoking status, tooth position, presence of both mesial and distal tooth, reason for extraction, FMPS, FMBS, KTH, GT, and thickness of the crest.

Clinical outcomes

All treated sites healed uneventfully, and no post-operative complications were recorded. No significant differences were assessed at 4 months follow up for FMPS, FMBS, KTH and GT in the three study groups. Slight but not significant differences were observed for KTH (-0.4 mm.) and GT (+0.35 mm.) for SH group, while no differences were observed for DBBM/CM group and IMPL/DBBM/CM group.

Radiographic outcomes

Dimensional alterations in mm. and percentage that occurred during healing for all sites are reported in **Table 2**.

Horizontal dimensional changes.

Horizontal changes were not significantly different between DBBM/CM group and IMPL/DBBM/CM group at 1 mm below the coronal crest, while significant differences were found between SH group and both DBBM/CM and IMPL/DBBM/CM group. At the most coronal aspect, ridge width decreased 3.37 ± 1.55 mm ($-43.2 \pm 25.1\%$) in the SH group, while DBBM/CM and IMPL/DBBM/CM groups presented a ridge reduction of 1.56 ± 0.76 mm ($-19.2 \pm 9.1\%$) and 1.29 ± 0.38 mm ($-14.9 \pm 4.9\%$) respectively.

Analyzing horizontal changes at the buccal (mid-buccal) and lingual (mid-lingual) aspect, significant differences were found at 1 and 3mm below the crest of the buccal side between SH group and both DBBM/CM and IMPL/DBBM/CM groups: a reduction of 2.45 ± 1.29 mm (at 1mm) and 1.92 ± 1.99 mm (at 3mm) was revealed for SH group, while a change of -0.91 ± 0.43 mm (at 1 mm.) and -0.53 ± 0.44 mm (at 3 mm.) was shown in DBBM/CM group and a change of -0.99 ± 0.21 mm (at 1 mm.) and -0.70 ± 0.33 mm (at 3 mm.) in IMPL/DBBM/CM group. Significant differences at the

lingual aspect were found at 1 mm below the crest between SH group ($-24.03 \pm 22\%$) and IMPL/DBBM/CM group ($-5.99 \pm 6.18\%$). (**Figure 4**)

Vertical changes

No statistically significant differences between the groups were observed for the vertical bone resorption on the buccal and the lingual side. (**Figure 5**).

DISCUSSION

The present study demonstrated that the insertion of an immediate implant does not affect the outcomes of the alveolar preservation technique. Even if an implant is inserted, the effectiveness of the alveolar preservation technique is guaranteed, at least in terms of linear bone reduction measured using DICOM data. Furthermore, this surgical protocol (with or without the insertion of an immediate implant) seems to limit hard tissue morphological changes that occur when an extraction site is left to heal spontaneously after a flap procedure.

Spontaneous healing

In this study a marked resorption of the alveolar ridge was observed at 4 months when this was left to heal spontaneously after a flapped procedure, revealing a horizontal change of 3.37 ± 1.55 mm ($43.2 \pm 25.1\%$) and a vertical change of 0.8 ± 1.1 mm ($12 \pm 17\%$) at the buccal aspect. These data are in agreement with those of a very recent similar radiographic study by Jung et al. (2013), in which a horizontal change of 3.3 ± 2 mm ($43.2 \pm 26.8\%$) and a vertical change of 0.5 ± 0.9 mm ($5.5 \pm 9.8\%$) at the buccal aspect was revealed after 6 months when the alveolar ridge was left to heal spontaneously after a flapless procedure.

The scientific literature has amply demonstrated in humans how, after the extraction of a tooth, significant changes occur in ridge size both horizontally and vertically (Pietrokovski & Massler, 1967; Schropp et al., 2003). A very recent systematic review demonstrated a horizontal dimensional reduction of 3.79 ± 0.23 mm. (29–63%) and a vertical bone loss at the buccal aspect of 1.24 ± 0.11 mm. (11–22%) at 6 months. (Tan et al., 2012).

In this study further analysis of mid-buccal and mid-lingual changes revealed that at 4 months vertical and horizontal resorption were more pronounced on the buccal (vertical: 0.8 ± 1.1 mm.; horizontal: 2.45 ± 1.29 mm.) than the lingual (vertical: 0.2 ± 0.3 mm.; horizontal: 0.98 ± 0.93 mm.) aspect, thus shifting the center of the crest towards a more palatal position. This observation is in agreement with preclinical studies by Araujo & Lindhe (2005), Fickl et al. (2008) and Discepoli et al. (2013) in which observed morphological changes were more significant at the buccal than the palatal/lingual aspects.

On the other hand, similarly to results from clinical trials in which radiographic analysis was performed at different levels below the alveolar crest (Jung et al., 2013; Kerr et al., 2008), this study demonstrated a relative decrease in horizontal ridge reduction as the distance from the alveolar crest increased, despite differences in the surgical method (flapped in this study, flapless in Jung et al., 2013 and Kerr et al., 2008). Different changes between the two cortices (buccal and palatal/lingual aspects) and at different heights (1-, 3-, 5mm.) below the crest may be explained by differences in thickness of the alveolar crest at baseline: although the sample size in the present study is insufficient to perform a statistical analysis, it seems that the thicker the crest the smaller the dimensional alteration. This resorption pattern may be due to the presence of bundle bone, in which the periodontal ligament fibers of a tooth invest, and which is lost following tooth extraction as it is a tooth-dependent structure. In pre-clinical studies from Araujo & Lindhe (2005) and Discepoli et al. (2013) it was observed that thin crestal regions (high resorption rate) were made up exclusively of bundle bone while the thick regions (low resorption rate) were comprised of a combination of bundle bone and lamellar bone.

Relatively large thickness of the marginal crest at baseline (buccal: 1.17 ± 0.39 mm.; lingual: 1.99 ± 1.05 mm.) and site selection (mostly premolars) may explain the discrepancy with respect to the amount of crestal resorption between this study and results from Araujo et al. (2015), in which a vertical change of 3.6 mm. (35.8%) at the buccal site and 1.4 mm. (13.4%) at the palatal site were

reported. In that article the study sample was mostly composed of anterior teeth, and further analysis of their data disclosed that the reduction in the buccal bone plate was more pronounced in the anterior than in the premolar regions. As demonstrated by Januario et al. (2011) from a radiographic study, about 50% of the coronal (5 mm) portion of the buccal bone wall in maxillary incisors and canines is <0.5 mm wide, with an average of 0.6 mm wide.

ARP

The observations in the present study established that the placement of a bone substitute material (DBBM) in the fresh extraction socket, covered by a collagen matrix, reduced vertical and horizontal ridge resorption. This is in agreement with data reported by Jung et al. (2013), in which both vertical and horizontal resorption were limited by the placement of DBBM, covered by a collagen matrix, in the fresh extraction socket, despite the fact that in that study a flapless approach was performed.

This is also in agreement with a number of recently published systematic reviews on ARP procedures (Ten Heggler et al., 2010; Vignoletti et al., 2012; Horvath et al., 2012; Vittorini Orgeas et al., 2013; Mardas et al., 2010; MacBeth et al., 2017) which conclude how no bone substitute material and/or membrane is able to completely preserve the alveolar ridge after tooth extraction, but may limit buccal plate resorption to a certain extent.

Findings from the present study revealed that mid-buccal horizontal changes 1 mm (0.91 ± 0.43 mm.), and 3 mm (0.53 ± 0.44 mm) below the marginal crest have been the ones which benefited the most from ARP procedure. This means, in agreement with Araujo et al. (2008), that graft material apparently promoted de novo hard tissue formation showing a radiographic appearance different from that of a cortical plate but maintaining the dimensions of the hard tissue wall. This is particularly true for sites made up exclusively of bundle bone, therefore regions with a very thin bone crest.

ARP + Immediate implant placement

In the present work no statistically significant difference resulted from the comparison between test group (IMPL/DBBM/CM) and control group (DBBM/CM), indicating that the preservation of bone volumes is quite similar in sites where the implant was inserted and in the sites where only ARP was performed.

When an implant was inserted simultaneously to an ARP procedure after flapped tooth extraction, horizontal mean changes at 1 mm. below the marginal crest were 1.29 ± 0.38 mm (14.9 ± 4.9 %) with changes at buccal aspect of 0.99 ± 0.21 mm (26.80 ± 7.07 %). These data are completely in agreement with a recent work by Sanz et al. (2016), aimed at evaluating differences in dimensional alterations of the ridge after 4 months between immediate implants and immediate implants associated with regenerative procedures. Reporting a bucco-lingual dimensional change (1 mm below the crest) in grafted sites of 1.3 (11%) and a reduction of the buccal cortical bone of 1.1 mm. (29%), they demonstrated that placement of DBBM in the void between the implant and the walls of the fresh extraction socket somewhat counteracted the contraction of the buccal hard tissue plate that normally occurs during healing.

Similar data were also presented in a radiographic study by Degidi et al. (2013), in which the mean reduction in the distance between implant surface and outer surface of buccal bone crest was 0.88 ± 0.51 mm (29.3%) after 1 year of a flapless immediate implant placement with simultaneous grafting of the buccal gap with DBBM and immediate restoration. Analyzing the height of the marginal buccal crest, the authors reported a mean reduction of 0.76 ± 0.96 mm., that is similar to 0.6 ± 0.4 mm. of vertical dimensional alteration obtained in this study at the buccal site when an immediate implant and an ARP procedure were simultaneously performed.

These data seems to confirm the trend towards better outcomes with the combined use of regenerative techniques observed in a clinical trial by Chen et al. (2007) and by a recent systematic review (Clementini et al., 2015) on dimensional changes after immediate implant placement with or without simultaneous regenerative procedures. In IMPL/DBBM/CM group of the present study a flapped procedure was performed and the inserted implant was not immediately restored. The use of a flapless procedure or an immediate restoration, as the placement of a soft-tissue graft or the use of

a platform-switching implant-abutment connection should further be investigated in well- designed clinical trials, since there are indications of their potential benefit in maintaining ridge volume after tooth extraction.

Due to the small sample size, this randomized controlled clinical trial was not able to identify correlations between some prognostic factors (i.e. thickness of the buccal bone plate at baseline, tooth location) and the radiographic outcomes (Ferrus et al., 2010; Tomasi et al., 2010). The short follow up period (4 months) of a radiographic analysis is another limit of this study since it does not allow an evaluation of the real benefits for patients of limiting morphological changes after tooth extraction: the necessity and the amount of a ridge augmentation procedure for the following implant placement, the occurrence of soft tissue dehiscence at longer follow up and patient related outcomes (overall treatment time, number of surgical procedures, esthetic satisfaction) should be radiologically and clinically evaluated after a minimum of 6-12 months after definitive prosthetic restoration.

Despite this, the present study is able to make important clinical considerations with some practical implications and these findings may allow for future investigations.

CONCLUSION

The present study demonstrates that after a flapped extraction of a tooth, vertical and horizontal changes of the alveolar ridge occur, regardless of whether alveolar ridge preservation is performed. This happens despite the placement of an implant simultaneously with the ridge preservation procedure. However, a preservation technique, with or without immediate implant placement, reduce the horizontal bone morphological changes that occur, mostly in the coronal portion of the buccal bone plate, when compared to spontaneous healing. For this reason, immediate implant placement in post-extraction sites plus an ARP technique may be a viable option, to reduce hard tissue morphological changes and treatment time.

REFERENCES

- Araújo, M.G. & Lindhe, J. (2005). Dimensional ridge alterations following tooth extraction. An experimental study in the dog. *Journal of Clinical Periodontology*, 32, 212–218.
- Araujo, M.G., Sukekava, F., Wennstrom, J.L. & Lindhe, J.. (2005) Ridge alterations following implant placement in fresh extraction sockets: an experimental study in the dog. *Journal of Clinical Periodontology*, 32, 645–652.
- Araújo, M.G., Linder, E., Wennström, J.L. & Lindhe, J. (2008). The influence of Bio-Oss collagen on healing of an extraction socket: an experimental study in the dog. *International Journal of Periodontics and Restorative Dentistry*, 28, 123–135.
- Araújo, M.G., da Silva, J.C.C., de Mendonça, A.F. & Lindhe, J. (2015). Ridge alterations following grafting of fresh extraction sockets in man. A randomized clinical trial. *Clinical Oral Implants Research*, 26, 407–412. doi: 10.1111/clr.1236.
- Avila-Ortiz, G., Chambrone, L. & Vignoletti, F. (2019). Effect of Alveolar Ridge Preservation Interventions Following Tooth Extraction: A Systematic Review and Meta-Analysis. *Journal of Clinical Periodontology* Jan 9. doi: 10.1111/jcpe.13057. [Epub ahead of print]
- Bliese, P. D. (2000). Within-group agreement, non-independence, and reliability: Implications for data aggregation and Analysis. In K. J. Klein & S. W. Kozlowski (Eds.), *Multilevel Theory, Research, and Methods in Organizations* (pp. 349-381). San Francisco, CA: Jossey-Bass, Inc.
- Botticelli, D., Berglundh, T. & Lindhe, J. (2004) Hard-tissue alterations following immediate implant placement in extraction sites. *Journal of Clinical Periodontology*, 31, 820–828.
- Clementini, M., Tiravia, L., De Risi, V., Vittorini Orgeas, G., Mannocci, A. & de Sanctis, M. (2015). Dimensional changes after immediate implant placement with or without simultaneous regenerative procedures: a systematic review and meta-analysis. *Journal of Clinical Periodontology*, 42, 666-677. doi: 10.1111/jcpe.12423

- Clementini, M., Discepoli, N., Danesi, C. & de Sanctis, M. (2018) Biologically guided flap stability: The role of flap thickness including periosteum retention on the performance of the coronally advanced flap—A double-blind randomized clinical trial. *Journal of Clinical Periodontology*, 45,1238–1246
- Chen, S. T., Darby, I. B. & Reynolds, E. C. (2007). A prospective clinical study of non-submerged immediate implants: clinical outcomes and esthetic results. *Clinical Oral Implants Research*, 18, 552–562.
- Chen, S.T. & Buser, D. (2014). Esthetic outcomes following immediate and early implant placement in the anterior maxilla – a systematic review. *The International Journal of Oral & Maxillofacial Implants*, 29, 186–215. doi: 10.11607/jomi.2014suppl.g3.3.
- Cosyn, J., Hooghe, N. & De Bruyn, H. (2012). A systematic review on the frequency of advanced recession following single immediate implant treatment. *Journal of Clinical Periodontology*, 39, 582–589. doi: 10.1111/j.1600-051X.2012.01888.x.
- De Risi, V., Clementini, M., Vittorini, G., Mannocci, A. & de Sanctis, M. (2015). Alveolar ridge preservation techniques: a systematic review and meta-analysis of histological and histomorphometrical data. *Clinical Oral Implants Research*, 26, 50–68. doi: 10.1111/clr.12288.
- Degidi, M., Daprile, G., Nardi, D. & Piattelli, A. (2012). Buccal bone plate in immediately placed and restored implant with Bio-Oss collagen graft: a 1-year follow-up study. *Clinical Oral Implants Research*, 24(11), 1201-1205. doi: 10.1111/j.1600-0501.2012.02561.x.
- Discepoli, N., Vignoletti, F., Laino, L., de Sanctis, M., Munoz, F. & Sanz, M. (2015). Fresh extraction socket: spontaneous healing vs. immediate implant placement. *Clinical Oral Implants Research*, 26, 1250–1255. doi: 10.1111/clr.12447.
- Discepoli, N., Vignoletti, F., Laino, L., de Sanctis, M., Munoz, F. & Sanz, M. (2013). Early healing of the alveolar process after tooth extraction. An experimental study in the beagle dog. *Journal of Clinical Periodontology*, 40, 638–644. doi: 10.1111/jcpe.12074.
- Evans, C.D. & Chen, S.T. (2008). Esthetic outcomes of immediate implant placements. *Clinical Oral Implants Research*, 19(1), 73–80.
- Ferrus, J., Cecchinato, D., Pjetursson, E. B., Lang, N. P., Sanz, M. & Lindhe, J. (2010). Factors influencing ridge alterations following immediate implant placement into extraction sockets. *Clinical Oral Implants Research*, 21, 22–29. doi: 10.1111/j.1600-0501.2009.01825.x.
- Fickl, S., Zuhr, O., Wachtel, H., Stappert, C.F.J., Stein, J.M. & Hürzeler, M.B. (2008). Dimensional changes of the alveolar ridge contour after different socket preservation techniques. *Journal of Clinical Periodontology*, 35, 906–913. doi: 10.1111/j.1600-051X.2008.01305.x.
- Hämmerle, C.H., Araújo, M.G. & Simion, M. (2012). Osteology Consensus Group 2011. Evidence-based knowledge on the biology and treatment of extraction sockets. *Clinical Oral Implants Research*, 23(5), 80–82. doi: 10.1111/j.1600-0501.2011.02370.x.
- Horvath, A., Mardas, N., Mezzomo, L.A., Needleman, I.G. & Donos, N. (2013). Alveolar ridge preservation. A systematic review. *Clinical Oral Investigations*, 17, 341–363. doi: 10.1007/s00784-012-0758-5.
- Januario, A.L., Duarte, W.R., Barriviera, M., Mesti, J.C., Araujo, M.G. & Lindhe, J. (2011). Dimension of the facial bone wall in the anterior maxilla: a cone-beam computed tomography study. *Clinical Oral Implants Research*, 10, 1168–1171. doi: 10.1111/j.1600-0501.2010.02086.x.
- Jung, R.E., Philipp, A., Annen, B.M., Signorelli, L., Thoma, D.S., Hämmerle, C.H., Attin, T. & Schmidlin, P. (2013). Radiographic evaluation of different techniques for ridge preservation after tooth extraction: a randomized controlled clinical trial. *Journal of Clinical Periodontology*, 1, 90–98. doi: 10.1111/jcpe.12027.
- Kerr, E.N, Mealey, B.L., Noujeim, M.E., Lasho, D.J, Nummikoski, P.V. & Mellonig, J.T. (2008). The effect of ultrasound on bone dimensional changes following extraction: a pilot study. *Journal of Periodontology*, 79(2), 283-290. doi: 10.1902/jop.2008.070289 .

- Lang, N.P., Pun, L., Lau, K.Y., Li, K.Y. & Wong, M.C. (2012). A systematic review on survival and success rates of implants placed immediately into fresh extraction sockets after at least 1 year. *Clinical Oral Implants Research*, 23(5), 39–66. doi: 10.1111/j.1600-0501.2011.02372.x.
- Lang, N.P. & Bartold, P.M. (2018). Periodontal health. *Journal of Clinical Periodontology*, 45(20), S9-S16. doi: 10.1111/jcpe.12936.
- Lazzara, R.G. (1989). Immediate implant placement into extraction sites: surgical and restorative advantages. *International Journal of Periodontics and Restorative Dentistry*, 9(5), 332-343.
- MacBeth, N., Trullenque-Eriksson, A., Donos, N. & Mardas, N. (2017). Hard and soft tissue changes following alveolar ridge preservation: a systematic review. *Clinical Oral Implant Research*, 28, 982–1004. doi: 10.1111/clr.12911.
- Mardas, N., Chadha, V. & Donos, N. (2010). Alveolar ridge preservation with guided bone regeneration and a synthetic bone substitute or a bovine-derived xenograft: a randomized, controlled clinical trial. *Clinical Oral Implants Research*, 21(7), 688-698. doi: 10.1111/j.1600-0501.2010.01918.x.
- Muhlemann, H. R., & Son, S. (1971). Gingival sulcus bleeding –a leading symptom in initial gingivitis. *Helvetica Odontologica Acta*, 15, 107–113.
- O’Leary, T. J., Drake, R. B., & Naylor, J. E. (1972). The plaque control record. *Journal of Periodontology*, 43, 38. <https://doi.org/10.1902/jop.1972.43.1.38>
- Pietrokovski, J. & Massler, M. (1967). Alveolar ridge resorption following tooth extraction. *Journal of Prosthetic Dentistry*, 17, 21–27.
- Sanz, M., Lindhe, J., Alcaraz, J., Sanz-Sanchez, I. & Cecchinato, D. (2017). The effect of placing a bone replacement graft in the gap at immediately placed implants: a randomized clinical trial. *Clinical Oral Implants Research*, 28(8), 902-910. doi: 10.1111/clr.12896.
- Schropp, L., Wenzel, A., Kostopoulos, L. & Karring, T. (2003). Bone healing and soft tissue contour changes following single-tooth extraction: a clinical and radiographic 12-month prospective study. *The International Journal of Periodontics & Restorative Dentistry*, 23, 313–323 .
- Schulte, W. & Heimke, G. (1976). The Tübingen immediate implant. *Die Quintessenz*, 27(6), 17–23.
- Tan, W. L., Wong, T. L., Wong, M. C. & Lang, N. P. (2012). A systematic review of post-extraction alveolar hard and soft tissue dimensional changes in humans. *Clinical Oral Implants Research*, 23(Suppl 5), 1–21. doi: 10.1111/j.1600-0501.2011.02375.x.
- Ten Heggeler, J.M.A.G., Slot, D.E. & Van der Weijden, G.A. (2011). Effect of socket preservation therapies following tooth extraction in non-molar regions in humans: a systematic review. *Clinical Oral Implants Research*, 22(8), 779–788. doi:10.1111/j.1600-0501.2010.02064.x.
- Tomasi, C., Sanz, M., Cecchinato, D., Pjetursson, B., Ferrus, J., Lang, N.P. & Lindhe, J. (2010). Bone dimensional variations at implants placed in fresh extraction sockets: a multilevel multivariate analysis. *Clinical Oral Implants Research*, 21, 30–36. doi: 10.1111/j.1600-0501.2009.01848.x.
- Tonetti, M.S., Cortellini, P., Graziani, F., Cairo, F., Lang, N.P., Abundo, R., Conforti, G.P., Marquardt, S., Rasperini, G., Silvestri, M., Wallkamm, B. & Wetzel, A. (2017) Immediate versus delayed implant placement after anterior single tooth extraction: the timing randomised controlled clinical trial. *Journal of Clinical Periodontology*, 44, 215–224. doi: 10.1111/jcpe.12666.
- Van der Weijden, F., Dell’Acqua, F. & Slot, D.E. (2009). Alveolar bone dimensional changes of post-extraction sockets in humans: a systematic review. *Journal of Clinical Periodontology*, 36, 1048–1058. doi: 10.1111/j.1600-051X.2009.01482.x.
- Vignoletti, F., Discepoli, N., Muller, A., de Sanctis, M., Munoz, F. & Sanz, M. (2012). Bone modelling at fresh extraction sockets: immediate implant placement versus spontaneous healing: an experimental study in the beagle dog. *Journal of Clinical Periodontology*, 39, 91–97. doi: 10.1111/j.1600-051X.2011.01803.x.
- Vignoletti, F., Matesanz, P., Rodrigo, D., Figuero, E., Martin, C. & Sanz, M. (2012). Surgical protocols for ridge preservation after tooth extraction. A systematic review. *Clinical Oral Implants Research*, 23(Suppl 5), 22–38. doi: 10.1111/j.1600-0501.2011.02331.x.

Vignoletti, F. & Sanz, M. (2014). Immediate implants at fresh extraction sockets: from myth to reality. *Periodontology* 2000, 66, 132–152. doi: 10.1111/prd.12044.

Vittorini Orgeas, G., Clementini, M., De Risi, V., de Sanctis, M. (2013). Surgical techniques for alveolar socket preservation: a systematic review. *International Journal of Oral and Maxillofacial Implants*, 28(4), 1049-1061. doi: 10.11607/jomi.2670.

Corresponding Author:

Dr. Marco Clementini
Università Vita-Salute San Raffaele
Via Olgettina 48, Milano, Italy
mail: mclementini@me.com

Figure 1. Baseline CBCT, intra-operative view and 4 months post-surgery CBCT representative of the 3 treatment modalities. 1) Spontaneous healing: (a) baseline, (b) intra-operative, (c) 4 months. 2) DBBM-CM site: (d) baseline, (e) intra-operative, (f) 4 months 3) IMPL / DBBM-CM site: (g) baseline, (h) intra-operative, (i) 4 months.

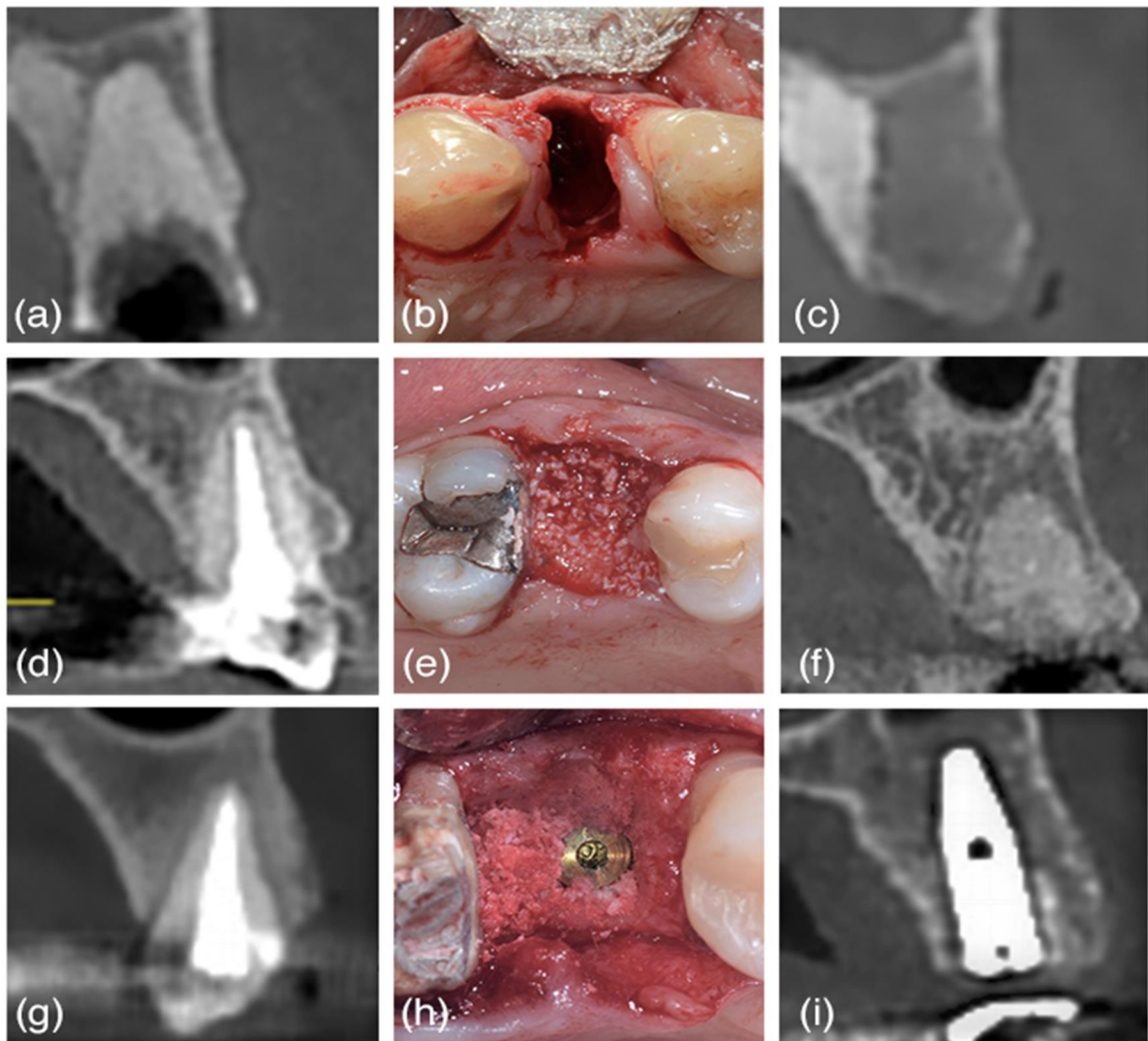


Table 1. Baseline demographic, clinical and radiographic data of included patients.

<i>Baseline characteristics</i>	SH	DBBM-CM	IMPL / DBBM-CM
Age (years)	50.5(12.2)	55.5(11.6)	52.5(7.5)
Male/Female	7/3	4/6	3/7
Smokers	3	4	3
Maxilla/Mandible	8/2	6/4	8/2
Anterior/Premolars	5/5	5/5	6/4
Presence of both mesial/distal tooth	9	9	9
Reason for extraction (endo/fracture/prosthetic/root resorption)	5/1/4	5/2/2/1	4/3/2/1
FMPS (%)	15.3(1.3)	15.1(1.9)	14.9(1.5)
FMBS (%)	8.9(0.4)	8.3(0.6)	8.6(0.5)
KTH (mm)	2.70(1.25)	3.70(0.95)	4.00(1.41)
GT (mm)	1.40(0.57)	1.30(0.59)	1.30(0.42)
Thickness 1 mm Buccal (mm)	1.17(0.39)	1.33(0.25)	1.34(0.45)
Thickness 3 mm Buccal (mm)	1.21(0.55)	1.35(0.48)	1.37(0.94)
Thickness 5 mm Buccal (mm)	1.59(0.41)	1.71(1.30)	1.64(0.90)
Thickness 1 mm Lingual (mm)	1.99(1.054)	2.43(1.64)	2.05(1.30)
Thikness 3 mm Lingual (mm)	2.38(0.91)	2.89(1.78)	3.08(1.81)
Thickness 5 mm Lingual (mm)	3.02(1.58)	4.12(2.16)	4.34(2.32)

Table 2. Calculated statistical differences for changes in ridge height and width over 4 months among the three treatment modalities.

Dimensional changes	SH	DBBM-CM	IMPL / DBBM-CM	Kruskal-Wallis (p-value)	Pairwise comparisons		
					SH vs. DBBM-CM	SH vs. IMPL / DBBM-CM	DBBM-CM vs. IMPL / DBBM-CM
Vertical buccal (mm)	-0.83(1.14)	-0.31(0.33)	-0.56(0.38)	0.3444			
Vertical lingual (mm)	-0.21(0.31)	-0.32(0.47)	-0.50(0.58)	0.4658			
Vertical buccal (%)	- 10.60(14.00)	-3.94(4.79)	-6.26(4.64)	0.4181			
Vertical lingual (%)	-2.15(3.23)	-3.58(4.72)	-4.98(5.83)	0.4586			
Horizontal 1 mm (mm)	-3.37(1.55)	-1.56(0.71)	-1.29(0.38)	0.0008	0.0133	0.0011	1
Horizontal 3 mm (mm)	-2.41(1.97)	-1.07(0.69)	-0.99(0.48)	0.0534			
Horizontal 5 mm (mm)	-1.88(1.55)	-0.96(0.61)	-0.92(0.59)	0.1858			
Horizontal 1 mm (%)	- 43.23(25.05)	-19.21(9.18)	-14.92(4.85)	0.001	0.0213	0.0011	1
Horizontal 3 mm (%)	- 30.62(28.60)	-12.27(8.56)	-10.78(5.64)	0.0738			
Horizontal 5 mm (%)	- 23.12(20.69)	-10.44(7.13)	-9.51(6.44)	0.1349			
Mid buccal 1 mm (mm)	-2.45(1.29)	-0.91(0.43)	-0.99(0.21)	0.0001	0.0003	0.0014	1
Mid buccal 3 mm (mm)	-1.92(1.99)	-0.53(0.44)	-0.70(0.33)	0.0292	0.0342	0.1461	1
Mid buccal 5 mm (mm)	-1.43(1.35)	-0.56(0.44)	-0.53(0.31)	0.0833			
Mid buccal 1 mm (%)	- 54.96(20.99)	- 25.96(11.01)	-26.80(7.07)	0.0004	0.0009	0.0034	1

Mid buccal 3 mm (%)	- 41.51(26.45)	- 15.76(13.86)	-19.22(9.44)	0.0335	0.056	0.095	1
Mid buccal 5 mm (%)	- 38.771(28.16)	- 16.90(15.21)	-14.87(8.78)	0.047	0.1262	0.076	1
Mid lingual 1 mm (mm)	-0.98(0.93)	-0.64(0.40)	-0.29(0.29)	0.0825			
Mid lingual 3 mm (mm)	-0.55(0.59)	-0.53(0.29)	-0.29(0.26)	0.1061			
Mid lingual 5 mm (mm)	-0.45(0.45)	-0.40(0.25)	-0.38(0.39)	0.9741			
Mid lingual 1 mm (%)	- 24.03(22.07)	-14.47(9.65)	-5.99(6.18)	0.0308	1	0.031	0.2061
Mid lingual 3 mm(%)	- 14.30(15.87)	-10.29(6.51)	-5.20(4.74)	0.1163			
Mid lingual 5 mm (%)	- 10.88(12.61)	-7.00(4.60)	-6.44(7.08)	0.7421			

Figure 2. Consort diagram showing the study design

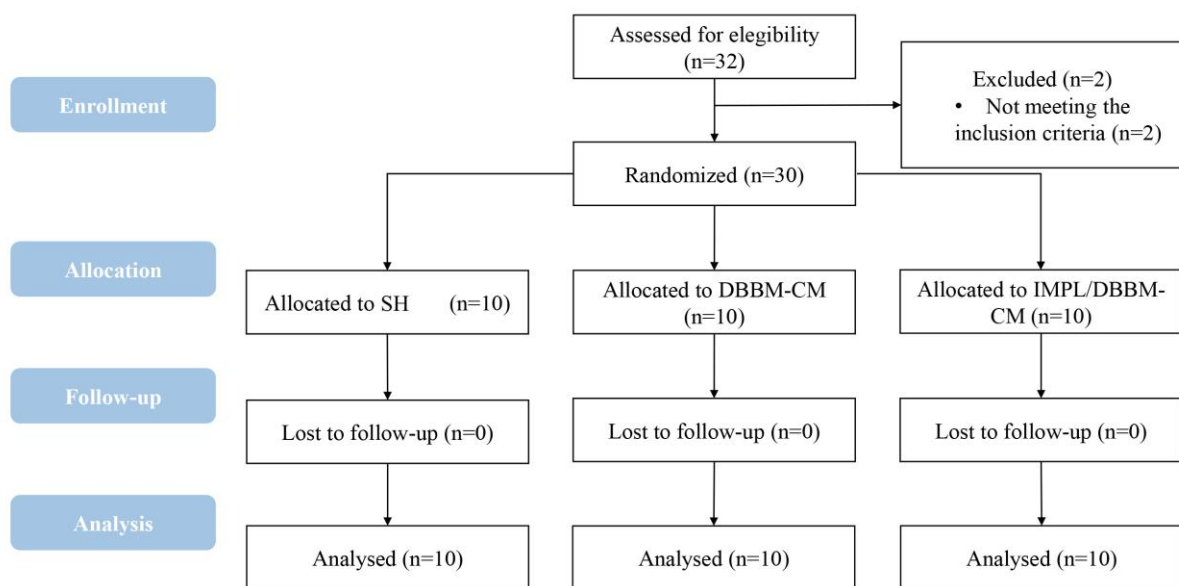


Figure 3. Bone changes measurements. ACP: apical central point. CCP: coronal central point. BCP: buccal coronal point. LCP: lingual central point.

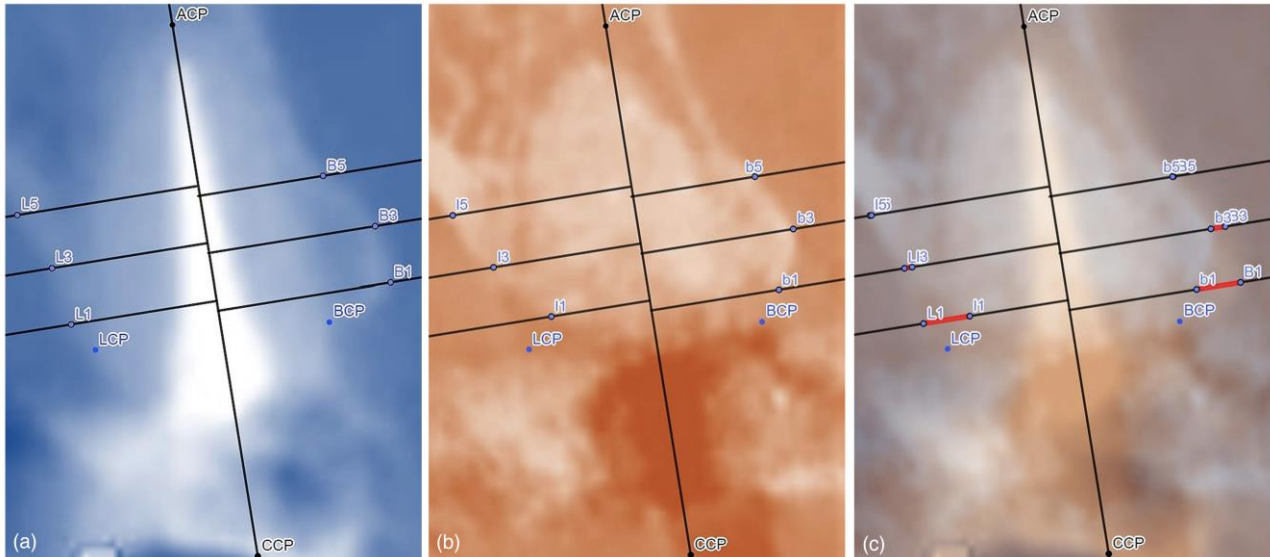


Figure 4. Changes in ridge width (mm) at buccal and lingual aspects over 4 months based on cone-beam computed tomography (CBCT) measurements.

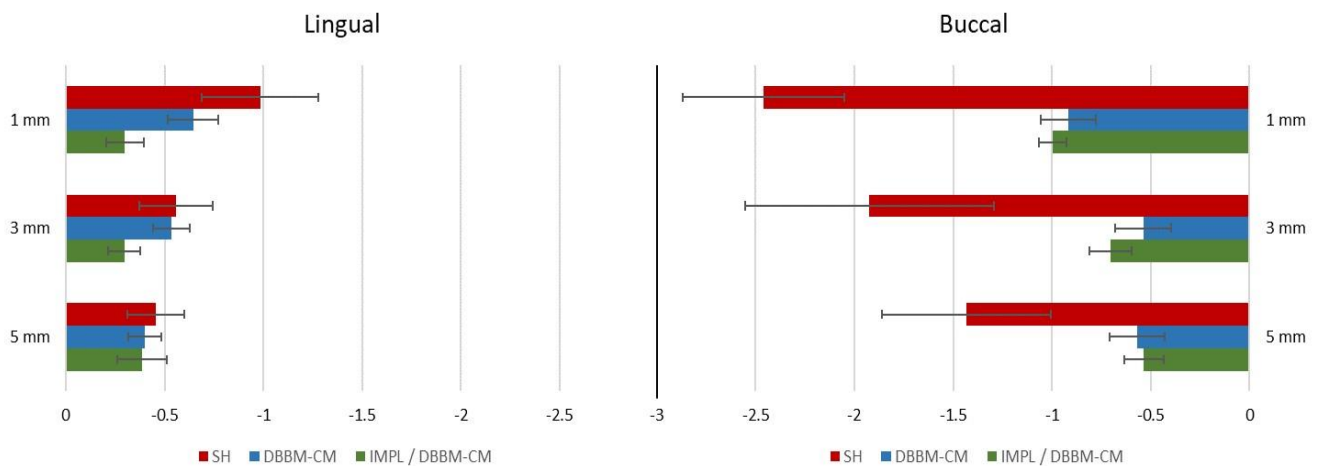
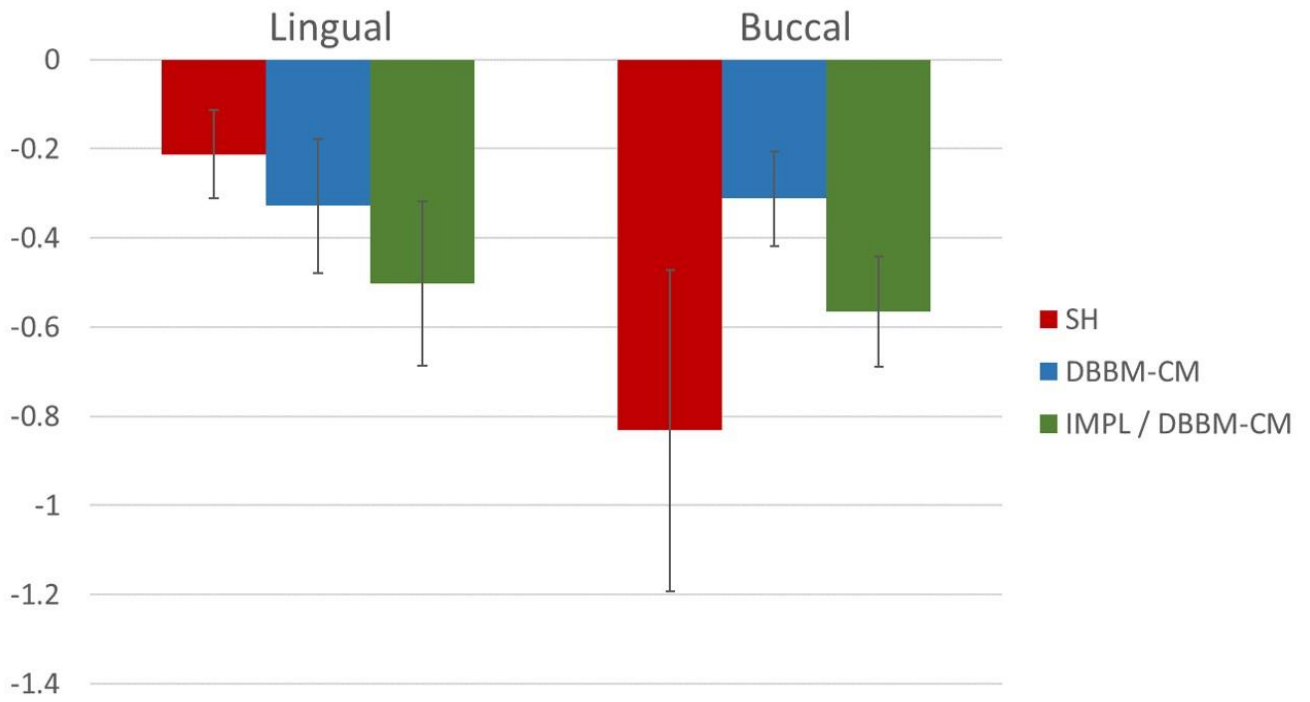


Figure 5. Changes in ridge height (mm) over 4 months based on cone-beam computed tomography (CBCT) measurements.



PREVALENCE OF PERI-IMPLANT DISEASES AMONG AN ITALIAN POPULATION OF PATIENTS WITH METABOLIC SYNDROME: A CROSS-SECTIONAL STUDY.

LA PREVALENZA DELLE PATOLOGIE PERI-IMPLANTARI IN UNA POPOLAZIONE ITALIANA DI PAZIENTI CON LA SINDROME METABOLICA: UNO STUDIO TRASVERSALE

Papi Piero, DDS*, **Di Murro Bianca, DDS ***, **Bisogni Valeria, MD ****, **Pranno Nicola, DDS ***, **Saracino Vincenza, MD****, **Letizia Claudio, MD ****, **Polimeni Antonella, MD, DDS ***, **Pompa Giorgio, MD, DDS ***

*Department of Oral and Maxillo-Facial Sciences, “Sapienza” University of Rome, Italy

** Department of Translational and Precision Medicine, “Sapienza” University of Rome, Italy

Abstract

Introduzione: Nel corso degli anni, solo pochi autori si sono concentrati sulla possibile correlazione tra patologie sistemiche e le malattie peri-implantari. L'obiettivo di questo studio trasversale è quello di valutare la prevalenza e la severità della peri-implantite nei pazienti con diagnosi di sindrome metabolica. **Materiali e Metodi:** Sono stati selezionati pazienti con almeno un impianto dentale, con minimo 5 anni di carico protesico, per effettuare uno screening parodontale, peri-implantare e metabolico. La diagnosi di Sindrome Metabolica è stata effettuata secondo i criteri diagnostici NCEP-ATP III, mentre la nuova classificazione delle malattie parodontali e peri-implantari del 2017 è stata utilizzata per la peri-implantite e la mucosite peri-implantare. La regressione multipla è stata eseguita per analizzare la relazione tra sindrome metabolica, presenza di malattia parodontale, sesso, tipo di protesi, sede implantare, fumo e la peri-implantite e la mucosite. **Risultati:** Sono stati arruolati 183 pazienti: nei pazienti con sindrome metabolica la prevalenza delle patologie peri-implantari riscontrata è stata del 97.6%, con un OR di 10.01 per la mucosite e 15.26 per la peri-implantite, mentre nei soggetti privi di Sindrome metabolica è stata evidenziata una frequenza dell'81.8%, con $p < 0.001$. **Conclusioni:** I pazienti con una diagnosi di sindrome metabolica hanno mostrato una nettissima prevalenza delle patologie peri-implantari.

Abstract

Purpose: The aim of this study is to detect frequency and severity of peri-implant diseases among an Italian population of patients affected by metabolic syndrome (MetS).

Methods: In this cross-sectional study, patients with at least one dental implant with >5 years of functional loading were screened to evaluate metabolic, periodontal and peri-implant status. MetS diagnosis was established in accordance with the NCEP ATP III criteria, while case definitions of the 2017 World Workshop were adopted for peri-implant diseases. Multinomial logistic regression analysed the relationship between gender, diagnosis of metabolic syndrome, presence of periodontitis, smoking, type of prosthesis and location of implants and peri-implant mucositis and peri-implantitis.

Results: A final sample of 183 patients was enrolled: in MetS subjects, 97.6% of implants were diagnosed with peri-implant diseases, with an OR of 10.01 for mucositis and OR 15.26 for peri-implantitis, compared to subjects without MetS, where frequency of peri-implant diseases was 81.8% , $p < 0.001$.

Patients with periodontitis showed a higher association with peri-implant mucositis (OR=4.33) and peri-implantitis (OR=9).

Conclusions: Based on the results of this study, patients with MetS showed a greater prevalence of peri-implant diseases, with further studies that need to confirm the possibility of this new possible risk indicator.

Introduction

The European population is getting older, with an increasing concern about oral health: according to Schimmel et al.¹, implant-prosthetic rehabilitation has become routine practice in elderly patients, however coexisting systemic risk factors should carefully be taken into account by clinicians².

Dental implants have shown well-documented long-term survival rates (> 10 years)³⁻⁴, however, implant success may be affected by either mechanical or biological complications⁵⁻⁶.

According to the 2017 World Workshop on the Classification of Periodontal and Peri-Implant Diseases and Conditions, plaque-related inflammatory conditions can be classified as peri-implantitis and peri-implant mucositis⁷.

Prevalence of peri-implant diseases is still controversial, according to Derks & Tomasi around 42% of dental implants are affected by mucositis, while a diagnosis of peri-implantitis could be established in 23% of dental implants⁸.

Schwarz et al.⁹ showed that there is strong evidence for history of periodontitis as a risk factor for peri-implantitis, an assumption supported by several longitudinal and cross-sectional studies¹⁰⁻¹².

Peri-implantitis, as well as periodontitis, is considered sensitive to factors inducing tissue inflammation (smoking, poor plaque control, hyperglycaemia) together with systemic oxidative stress and up-regulation of inflammatory cytokines¹³⁻¹⁴.

Over the years, correlation between metabolic and cardiovascular diseases has been described in literature¹⁵⁻¹⁷, while only few authors have studied the association of these conditions with peri-implantitis¹⁸⁻¹⁹.

In particular, Monje et al.²⁰ found out that diabetes patients no-smokers showed a 3.39 higher risk for peri-implantitis compared to normoglycaemia subjects, however several studies included in the systematic review failed to identify diabetes as a risk factor for peri-implantitis.

Renvert et al.²¹ concluded that history of cardiovascular disease (CVD) had a high likelihood of comorbidity with peri-implantitis, expressing an Odds Ratio (OR) of 8.7, while Koldslund et al.²² found no association between CVD and peri-implant diseases.

Metabolic syndrome

Metabolic syndrome (MetS) is a clustering of clinical findings made up of abdominal obesity, high glucose, high triglycerides and low high-density lipoprotein (HDL) cholesterol levels, and arterial hypertension (HT)²³. Its overall prevalence is more than 40%, but ranged from 38% to 60%, depending on age, sex, socioeconomic status, the ethnic background of study cohorts, and the definition used²³⁻²⁴. Several definitions of MetS, indeed, have been proposed, with varied requirements, including those by the International Diabetes Federation and the National Cholesterol Education Program (NCEP) Adult Treatment Panel (ATP) III²⁵ that has been recognized as more accurate and sensitive for prediction of CVD²⁶. According to the NCEP ATP III, a diagnosis of MetS is made by fulfilment of 3 of the following 5 criteria: (1) waist circumference (WC) \geq 102 cm for males or \geq 88 cm for females; (2) fasting glucose \geq 110 mg/dL; (3) triglycerides \geq 150 mg/dL; (4) HDL - cholesterol < 40 mg/dL for males or < 50 mg/dL for females; (5) blood pressure (BP) \geq 130/85 mmHg²⁵.

MetS is associated to higher cardiovascular (CV) and metabolic complications with increased risk of type 2 diabetes mellitus and CVD mortality²⁷.

Recently, it has been highlighted by several cross-sectional²⁸⁻³⁰ and case-control³¹⁻³² studies that there is an interrelationship between periodontitis and MetS³³. Therefore, it has been suggested that the evaluation of periodontal parameters should become part of routine diagnostic procedures for patients affected by MetS³⁴.

However, data about the association between MetS, its components and peri-implant diseases is lacking and only lately it has been highlighted the relevance of this feasible relationship in the management of patients with implants affected by MetS³⁵.

The aim of this cross-sectional survey is to detect frequency and severity of peri-implant diseases among an Italian population of patients affected by MetS, and to further identify possible role of MetS as a risk indicator.

Material and Methods

Study design

To address the research purpose, the authors developed and implemented a cross-sectional study, conducted at the Departments of Oral and Maxillo-Facial Sciences and Translational and Precision Medicine, at “Sapienza” University of Rome.

Study population

From April 2018 to September 2018, all subjects referred to the Tertiary Centre of Secondary Hypertension Unit, Policlinico Umberto I, “Sapienza” University of Rome, for screening, diagnosis, and treatment of primary and/or secondary hypertension were consecutively evaluated.

Patients were enrolled in the study based on the following inclusion and exclusion criteria:

age \geq 18 years and presence of at least one osseointegrated implant functioning for >5 years.

Each patient received detailed descriptions of the study protocol and all subjects signed the informed consent form and gave written approval to be included in the study population, according to the latest version of the World Medical Declaration of Helsinki (2013). The study was approved by the institution review board of “Sapienza” University of Rome (Ref. 4948/2018) and reported according to the STROBE statement (www.strobe-statement.org).

Medical Examination

Anthropometric measurements and venous blood samples were obtained from all patients in the early morning after an overnight fast. Data about smoking habit, as well as current medications, past medical history, including CV events, was collected, and we performed a complete screening to exclude secondary forms of hypertension, such as primary aldosteronism, renovascular diseases, Cushing’s syndrome, and pheochromocytoma. The instrumental evaluation included the 24-hours ambulatory blood pressure monitoring (ABPM) and the Doppler ultrasound for carotid arteries to estimate the intima media thickness (IMT) value and the presence of plaques, as markers of hypertensive- and metabolic-related vascular damage³⁶.

The 24-hours ABPM was performed by the Spacelabs 90207 (SpaceLabs®, Washington, USA). For each registration, the blood pressure (BP) values were obtained every 15 minutes during the day and every 30 minutes during the night time period. The parameters collected include: mean 24-hours systolic and diastolic BP and its standard deviation (SD), mean daily and night-time systolic and diastolic BP and their SD, the dipping values.

A Doppler scan was used to detect IMT and plaques. The common carotid artery, the carotid bulb, and the near and far wall segments of the internal carotid artery were scanned bilaterally. Images were obtained in longitudinal sections with a single lateral angle of insonation, optimizing the image for the far wall. According to the consensus statement from the American Society of Echocardiography Carotid Intima-Media Thickness Task Force, endorsed by the Society for Vascular Medicine³⁶, IMT was defined as the distance between the ultrasound interfaces of the lumen-intima and media-adventitia. Six manual measurements were performed, with automatic border detection, at equal distances along 1 cm on the far wall of the common carotid. Carotid plaque was defined as the presence of focal wall thickening that is at least 50% greater than that of the surrounding vessel wall or as a focal region with IMT greater than 1.5 mm that protrudes into the lumen that is distinct from the adjacent boundary.

All patients were screened for the MetS according to the NCEP ATP III criteria²³. The diagnosis was made by the evidence of ≥ 3 of the following criteria: (1) WC ≥ 102 cm (M) or ≥ 88 cm (F). The WC was measured placing the measuring tape horizontally around the patient's abdomen and aligning the bottom edge of the tape with the belly bottom. We used a measuring tape with a spring handle in order to control the pressure exerted on the patient's abdomen. (2) Fasting plasma glucose value ≥ 110 mg/dL; (3) serum triglycerides concentration ≥ 150 mg/dL; (4) serum HDL - cholesterol concentration < 40 mg/dL (M) or < 50 mg/dL (F); (5) BP $\geq 130/85$ mmHg, obtained by 24-hours ABPM²³.

Dental examination

All patients with at least one dental implant with >5 years of functional loading were referred at the Oral Surgery Unit, Policlinico Umberto I, "Sapienza" University of Rome to evaluate periodontal and peri-implant status.

Patients' data collected included: sex, age, referred medical systemic condition and periodontal status (presence or absence of periodontitis).

A full mouth periodontal examination at six sites per teeth and implant [mesio-vestibular (mv), mid-vestibular (v), disto-vestibular (dv), mesio-palatine/lingual (mp/ml), mid-palatine/lingual (p/l), and disto-palatine/lingual (dp/dl)] was performed by using a periodontal probe (PCP-Unc 15, Hu-Friedy®, Chicago, Illinois, USA) with a light force (approximately 0.15 N), without anaesthesia, by the same trained previously calibrated examiner (BDM).

A patient was defined as a "periodontitis case" in accordance with the 2017 World Workshop on the Classification of Periodontal and Peri-Implant Diseases and Conditions³⁷ if:

- Interdental CAL was detectable at ≥ 2 non-adjacent teeth, or
- Buccal or oral CAL ≥ 3 mm with pocketing >3 mm was detectable at ≥ 2 teeth and the observed CAL cannot be ascribed to non-periodontal causes such as: 1) gingival recession of traumatic origin; 2) dental caries extending in the cervical area of the tooth; 3) the presence of CAL on the distal aspect of a second molar and associated with malposition or extraction of a third molar, 4) an endodontic lesion draining through the marginal periodontium; and 5) the occurrence of a vertical root fracture

To achieve intra-examiner reliability, the examiner was calibrated to show an agreement of 90% within 1 mm by duplicate measurements of probing depths on randomly selected teeth (10) and implants (10).

For each implant, the following clinical measurements were recorded:

- Probing Pocket Depth (PPD). Measured in millimetres, is the distance from the mucosal margin to the bottom of the probable pocket
- Plaque Index (PI) recorded with dichotomic values (present/absent)

- Mucosal redness defined as the phenomenon of inflammation presents as a biological response to extrinsic or intrinsic insult and recorded with dichotomic values (present/absent)
- Suppuration defined as a pus formation followed by discharge within a natural aperture or fistula and recorded with dichotomic values (present/absent)
- Bleeding on probing recorded with dichotomic values (present/absent)

Furthermore, years of functional loading, implant location (maxilla or mandible) and type of prostheses (single crown or multiple unit) were recorded.

In addition, mesial and distal implant crestal bone levels were measured on standardized (Rinn Centratore XCP Evolution 2003, Dentsply, Rome, Italy) digital periapical x-rays for each implant obtained by using an imaging plate scanner (PSPIX²®, Acteon Group, Norwich, UK).

A calibrated software (SOPRO Imaging, Acteon Group, Norwich, UK) was used to estimate variations in the marginal peri-implant bone level. The implant length and width were used as references for calibration of measurements. Two expert investigators who were blinded to other aspects of the study conducted the radiographic assessment. Any disagreement was solved by consensus, and a third investigator was consulted when it was not initially possible to achieve complete agreement (defined as a difference between the measurements made by the two experts of >0.1 mm).

The reference point for the bone level measurement was the implant shoulder. The bone level was digitally evaluated by measuring the distance between the implant shoulder and the first visible bone contact on the implant. The bone level measurements were recorded on the mesial and distal aspect of each implant.

An error of 0.75 mm was considered when reporting marginal bone loss (MBL), a threshold exceeding the measurement error (mean 0.5 mm) by 50%, as recommended by Berglundh et al⁷.

Case definitions for epidemiological or disease surveillance studies of the 2017 World Workshop on the Classification of Periodontal and Peri-Implant Diseases and Conditions were adopted to establish diagnosis of peri-implant diseases⁷.

Peri-implant health was defined as absence of clinical signs of inflammation, bleeding and/or suppuration on gentle probing, without radiographic bone loss.

Peri-implant mucositis was characterized by presence of bleeding and/or suppuration on gentle probing, without radiographic bone loss.

Peri-implantitis was defined as presence of bleeding and/or suppuration on gentle probing, with radiographic bone levels ≥ 3 mm apical of the most coronal portion of the intra-osseous part of the implant.

Statistical analysis

A database was created using Excel (Microsoft, Redmond, WA, USA). Descriptive statistics including mean \pm SD values were calculated for each variable, and box plots were used to evaluate data outliers. The Shapiro-Wilk test was used to determine whether or not the data conformed to a normal distribution.

Risk indicators for peri-implant mucositis and peri-implantitis were analysed at the patient level. The outcomes were explored by multinomial logistic regression to evaluate the relationship between gender, diagnosis of metabolic syndrome, periodontal status, smoking, type of prosthesis and location of implants and peri-implant mucositis and peri-implantitis.

An independent-samples t-test was run to determine if there were differences in mean value of marginal peri-implant bone level and in probing depth between patients with or without diagnosis of metabolic syndrome and with or without periodontitis.

Data were evaluated using standard statistical analysis software (version 20.0, Statistical Package for the Social Sciences, IBM Corporation, Armonk, NY, USA). In each test, the cut-off for statistical significance was $p \leq 0.05$.

Results

A total of 784 patients was consecutively evaluated at the Secondary Hypertension Unit in the study period: 363 subjects declared they had dental implants placed, however 134 had implants functioning by less than 5 years and were, therefore, excluded from the study.

The remaining 229 patients were referred at the Oral Surgery Unit in order to evaluate peri-implant status: 26 refused to be included in the study, 20 did not attend the scheduled visit and refused a new dental examination.

A final sample of 183 patients was enrolled in this study: 112 females (61.2%) and 71 males (38.8%) with a mean age of 66.08 ± 10.42 years (age range 42-85).

Eighty-four patients had a diagnosis of metabolic syndrome (45.9%), while the remaining 99 (54.1%) did not meet MetS criteria (Table 1).

The subgroup with MetS, compared to patients without MetS, showed significantly higher values of waist circumference and triglycerides (103.4 ± 9.7 vs 92.2 ± 11.0 cm, $p=0.01$, 147.5 ± 62.2 vs 87.9 ± 30.4 mg/dl, $p=0.002$, respectively), and lower HDL cholesterol levels (50.3 ± 16.1 vs 66.8 ± 14.5 mg/dl, $p=0.01$).

Presence of periodontitis was detected in 115 subjects (64.8%).

Subjects enrolled had 567 dental implants placed, with a mean of 3.1 implants per patient.

Out of the 183 dental implants included, mucositis was diagnosed in 57.9% of cases, peri-implantitis in 31.1% and only 10.9% of implants were classified as healthy. Mean functional time was 7.61 ± 4.04 years (range: 5-24 years).

Mean values of MBL were mesially 1.765 ± 1.424 and distally 1.918 ± 1.576 mm.

The mean PPD was 3.71 ± 1.48 mm (Table 1).

The multinomial logistic regression revealed that two of the six predictor variables were statistically significant for a diagnosis of mucositis: presence of metabolic syndrome ($p=0.005$; odds ratio 10.01) and periodontitis ($p=0.25$; odds ratio 4.33); and two of the six predictor variables were statistically significant for a diagnosis of peri-implantitis: metabolic syndrome ($p=0.001$; odds ratio 15.26) and periodontitis ($p=0.002$; odds ratio 9) (Table 2).

No difference was found in mean values of MBL between patients with metabolic syndrome (1.96 ± 1.41 mm) and without metabolic syndrome (1.6 ± 1.42 mm) ($p=0.081$).

By contrast, mean PPD values in patients with MetS (4.26 ± 1.74 mm) were statistically significant ($p=0.013$), compared to subjects without metabolic syndrome (3.71 ± 1.55 mm).

The sub-group with periodontitis showed statistically significant greater values of PPD and MBL (4.17 ± 1.85 vs 3.6 ± 1.21 mm, $p=0.024$, 2.05 ± 1.44 vs 1.28 ± 1.27 mm, $p<0.001$), compared to patients without periodontitis.

Conclusions

Risk indicators for implant biologic complications are still debated in literature and, among others, poor plaque control, smoking, lack of keratinized tissue, years in function, number of rehabilitated dental implants, history of periodontal disease and co-existing systemic medical conditions were individuated³⁹.

Implant treatment in the medically compromised patient represents, nowadays, a common clinical situation for dentists⁴⁰ and MetS prevalence has been constantly rising in the last years, involving approximately 30% of the population⁴¹.

Several studies have reported an inter-relationship between periodontal disease and MetS⁴², although, to the best of the authors' knowledge this is the first article to report data regarding MetS and peri-implant diseases.

A high prevalence of peri-implant diseases has been described by various authors: Atieh et al.⁴³ and Gurgel et al.⁴⁴ revealed that peri-implant diseases were diagnosed in around 82% of individuals, while in the study conducted by Pimentel et al.⁴⁵, they were observed in 94.5% of implants and 100% of individuals.

On the other hand, Wada et al.⁴⁶ reported a significant lower prevalence, with peri-implant mucositis and peri-implantitis being diagnosed at subject level in 23.9% and 15.8%, respectively. According to our results, patients with Metabolic Syndrome had a strong association with peri-implant mucositis (OR= 10.01) and even stronger with peri-implantitis (OR=15.26) (Table 2).

In MetS patients, 97.6% of implants (n=82/84) were diagnosed with either mucositis or peri-implantitis, a highly statistically significant difference ($p<0.001$) compared to subjects without MetS, where frequency of peri-implant diseases was 81.8% (n=81/99).

No differences were found among patients for smoking habits, implant location, gender and type of prosthetic rehabilitation.

Patients with presence of periodontitis were found to have a higher association with peri-implant mucositis (OR= 4.33) and peri-implantitis (OR=9): they showed also statistically significant greater values of PPD ($p=0.024$) and MBL ($p<0.001$), a result in accordance with previous studies⁴⁷⁻⁴⁸ (Table 2).

In line with our data, Renvert et al.²¹ showed an Odds ratio (OR) of 10.8 for peri-implantitis in patients with a diagnosis of periodontitis, while Derks et al.⁴⁹ reported an OR of 4.08.

Although, Ferreira et al.¹⁰, in a recent systematic review with meta-analysis, highlighted the heterogeneity of studies present in literature, with OR ranging from 1.74 to 22.9 depending on the different study design.

They concluded that there was evidence that patients with diagnosis or history of periodontitis were associated with the occurrence of peri-implantitis.

In this study, the diagnostic criteria proposed by the latest 2017 World Workshop on the Classification of Periodontal and Peri-Implant Diseases and Conditions were applied.

Previous systematic reviews highlighted how differences in the occurrence of peri-implant diseases were mostly due to the different clinical and radiographic parameters adopted, with minor changes in the diagnostic criteria producing a great difference in detection and frequency⁵⁰.

Main limitations of our study are represented by the absence of several important implant-related data, such as implant brand, shape, connection, surface treatment or guided bone regeneration (GBR) procedures.

These data were not available due to the cross-sectional nature of our study: the vast majority of implants were installed in private settings all over Italy, either by general practitioners, oral surgeons or periodontists.

Furthermore, absence of a retrospective standardized baseline (at prostheses delivery) radiological examination did not allow performing accurate bone level measurements, however, as recommended by Berglundh et al.⁷, an error of 0.75 mm was taken into account when performing the assessment.

There are no previous studies to which our findings can be compared and the design of this study do not allow establishing direct cause-effect relationships, however, the present study demonstrated a high prevalence of peri-implant diseases at the patient level in an Italian population of MetS subjects (97.6%).

This possible association need to be evaluated by further studies, with greater power and a longitudinal design: directionality of the relationship should be investigated and patient's therapeutic response analyzed.

Based on the results of this cross-sectional study, patients affected by metabolic syndrome showed a greater prevalence of peri-implant diseases, with further studies that need to confirm this new possible risk indicator.

References

1. Schimmel M, Müller F, Suter V, Buser D. Implants for elderly patients. *Periodontol 2000* 2017; 73: 228-240.
2. Srinivasan M, Meyer S, Mombelli A, Müller F. Dental implants in the elderly population: a systematic review and meta-analysis. *Clin Oral Implants Res.* 2017;28: 920-930.
3. De Angelis F, Papi P, Mencio F, Rosella D, Di Carlo S, Pompa G. Implant survival and success rates in patients with risk factors: results from a long-term retrospective study with a 10 to 18 years follow-up. *Eur Rev Med Pharmacol Sci* 2017; 21:433-437.
4. Rossi F, Lang NP, Ricci E, Ferraioli L, Baldi N, Botticelli D. Long-term follow-up of single crowns supported by short, moderately rough implants-A prospective 10-year cohort study. *Clin Oral Implants Res.* 2018;29: 1212-1219.
5. Heitz-Mayfield LJ, Aaboe M, Araujo M, et al. Group 4 ITI Consensus Report: Risks and biologic complications associated with implant dentistry. *Clin Oral Implants Res.* 2018;29 Suppl 16:351-358.
6. Hämmerle CHF, Cordaro L, Alccayhuaman KAA, et al. Biomechanical aspects: Summary and consensus statements of group 4. The 5th EAO Consensus Conference 2018. *Clin Oral Implants Res.* 2018;29 Suppl 18:326-331.
7. Berglundh T, Armitage G, Araujo MG, et al. Peri-implant diseases and conditions: Consensus report of workgroup 4 of the 2017 World Workshop on the Classification of Periodontal and Peri-Implant Diseases and Conditions. *J Periodontol.* 2018;89 Suppl 1:S313-S318.
8. Derks J, Tomasi C. Peri-implant health and disease; a systematic review of current epidemiology. *J Clin Periodontol* 2015; 42 Suppl 16: S158-S171.
9. Schwarz F, Derks J, Monje A, Wang HL. Peri-implantitis. *J Periodontol.* 2018;89 Suppl 1:S267-S290.
10. Ferreira SD, Martins CC, Amaral SA, et al. Periodontitis as a risk factor for peri-implantitis: Systematic review and meta-analysis of observational studies. *J Dent.* 2018;79:1-10.
11. Smith MM, Knight ET, Al-Harathi L, Leichter JW. Chronic periodontitis and implant dentistry. *Periodontol 2000.* 2017;74: 63-73.
12. Renvert S, Quirynen M. Risk indicators for peri-implantitis. A narrative review. *Clin Oral Implants Res.* 2015;26 Suppl 11:15-44
13. Acharya A, Koh ML, Kheur S, Watt RM, Jin L, Mattheos N. Salivary IL-1 β and red complex bacteria as predictors of the inflammatory status in sub-peri-implant niches of subjects with peri-implant mucositis. *Clin Oral Implants Res.* 2016;27: 662-667
14. Severino VO, Beghini M, de Araújo MF, et al. Expression of IL-6, IL-10, IL-17 and IL-33 in the peri-implant crevicular fluid of patients with peri-implant mucositis and peri-implantitis. *Arch Oral Biol.* 2016;72:194-199.
15. Sabharwal A, Gomes-Filho IS, Stellrecht E, Scannapieco FA. Role of periodontal therapy in management of common complex systemic diseases and conditions: An update. *Periodontol 2000.* 2018;78: 212-226.
16. Pietropaoli D, Del Pinto R, Ferri C, et al. Poor Oral Health and Blood Pressure Control Among US Hypertensive Adults: Results From the National Health and Nutrition Examination Survey 2009 to 2014. *Hypertension.* 2018 22;72:1365-1373.
17. D'Aiuto F, Orlandi M, Gunsolley JC. Evidence that periodontal treatment improves biomarkers and CVD outcomes. *J Periodontol.* 2013;84: S85-S105.

18. Turri A, Rossetti PH, Canullo L, Grusovin MG, Dahlin C. Prevalence of peri-implantitis in medically compromised patients and smokers: a systematic review. *Int J Oral Maxillofac Implants* 2016; 31: 111-118.
19. Dalago H, Schuldt Filho G, Rodrigues M, Renvert S, Bianchini M. Risk indicators for peri-implantitis: A cross-sectional study with 916 implants. *Clin Oral Implants Res.* 2017; 28: 144-150.
20. Monje A, Catena A, Borgnakke W. Association between diabetes mellitus/hyperglycemia and peri-implant diseases: Systematic review and meta-analysis. *J Clin Periodontol* 2017; 44: 636-648.
21. Renvert S, Aghazad eh A, Hallström H, Persson GR. Factors related to peri-implantitis - a retrospective study. *Clin Oral Implants Res.* 2014; 25: 522-529.
22. Koldslund OC , Scheie AA, Aass AM. The association between selected risk indicators and severity of peri-implantitis using mixed model analyses. *J Clin Periodontol* 2011; 38: 285-292.
23. Samson SL, Garber AJ. Metabolic syndrome. *Endocrinol Metab Clin North Am.* 2014;43: 1-23.
24. Beltran-Sanchez H, Harhay MO, Harhay MM, et al. Prevalence and trends of metabolic syndrome in the adult US population, 1999–2010. *J Am Coll Cardiol* 2013;62:697–703.
25. Expert Panel on Detection, Evaluation, and Treatment of High Blood Cholesterol in Adults. Executive summary of the third report of The National Cholesterol Education Program (NCEP) expert panel on detection, evaluation, and treatment of high blood cholesterol in adults (adult treatment panel III). *JAMA* 2001;285: 2486–2497.
26. Nilsson PM, Engstrom G, Hedblad B. The metabolic syndrome and incidence of cardiovascular disease in non-diabetic subjects—a population-based study comparing three different definitions. *Diabet Med* 2007;24:464–472.
27. Eberly LE, Prineas R, Cohen JD, et al. Metabolic syndrome: risk factor distribution and 18-year mortality in the multiple risk factor intervention trial. *Diabetes Care* 2006;29:123–130
28. Shimazaki Y, Saito T, Yonemoto K, Kiyohara Y, Iida M, Yamashita Y. Relationship of metabolic syndrome to periodontal disease in Japanese women: the Hisayama Study. *J Dent Res* 2007; 86: 271-275.
29. Nascimento GG, Leite FRM, Peres KG, Demarco FF, Corrêa MB, Peres MA. Metabolic syndrome and periodontitis: A structural equation modeling approach. [published online ahead of print November 17, 2018] *J Periodontol.*
30. D’Aiuto F, Sabbah W, Netuveli G, et al. Association of the metabolic syndrome with severe periodontitis in a large U.S. population-based survey. *J Clin Endocrinol Metab* 2008; 93: 3989-3994.
31. Khader Y, Khassawneh B, Obeidat B, et al. Periodontal status of patients with metabolic syndrome compared to those without metabolic syndrome. *J Periodontol.* 2008;79:2048–2053.
32. Li P, He L, Sha YQ, Luan QX. Relationship of metabolic syndrome to chronic periodontitis. *J Periodontol.* 2009;80:541-549.
33. Watanabe K, Cho YD. Periodontal disease and metabolic syndrome: a qualitative critical review of their association. *Arch Oral Biol.* 2014;59:855-870.
34. Nibali L, Tatarakis N, Needleman I, et al. Clinical review: association between metabolic syndrome and periodontitis: a systematic review and meta-analysis. *J Clin Endocrinol Metab* 2013; 98: 913-920.
35. Papi P, Letizia C, Piloni A, et al. Peri-implant diseases and metabolic syndrome components: a systematic review. *Eur Rev Med Pharmacol Sci.* 2018;22: 866-875.
36. Stein JH, Korcarz CE, Hurst RT, et al. Use of carotid ultrasound to identify subclinical vascular disease and evaluate cardiovascular disease risk: a consensus statement from the American Society of Echocardiography Carotid Intima-Media Thickness Task Force. Endorsed by the Society for Vascular Medicine. *J Am Soc Echocardiogr* 2008; 21:93–111.
37. Tonetti MS, Greenwell H, Kornman KS. Staging and grading of periodontitis: Framework and proposal of a new classification and case definition. *J Periodontol.* 2018;89 Suppl 1:S159-S172.
38. Mombelli A, van Oosten MA, Schurch E Jr, Land NP. The microbiota associated with successful or failing osseointegrated titanium implants. *Oral Microbiol Immunol.* 1987;2:145-151.
39. de Araújo Nobre M, Maló P. Prevalence of periodontitis, dental caries, and peri-implant pathology and their relation with systemic status and smoking habits: Results of an open-cohort study with 22009 patients in a private rehabilitation center. *J Dent.* 2017;67:36-42.
40. Vissink A, Spijkervet F, Raghoobar GM. The medically compromised patient: Are dental implants a feasible option? *Oral Dis.* 2018;24: 253-260.
41. Engin A. The Definition and Prevalence of Obesity and Metabolic Syndrome. *Adv Exp Med Biol.* 2017;960:1-17.
42. Lamster IB, Pagan M. Periodontal disease and the metabolic syndrome. *Int Dent J* 2017; 67: 67-77.

43. Atieh MA, Alsabeeha NH, Faggion CM Jr, Duncan WJ. The frequency of peri-implant diseases: a systematic review and meta-analysis. *J Periodontol* 2013; 84: 1586-1598.
44. Gurgel BCV, Montenegro SCL, Dantas PMC, Pascoal ALB, Lima KC, Calderon PDS. Frequency of peri-implant diseases and associated factors. *Clin Oral Implants Res.* 2017;28:1211-1217.
45. Pimentel SP, Shiota R, Cirano FR, et al. Occurrence of peri-implant diseases and risk indicators at the patient and implant levels: A multilevel cross-sectional study. *J Periodontol.* 2018;89:1091-1100.
46. Wada M, Mameno T, Onodera Y, Matsuda H, Daimon K, Ikebe K. Prevalence of peri-implant disease and risk indicators in a Japanese population with at least 3 years in function-A multicentre retrospective study. [published online ahead of print December 23, 2018] *Clin Oral Implants Res.*
47. Chrcanovic BR, Albrektsson T, Wennerberg A. Periodontally compromised vs. periodontally healthy patients and dental implants: a systematic review and meta-analysis. *J Dent.* 2014;42: 1509-1527.
48. Cho-Yan Lee J, Mattheos N, Nixon KC, Ivanovski S. Residual periodontal pockets are a risk indicator for peri-implantitis in patients treated for periodontitis. *Clin Oral Implants Res.* 2012;23: 325-333.
49. Derks J, Schaller D, Hakansson J, Wennstrom JL, Tomasi C, Berglundh T. Effectiveness of implant therapy analyzed in a Swedish population: prevalence of peri-implantitis. *J Dent Res.* 2016;95:43-49.
50. Dreyer H, Grischke J, Tiede C, et al. Epidemiology and risk factors of peri-implantitis: A systematic review. *J Periodontol Res.* 2018;53: 657-681.

Corresponding Author:

Dr Piero Papi

E-mail: piero.papi@uniroma1.it

Table 1: Sample demographics

Variable (categories)	Mean \pm SD or % distribution
<i>Patients without metabolic syndrome (P = 99; I = 288)</i>	
Sex, % (Male – Female)	46.5 – 53.5
Age (years)	64 \pm 10
Smoking, % (yes – no)	43.4 – 56.6
Presence of periodontitis, % (yes – no)	69.7 – 30.3
Implant years in function	8.8 \pm 5.2
Implant location (maxilla – mandible)	62.6 – 37.4
Type of prosthesis (multiple unit – single crown)	58.6 – 41.4
Probing pocket depth (mm)	3.7 \pm 1.5
Marginal bone loss (mm)	1.6 \pm 1.4
Plaque Index (%)	65.6
Mucosal Redness (%)	18.1
Suppuration (%)	12.1
Bleeding on probing (%)	71.7
Peri-implant mucositis (%)	55.6
Peri-implantitis (%)	26.3
Healthy implants (%)	18.1
<i>Patients with metabolic syndrome (P = 84; I = 279)</i>	
Sex, % (Male – Female)	29.8 – 70.2
Age (years)	68 \pm 11
Smoking, % (yes – no)	25 – 75
Presence of periodontitis, % (yes – no)	54.8 – 45.2
Implant years in function	6.5 \pm 2.3
Implant location (maxilla – mandible)	72.6 - 27.4
Type of prosthesis (multiple unit – single crown)	59.5 - 40.5
Probing depth (mm)	4.3 \pm 1.7
Marginal bone loss (mm)	2 \pm 1.4
Plaque Index (%)	69
Mucosal Redness (%)	16.6

Suppuration (%)	22.6
Bleeding on probing (%)	90.4
Peri-implant mucositis (%)	60.7
Peri-implantitis (%)	36.9
Healthy implants (%)	2.4

SD = standard deviation; mm = millimetre; P = number of patients; I = number of dental implants

Table 2: Effects of gender, diagnosis of metabolic syndrome, presence of periodontitis, smoking, type of prosthesis and location of implants on the diagnosis of mucositis and peri-implantitis.

	Peri-implant mucositis						95% Confidence Interval for Odds Ratio	
	B	S.E.	Wald	df	Sig.	Odds Ratio	Lower	Upper
Intercept	-.579	.597	.943	1	.331			
Female	.945	.582	2.633	1	.105	2.572	.822	8.052
Male	0 ^b	.	.	0
Patients with metabolic syndrome	2.309	.818	7.969	1	.005	10.066	2.026	50.021
Patients without metabolic syndrome	0 ^b	.	.	0
Patients with periodontitis	1.466	.652	5.057	1	.025	4.331	1.207	15.540
Patients without periodontitis	0 ^b	.	.	0
Smoker	-.325	.641	.257	1	.612	.723	.206	2.540
No smoker	0 ^b	.	.	0
Multiple unit	.498	.598	.694	1	.405	1.645	.510	5.306
Single crown	0 ^b	.	.	0
Implant located in mandible	.679	.570	1.423	1	.233	1.973	.646	6.024
Implant located in maxilla	0 ^b	.	.	0

Peri-implantitis							95% Confidence Interval for Odds Ratio	
	B	S.E.	Wald	df	Sig.	Odds Ratio	Lower	Upper
Intercept	-.802	.648	1.528	1	.216			
Female	.464	.622	.556	1	.456	1.590	.470	5.378
Male	0 ^b	.	.	0
Patients with metabolic syndrome	2.725	.847	10.362	1	.001	15.259	2.903	80.196
Patients without metabolic syndrome	0 ^b	.	.	0
Patients with periodontitis	2.198	.706	9.688	1	.002	9.004	2.256	35.932
Patients without periodontitis	0 ^b	.	.	0
Smokers	.111	.671	.027	1	.869	1.117	.300	4.161
No smokers	0 ^b	.	.	0
Multiple unit	-.630	.635	.985	1	.321	.532	.153	1.848
Single crown	0 ^b	.	.	0
Implant located in mandible	-.468	.644	.529	1	.467	.626	.177	2.212
Implant located in maxilla	0 ^b	.	.	0

The reference category is: No diagnosis of peri-implant disease

b. This parameter is set to zero because it is redundant

RADIOGRAPHIC OUTCOMES OF TRANSCRESTAL AND LATERAL SINUS FLOOR ELEVATION: ONE-YEAR RESULTS OF A BI-CENTER, PARALLEL-ARM RANDOMIZED TRIAL

Giovanni Franceschetti¹, **Roberto Farina**^{1,2}, **Domenico Travaglini**^{3,4}, **Ugo Consolo**^{3,4}
Luigi Minenna², **Gian Pietro Schincaglia**^{2,5}, **Orio Riccardi**^{2,6}, **Alberto Bandieri**^{3,4}, **Elisa Maietti**⁷, **Leonardo Trombelli**^{1,2}

¹ Operative Unit of Dentistry, University-Hospital of Ferrara, Italy

² Research Centre for the Study of Periodontal and Peri-implant Diseases, University of Ferrara, Italy

³ Operative Unit of Dentistry and Maxillofacial Surgery, Department Integrated Activity - Specialist Surgeries, University-Hospital of Modena, Italy

⁴ Department of Specialistic Surgeries Head-Neck, University of Modena and Reggio Emilia, Italy

⁵ Department of Periodontics, School of Dentistry, West Virginia University, Morgantown WV, (USA)

⁶ Private practice Torre Pedrera, Rimini, Italy

⁷ Center of Clinical Epidemiology, University of Ferrara, Italy

Abstract

The aim is to comparatively evaluate the radiographic outcomes of transcrestal and lateral sinus floor elevation (tSFE and lSFE, respectively) when applied concomitantly with implant placement.

Patients with ≥ 1 site with residual bone height (RBH) of 3-6 mm were enrolled in a randomized trial. Both tSFE (n= 26) and lSFE (n= 28) were associated with a xenograft, and implants were inserted concomitantly. Marginal bone loss and the maturation of the grafted area were evaluated on periapical radiographs at 6 and 12 months. Twelve-month CT/CBCT was used to assess the effect of grafting procedures circumferentially around the implant.

At 12 months, the implant surface was, on average, entirely embedded in a radiopaque area in both tSFE and lSFE groups. Sub-optimal bone-to-implant contact was observed in 13% and 3.6% of tSFE and lSFE cases, respectively. In both groups, marginal bone loss was minimal (≤ 1 mm) and infrequent, and the radiographic aspect was suggestive of an advanced stage of maturation.

At sites with RBH of 3-6 mm, tSFE and lSFE can similarly result in a substantial increase in peri-implant bone support at 12 months.

(ClinicalTrials.gov ID: NCT02415946)

Introduction

At maxillary posterior sites where post-extraction pneumatization of the maxillary sinus has contributed the dimensional reduction of the residual bone crest following tooth loss (Eufinger et al. 1997, 1999, Farina et al. 2011, Pramstraller et al. 2011), maxillary sinus floor elevation with a lateral (lSFE) or transcrestal (tSFE) approach represent two options to enhance the available bone and restore the local conditions compatible with the placement and long-term survival of dental implants (Pjetursson et al. 2008, Tan et al. 2008, Listl & Faggion 2010, Tetsch et al. 2010, Esposito et al. 2014).

Indications to apply tSFE or lSFE should be determined primarily on the basis of their potential to enhance the peri-implant bony support. Due to the possibility to visualize directly the sinus cavity through the lateral antrotomy and extend the elevation of the sinus membrane according to individual needs and local anatomy, lSFE has several technical premises for achieving substantial augmentation. Confirmatory data come from studies

reporting a mean vertical extent of sinus lift (as evaluated radiographically) varying from about 8 mm to more than 14 mm when ISFE was obtained with a bovine-derived xenograft (Felice et al. 2009, Chackartchi et al. 2011, Merli et al. 2013). On the other hand, tSFE has limitations related to its closed approach to the sinus, including the difficulty in determining the extent of sinus lift achievable in relation to the presumed tensile resistance of the sinus membrane. Consistently, several clinical trials reported a vertical extent of sinus lift (as assessed radiographically) lower than that reported for ISFE, with mean values ranging between 1.7 mm (Pjetursson et al. 2009) and more than 8 mm (Kfir et al. 2007, Sisti et al. 2012).

To date, studies that comparatively evaluated tSFE and ISFE either lack of a randomized design or refer to different surgical conditions between treatments (Zitzmann & Schärer 1998, Rodoni et al. 2005, Krenmair et al. 2007, Jurisic et al. 2008, Cannizzaro et al. 2009, Tetsch et al. 2010, Kim et al. 2011, Al-Almaie et al. 2013, Yu et al. 2017, Temmerman et al. 2017). Most of them included a radiographic assessment based on bi-dimensional radiographic exams such as ortopantomography and/or periapical radiographs (Rodoni et al. 2005, Krenmair et al. 2007, Jurisic et al. 2008, Cannizzaro et al. 2009, Tetsch et al. 2010, Kim et al. 2011, Al-Almaie et al. 2013, Yu et al. 2017), with the impossibility to evaluate the extent of peri-implant bone augmentation circumferentially around the implant. Tridimensional radiographic exams such as conventional or cone-beam computed tomography (CT or CBCT, respectively) were used in a limited number of studies, only in a subsample of consenting patients (Zitzmann & Schärer 1998) or at very short post-surgery intervals (Temmerman et al. 2017).

Recently, we performed a bi-center, parallel-arm, randomized trial comparatively evaluating tSFE and ISFE when applied concomitantly with implant placement at sites with limited (3-6 mm) residual bone. The results of the study have been partly published, and allowed for the identification of differences in the morbidity following the two interventions (Farina et al. 2018). Based on bi- and tri-dimensional radiographic assessments conducted by Farina et al. (2018), the purpose of the present study is to comparatively evaluate the extent of bone augmentation (with particular emphasis to the contribution of each intervention to the peri-implant bony support) obtained at 1 year following either tSFE or ISFE and concomitant implant placement.

Materials and Methods

Experimental design

The study is a bi-center, parallel-arm, single-blind, randomized controlled clinical trial, and is part of a larger project which comparatively evaluated tSFE and ISFE under several perspectives. Information on ethical approval and trial registration, the methodological aspects of the study and the surgical aspects of the procedures have been reported in a recent publication on the morbidity of tSFE and ISFE (Farina et al. 2018). The present study reports only methodological aspects and data functional to evaluate the radiographic outcomes of the two investigated interventions.

Study population

Patients were recruited at two University-Hospitals (Ferrara and Modena, Italy) according to selection criteria reported by Farina et al. (2018). Briefly, each patient contributed the study with one maxillary quadrant (identified as “experimental”) with ≥ 1 maxillary posterior site edentulous for at least 6 months and showing a residual bone height (RBH) of $3 \div 6$ mm. RBH was measured on CT or CBCT performed while wearing a radiological stent with 4-mm thick radiopaque indicators.

Surgical and post-surgical procedures

The surgical aspects of tSFE and lSFE and the post-surgical procedures are described briefly in the following paragraphs. Additional details have been reported in a previous publication (Farina et al. 2018).

tSFE was performed according to the *Smart Lift* technique (Trombelli et al. 2008, 2010a,b). After placing a plug of collagen matrix (Mucograft Seal®; Geistlich Pharma, AG, Wolhusen, Switzerland), the trephined bone core was condensed and malleted with a calibrated osteotome (*Smart Lift Elevator*) to fracture the sinus floor. Membrane perforation was assessed by the Valsalva maneuver. If no perforation was detected, a pre-determined amount of deproteinized bovine bone mineral (DBBM; Bio-Oss® spongiosa granules, particle size 0.25-1.0 mm; Geistlich Pharma, AG, Wolhusen, Switzerland), which was related to the programmed extent of implant penetration into the sinus, was pushed through each implant site by gradual increments with the *Smart Lift Elevator*. When membrane perforation was detected, it was treated with repeated insertions of plugs trimmed from a collagen matrix (Mucograft Seal®; Geistlich Pharma AG, Wolhusen, Switzerland) in the apical portion of the crestal access. The Valsalva maneuver was then re-assessed: if negative, the grafting procedure was completed and the implant was inserted; if positive, the patient exited the study, and tSFE and concomitant implant placement were postponed at 4 months following first surgery.

In patients assigned to lSFE, lateral access to the maxillary sinus was obtained with rotating and/or manual instruments. The grafting procedure was performed with DBBM (Bio-Oss® spongiosa granules, particle size 0.25-1.0 mm or 1-2 mm; Geistlich Pharma, AG, Wolhusen, Switzerland) immediately after the elevation of the sinus membrane with manual instruments (Hu-Friedy, Chicago, US). The particle size and amount of graft material were left at operator discretion. Implant bed preparation was, then, performed according to the sequence of burs recommended by the implant manufacturer (Thommen Medical AG; Grenchen, Switzerland). The window in the lateral wall was covered with a resorbable collagen membrane (Bio-Gide; Geistlich Pharma, AG, Wolhusen, Switzerland). When membrane perforation (as visually detected) occurred, it was treated according to Fugazzotto & Vlassis (2003), and the grafting procedure was completed.

In both tSFE and lSFE groups, implants (SPI Inicell Element®; Thommen Medical AG, Grenchen, Switzerland) were inserted immediately after the completion of the grafting procedure with the 1.0 mm polished collar above the bone crest. The healing protocol (submerged or transmucosal) was left at the operator's discretion.

Implants placed with a submerged healing protocol at day 0 were surgically exposed at 20 weeks post-surgery, and a healing abutment was positioned. Implants were loaded with a provisional or definitive restoration (according to their treatment plan) between week +24 and week +32. The patient exited the study at week +48.

Radiographic exams and measurements

At the time of implant loading with a provisional or definitive restoration (performed between week +24 and week +32) and at week +48 ± 4 weeks (identified as 6- and 12-month follow-up visits, respectively), peri-apical radiographs were obtained with a paralleling technique using a Rinn film holder with a rigid film-object X-ray source, and were then scanned, digitized, and stored at a resolution of 600 dpi. Also, a CT or a CBCT of the implant areas was performed at 12-month visit, and data were saved in Digital Imaging and Communications in Medicine (DICOM) file format.

Measurements on digitized periapical radiographs were performed using an image-processing software (NIS Elements® v4.2; Nikon Instruments, Campi Bisenzio, Firenze, Italy), while a software for implant planning was used for measurements on CT and CBCT scans

(Nobel clinician® v2.6.3.2; Nobel Biocare Services AG, Kloten, Switzerland). All radiographic measurements were performed by a single trained examiner (G.F.) who had previously undergone a calibration session for linear radiographic measurements on a sample of 15 patients not included in the study (Cohen's k-coefficient for intra-examiner agreement: 0.981) and had participated as clinical examiner in previous clinical trials on sinus lift procedures (Trombelli et al. 2008, 2010a,b, 2012, 2014, 2015, Franceschetti et al. 2014, 2015, 2017, Farina et al. 2018). The examiner was kept blinded as to treatment group and observation interval.

On digitized periapical radiographs taken at 6- and 12-month visit, the following measurements were performed using a digital caliper:

- radiographic implant length (rIL): distance (in mm) from the apical margin of the implant shoulder to the implant apex as assessed at the mesial or distal aspect of the implant;
- peri-implant bone level at the mesial (mPBL) and distal (dPBL) aspects of the implant: distance (in mm) from the apical margin of the implant shoulder to the first bone-to-implant contact at the mesial and distal aspect of the implant, respectively. To account for radiographic distortion, mPBL and dPBL were adjusted for a coefficient derived from the ratio: true length of the implant / radiographic implant length (rIL);
- maturation of the grafted space: assessed using the sinus grafting remodeling index (SGRI) (Brägger et al. 2004).

On CT and CBCT scans performed at 12-month visit, the following parameters were assessed:

- percentage ratio between the linear length (in mm) of the implant surface in direct contact with the peri-implant radiopaque area (native bone + newly formed bone) and the linear length (in mm) of implant surface (CON%). CON% measurements were performed on each of 180 CT/CBCT sections (with a 1° difference in angle between adjacent sections) parallel to the long axis of the implant and passing through the mid portion of the implant. CON% measurements from the 180 CT/CBCT sections were averaged (totCON%). Also, CON% were reported separately for the mesial, distal and apical aspect of the implant as assessed on the CT/CBCT mesio-distal section (mCON%, dCON%, and aCON%_{m-d}, respectively) and for the buccal, palatal and apical aspect of the implant as assessed on bucco-lingual CT/CBCT section (bCON%, pCON%, and aCON%_{b-p}, respectively);
- height of the radiopaque area apical to the implant apex (aGH): distance (in mm) occupied by a radiopaque area between the implant apex and the most apical position of the radiopaque area as assessed at the mid portion of the implant on the CT/CBCT section passing through the mid portion of the implant apex.

Statistical Analysis

Sample size calculation

totCON% was the primary outcome variable of the study. Since no data on totCON% related to the investigated interventions could be derived from previous comparative studies, sample size calculation was based on aGH. Assuming a standard deviation in sinus lift of 2.0 mm for both tSFE, as derived from an internal analysis of data from the studies by Trombelli et al. (2012, 2014) and Franceschetti et al. (2014), and lSFE (Chackartchi et al. 2011, Merli et al. 2013), and an expected inter-group difference in sinus lift of 3.0 mm (Zitzmann & Schärer 1998), a *per protocol* study population of at least 48 patients (24 treated with tSFE, 24 treated with lSFE) was needed for a two-tailed test to detect an inter-group difference in aGH with a power higher than 95% and a p-level of 0.05.

Descriptive and inferential statistics

A *per-protocol* (PP) analysis was performed. The patient was regarded as the statistical unit. Therefore, for patients receiving two implants concomitantly with sinus floor elevation in the

experimental quadrant, only the implant showing the lowest totCON% was included for analysis. If multiple implants within the experimental quadrant had the same totCON%, only the implant with the lowest aGH was included for analysis. Since all numerical variables showed a non-normal and non-symmetric distribution, they were expressed as median and interquartile range (IR). Within-group comparisons for mPBL, dPBL and SGRI were performed between 6- and 12-month visits using Wilcoxon test. Treatment groups were compared using χ^2 test or Fisher's exact test for categorical variables and Mann-Whitney U-test for numerical and ordinal variables. The level of statistical significance was fixed at 0.05, and the analysis was done using Stata 13 for Windows (StataCorp, College Station, TX).

Results

Study population

Twenty-nine patients and 28 patients were randomly allocated to tSFE and lSFE group, respectively (Figure 1). In tSFE group, 1 implant was immediately removed after placement due to the lack of primary stability, while 1 implant in another patient failed to osseointegrate and was removed at 2 months after insertion. Both patients were excluded from the present analysis, and received an implant of same dimensions 6 months later without additional bone augmentation. Another patient in tSFE group suffered acute myocardial infarction after the 6-month visit, postponed all the 12-month radiographic exams and was therefore excluded from the study. The PP study population consisted of 26 patients in the tSFE group and 28 patients in the lSFE group (Figure 1). Patient and implant characteristics in tSFE and lSFE groups are reported in Table 1.

Radiographic outcomes

In tSFE group, DICOM files of three 12-month CT/CBCT exams could not be analyzed due to technical issues. Therefore, totCON% and aGH measurements in tSFE group were performed on 23 patients. Radiographic outcomes are reported in Table 2 and Figures 2-5. Each patient is consistently identified with the same numeric code through Figures 2-5.

No center effect on totCON% and aGH was found. Data on CON% are reported in Table 2 and Figure 2. totCON% was 100% in both groups, with no significant inter-group difference ($p=0.580$) (Table 2). Three patients (13.0%) in the tSFE group showed totCON% lower than 100%, with totCON% values ranging between 71.1% and 86.3%. In tSFE group, totCON% lower than 100% was mainly due to the absence of a peri-implant radiopaque area in the apical part of the implant (i.e., aCON%_{ob-p} and aCON%_{m-d} = 0) (Figure 2). One patient (3.6%) in lSFE group showed totCON% lower than 100% (totCON%= 77.6%) due to the partial absence of a peri-implant radiopaque area at the palatal aspect (i.e., pCON%= 60%) (Figure 2).

aGH was significantly higher in lSFE group (6.2 mm; IR: 3.3 – 8.3) compared to tSFE group (0.6 mm; IR: 0.5 – 1.6) ($p<0.0001$). aGH was positive in 20 patients (87.0%) and 27 patients (96.4%) in tSFE and lSFE groups, respectively, and was 0 in the other patients (Figure 3).

At 6 months, mPBL and dPBL were 0 mm (IR: 0 - 0) in both groups ($p=0.637$ and $p=0.790$, respectively). Two patients (7.7%) in the tSFE group and 1 patient (3.6%) in the lSFE group showed mPBL and/or dPBL > 0 mm. At 12 months, mPBL and dPBL were 0 mm (IR: 0 – 0) in both groups ($p=0.600$ and $p=0.553$, respectively). Four (15.4%) patients in the tSFE group and 5 (17.9%) patients in the lSFE group showed mPBL and/or dPBL > 0 mm (Figure 4). No significant changes in mPBL and dPBL were observed between the 6-month and 12-month visit.

SGRI values as observed at 6 and 12 months in each patient are reported in Figure 5. At 6 months, SGRI was significantly higher in ISFE group (3.0; IR: 2.0 - 3.0) compared to tSFE group (2.0; IR: 2.0 - 3.0) ($p= 0.006$). The score was 3 at 20 sites, and 2 at 8 sites in ISFE group, whereas 3 at 9 sites, 2 at 11 sites, 1 at 4 sites, and 0 at 2 sites in the tSFE group. At 12 months, SGRI was significantly higher in ISFE group (3.0; IR: 3.0 - 3.0) compared to tSFE group (3.0; IR: 2.0 - 3.0) ($p= 0.026$). The score was 3 at 24 sites, and 2 at 4 sites in ISFE group, whereas 3 at 14 sites, 2 at 6 sites, 1 at 4 sites, and 0 at 2 sites in the tSFE group. The variation in SGRI as observed between 6 and 12-month visit was significant only in tSFE group ($p= 0.043$).

Conclusions

In conclusion, the results of the present study demonstrated that tSFE (when performed according to the *Smart Lift* technique) and ISFE similarly contribute to increase substantially the peri-implant bone support at sites with residual bone height of 3-6 mm at 12 months post-surgery.

Acknowledgements

The study was supported by a research grant by Regione Emilia-Romagna (Programma di Ricerca Regione-Università, Area 1 “Ricerca Innovativa”, Bando Giovani Ricercatori “Alessandro Liberati” 2013; project PRUA1GR-2013-00000168), and by a research grant of the Osteology Foundation, Lucerne, Switzerland (project #13-063).

Regenerative devices were kindly provided by Geistlich Biomaterials Italia, Thiene, Italy. Dental implants were kindly provided by Dental Trey, Fiumana-Predappio, Italy.

Conflict of interest

The Authors declare they have no conflict of interest related to the present study.

References

1. Abdulkarim, H.H., Miley, D.D., McLeod, D.E. & Garcia, M.N. (2013) Short-term evaluation of bioactive glass using the modified osteotome sinus elevation technique. *Implant Dentistry* **22**, 491-498.
2. Al-Almaie, S., Kavarodi, A.M. & Al Faidhi, A. (2013) Maxillary sinus functions and complications with lateral window and osteotome sinus floor elevation procedures followed by dental implants placement: a retrospective study in 60 patients. *Journal of Contemporary Dental Practice* **14**, 405-413.
3. Brägger, U., Gerber, C., Joss, A., Haenni, S., Meier, A., Hashorva, E. & Lang, N.P. (2004) Patterns of tissue remodeling after placement of ITIs dental implants using an osteotome technique: a longitudinal radiographic case cohort study. *Clinical Oral Implants Research* **15**, 158-166.
4. Cannizzaro, G., Felice, P., Leone, M., Viola, P. & Esposito, M. (2009) Early loading of implants in the atrophic posterior maxilla: lateral sinus lift with autogenous bone and Bio-Oss versus crestal mini sinus lift and 8-mm hydroxyapatite-coated implants. A randomised controlled clinical trial. *European Journal of Oral Implantology* **2**, 25-38.
5. Chackartchi, T., Iezzi, G., Goldstein, M., Klinger, A., Soskolne, A., Piattelli, A. & Shapira, L. (2011) Sinus floor augmentation using large (1-2 mm) or small (0.25-1 mm) bovine bone mineral particles: a prospective, intra-individual controlled clinical, micro-computerized tomography and histomorphometric study. *Clinical Oral Implants Research* **22**, 473-480.
6. Esposito, M., Felice, P. & Worthington, H.V. (2014) Interventions for replacing missing teeth: augmentation procedures of the maxillary sinus. *Cochrane Database of Systematic Reviews* Issue 5. Art. No.: CD008397.
7. Eufinger, H., König, S. & Eufinger, A. (1997) The role of alveolar ridge width in dental implantology. *Clinical Oral Investigations* **1**, 169-177.
8. Eufinger, H., König, S., Eufinger, A. & Machtens, E. (1999) Significance of the height and width of the alveolar ridge in implantology in the edentulous maxilla. Analysis of 95 cadaver jaws and 24 consecutive patients. *Mund-, Kiefer- und Gesichtschirurgie* **3 (Suppl 1)**, S14-18. (article in german)
9. Farina, R., Pramstraller, M., Franceschetti, G., Pramstraller, C. & Trombelli, L. (2011) Alveolar ridge dimensions in maxillary posterior sextants: a retrospective comparative study of dentate and edentulous sites using computerized tomography data. *Clinical Oral Implants Research* **22**, 1138-1144.
10. Farina, R., Franceschetti, G., Travaglini, D., Consolo, U., Minenna, L., Schincaglia, G.P., Riccardi, O., Bandieri, A., Maietti, E. & Trombelli, L. (2018) Morbidity following transcresal and lateral sinus floor elevation: A randomized trial. *Journal of Clinical Periodontology* **45**, 1128-1139.
11. Felice, P., Scarano, A., Pistilli, R., Checchi, L., Piattelli, M., Pellegrino, G. & Esposito, M. (2009) A comparison of two techniques to augment maxillary sinuses using the lateral window approach: rigid synthetic resorbable barriers versus anorganic bovine bone. Five-month post-loading clinical and histological results of a pilot randomised controlled clinical trial. *European Journal of Oral Implantology* **2**, 293-306.
12. Fornell, J., Johansson, L.-Å., Bolin, A., Isaksson, S. & Sennerby, L. (2012) Flapless, CBCT-guided osteotome sinus floor elevation with simultaneous implant installation. I: radiographic examination and surgical technique. A prospective 1-year follow-up. *Clinical Oral Implants Research* **23**, 28-34.
13. Franceschetti, G., Farina, R., Stacchi, C., Di Lenarda, R., Di Raimondo, R. & Trombelli, L. (2014) Radiographic outcomes of transcresal sinus floor elevation performed with a minimally invasive technique in smoker and non-smoker patients. *Clinical Oral Implants Research* **25**, 493-499.
14. Franceschetti, G., Farina, R., Minenna, L., Franceschetti, G. & Trombelli, L. (2015) Learning curve of a minimally invasive technique for transcresal sinus floor elevation: a split-group analysis in a prospective case series with multiple clinicians. *Implant Dentistry* **24**, 517-526.
15. Franceschetti, G., Rizzi, A., Minenna, L., Pramstraller, M., Trombelli, L. & Farina, R. (2017) Patient-reported outcomes of implant placement performed concomitantly with transcresal sinus floor elevation or entirely in native bone. *Clinical Oral Implants Research* **28**, 156-162.
16. Fugazzotto, P.A. & Vlassis, J. (2003) A simplified classification and repair system for sinus membrane perforations. *Journal of Periodontology* **74**, 1534-1541.
17. Jung, J.-H., Choi, S.-H., Cho, K.-S. & Kim, C.-S. (2010) Bone-added osteotome sinus floor elevation with simultaneous placement of non-submerged sand blasted with large grit and acid etched implants: a 5-year radiographic evaluation. *Journal of Periodontal & Implant Science* **40**, 69-75.
18. Jurisic, M., Markovic, A., Radulovic, M., Brkovic, B.M. & Sándor, G.K. (2008) Maxillary sinus floor augmentation: comparing osteotome with lateral window immediate and delayed implant placements. An interim report. *Oral Surgery Oral Medicine Oral Pathology Oral Radiology and Endodontics* **106**, 820-827.

19. Kfir, E., Kfir, V., Eliav, E., & Kaluski, E. (2007) Minimally Invasive Antral Membrane Balloon Elevation: Report of 36 Procedures. *Journal of Periodontology* **78**, 2032-2035.
20. Kim, S.M., Park, J.W., Suh, J.Y., Sohn, D.S. & Lee, J.M. (2011) Bone-added osteotome technique versus lateral approach for sinus floor elevation: a comparative radiographic study. *Implant Dentistry* **20**, 465-470.
21. Krennmair, G., Krainhöfner, M., Schmid-Schwab, M. & Piehslinger, E. (2007) Maxillary sinus lift for single implant-supported restorations: a clinical study. *International Journal of Oral and Maxillofacial Implants* **22**, 351-358.
22. Listl, S. & Faggion, C.M. Jr. (2010) An economic evaluation of different sinus lift techniques. *Journal of Clinical Periodontology* **37**, 777-787.
23. Mardinger, O., Chaushu, G., Sigalov, S., Herzberg, R., Shlomi, B. & Schwartz-Arad, D. (2011) Factors affecting changes in sinus graft height between and above the placed implants. *Oral Surgery Oral Medicine Oral Pathology Oral Radiology and Endodontics* **111**, e6-11.
24. Markovic, A., Mišić, T., Calvo-Guirado, J.L., Delgado-Ruiz, R.A., Janjic, B. & Abboud, M. (2016) Two-Center Prospective, Randomized, Clinical, and Radiographic Study Comparing Osteotome Sinus Floor Elevation with or without Bone Graft and Simultaneous Implant Placement. *Clinical Implant Dentistry and Related Research* **18**, 873-882.
25. Mazzocco, F., Lops, D., Gobbato, L., Lolato, A., Romeo, E. & Del Fabbro, M. (2014) Three-Dimensional Volume Change of Grafted Bone in the Maxillary Sinus. *International Journal of Oral and Maxillofacial Implants* **29**, 178-184.
26. Merli, M., Moscatelli, M., Mariotti, G., Rotundo, R. & Nieri, M. (2013) Autogenous bone versus deproteinised bovine bone matrix in 1-stage lateral sinus floor elevation in the severely atrophied maxilla: a randomised controlled trial. *European Journal of Oral Implantology* **6**, 27-37.
27. Nishida, T., Takenouchi, Y., Mori, K., Arijii, M., Nishida, K. & Ito, K. (2013) Remodeling of autogenous bone grafts after osteotome sinus floor elevation assessed by limited cone beam computed tomography. *International Journal of Dentistry* 931708.
28. Pramstraller, M., Farina, R., Franceschetti, G., Pramstraller, C. & Trombelli, L. (2011) Ridge dimensions of the edentulous posterior maxilla: a retrospective analysis of a cohort of 127 patients using computerized tomography data. *Clinical Oral Implants Research* **22**, 54-61. Erratum in: *Clinical Oral Implants Research* 2011;**22**:235.
29. Pjetursson, B.E., Tan, W.C., Zwahlen, M. & Lang, N.P. (2008) A systematic review of the success of sinus floor elevation and survival of implants inserted in combination with sinus floor elevation. *Journal of Clinical Periodontology* **35(8 Suppl)**, 216-240.
30. Pjetursson, B.E., Rast, C., Bragger, U., Zwahlen, M. & Lang, N.P. (2009) Maxillary sinus floor elevation using the osteome technique with or without grafting material. Part I – Implant survival and patient's perception. *Clinical Oral Implants Research* **20**, 667-676.
31. Rodoni, L., Glauser, R., Feloutzis, A. & Hämmerle, C.H.F. (2005) Implants in the Posterior Maxilla: A Comparative Clinical and Radiologic Study. *International Journal of Oral and Maxillofacial Implants* **20**, 231-237.
32. Sisti, A., Canullo, L., Mottola, M.P. & Ianello, G. (2012) Crestal minimally-invasive sinus lift on severely resorbed maxillary crest: prospective study. *Biomedizinische Technik. Biomedical Engineering (Berl)* **57**, 45-51.
33. Tallarico, M., Cochran, D.L., Khanari, E., Dellavia, C., Canciani, E., Mijiritsky, E. & Meloni, S.M. (2017) Crestal sinus lift using an implant with an internal L-shaped channel: 1-year after loading results from a prospective cohort study. *European Journal of Oral Implantology* **10**, 325-336.
34. Tan, W.C., Lang, N.P., Zwahlen, M. & Pjetursson, B.E. (2008) A systematic review of the success of sinus floor elevation and survival of implants inserted in combination with sinus floor elevation. Part II: transalveolar technique. *Journal of Clinical Periodontology* **35(8 Suppl)**, 241-254.
35. Temmerman, A., Van Dessel, J., Cortellini, S., Jacobs, R., Teughels, W. & Quirynen, M. (2017) Volumetric changes of grafted volumes and the Schneiderian membrane after transcresal and lateral sinus floor elevation procedures: A clinical, pilot study. *Journal of Clinical Periodontology* **44**, 660-671.
36. Tetsch, J., Tetsch, P. & Lysek, D.A. (2010) Long-term results after lateral and osteotome technique sinus floor elevation: a retrospective analysis of 2190 implants over a time period of 15 years. *Clinical Oral Implants Research* **21**, 497-503.
37. Trombelli, L., Minenna, P., Franceschetti, G., Farina, R. & Minenna, L. (2008) [Smart Lift: una nuova procedura minimamente invasiva per la elevazione del pavimento del seno mascellare]. *Dental Cadmos* **76**, 71-83. [article in italian]
38. Trombelli, L., Minenna, P., Franceschetti, G., Minenna, L., Itró, A. & Farina, R. (2010a) Minimally invasive technique for transcresal sinus floor elevation: a case report. *Quintessence International* **41**, 363-369.

39. Trombelli, L., Minenna, P., Franceschetti, G., Minenna, L. & Farina, R. (2010b). Transcrestal sinus floor elevation with a minimally invasive technique. *Journal of Periodontology* **81**, 158-166.
40. Trombelli, L., Franceschetti, G., Rizzi, A., Minenna, P., Minenna, L. & Farina, R. (2012) Minimally invasive transcrestal sinus floor elevation with graft biomaterials. A randomized clinical trial. *Clinical Oral Implants Research* **23**, 424-432.
41. Trombelli, L., Franceschetti, G., Stacchi, C., Minenna, L., Riccardi, O.L., Di Raimondo, R., Rizzi, A. & Farina, R. (2014) Minimally-invasive transcrestal sinus floor elevation with a deproteinized bovine bone or β -tricalcium phosphate: a multicenter, randomized, controlled clinical trial. *Journal of Clinical Periodontology* **41**, 311-319.
42. Trombelli, L., Franceschetti, G., Trisi, P. & Farina, R. (2015) Incremental, transcrestal sinus floor elevation with a minimally invasive technique in the rehabilitation of severe maxillary atrophy. Clinical and histological findings from a proof-of-concept case series. *Journal of Oral and Maxillofacial Surgery* **73**, 861-888.
43. Umanjec-Korac, S., Wu, G., Hassan, B., Liu, Y. & Wismeijer, D. (2014) A retrospective analysis of the resorption rate of deproteinized bovine bone as maxillary sinus graft material on cone beam computed tomography. *Clinical Oral Implants Research* **25**, 781-785.
44. Yu, H., Wang, X. & Qiu, L. (2017) Outcomes of 6.5-mm Hydrophilic Implants and Long Implants Placed with Lateral Sinus Floor Elevation in the Atrophic Posterior Maxilla: A Prospective, Randomized Controlled Clinical Comparison. *Clinical Implant Dentistry and Related Research* **19**, 111-122.
45. Zitzmann, N.U. & Schärer, P. (1998) Sinus elevation procedures in the resorbed posterior maxilla. Comparison of the crestal and lateral approaches. *Oral Surgery Oral Medicine Oral Pathology Oral Radiology and Endodontics* **85**, 8-17.

Corresponding Author:

Dr Giovanni Franceschetti

E-mail: frngnn1@unife.it

Table 1. Patient and implant characteristics in tSFE and ISFE groups.

	n° patients/ implants	age (years)	gender	smoking status	RBH (mm)	implant diameter (mm)	implant length (mm)
	n	median (IR)	n° males / n° females	n° current smokers / former smokers/never smoked	median (IR)	median (IR)	median (IR)
tSFE group	26	51.6 (47.0 – 58.5)	15 / 11	4 / 2 / 20	5.0 (4.1 - 5.4)	4.0 (4.0 - 4.0)	9.5 (9.5 – 11.0)
ISFE group	28	53.0 (48.5 - 59.0)	11 / 17	3 / 2 / 23	4.1 (4.0 – 5.1)	4.0 (4.0 - 4.0)	9.5 (9.5 – 11.0)
<i>p</i> value		0.461	0.176	0.882	0.123	0.146	0.485

Table legend

IR: inter-quartile range; RBH: residual bone height; tSFE: transcrestal sinus floor elevation (*Smart Lift* technique); ISFE: lateral sinus floor elevation.

Table 2. Proportion of the implant surface in direct contact with the radiopaque area (CON%) as assessed at 12 months post-surgery on the CT/CBCT. CON% measurements were performed on the CT/CBCT mesio-distal section assessing CON% on mesial, distal and apical aspect of the implant (mCON%, dCON%, and aCON%_{m-d}, respectively) and on bucco-lingual CT/CBCT section assessing CON% on buccal, palatal and apical aspect of the implant (bCON%, pCON%, and aCON%_{b-p}, respectively). totCON% expresses the proportion of the implant surface in direct contact with the radiopaque area obtained by averaging CON% measurements of all 180 CT/CBCT sections parallel to the long axis of the implant and passing through the mid portion of the implant.

	totCON%	bCON%	aCON%_{b-p}	pCON%	mCON%	aCON%_{m-d}	dCON%
tSFE group *	100 (IR: 100 - 100; min: 71.1 - max: 100)	100 (IR: 100 - 100; min: 72.6 - max: 100)	100 (IR: 100 - 100; min: 0 - max: 100)	100 (IR: 100 - 100; min: 60.0 - 100)	100 (IR: 100 - 100; min: 73.6 - max: 100)	100 (IR: 100 - 100; min: 0 - max: 100)	100 (IR: 100 - 100; min: 100 - max: 100)
ISFE group	100 (IR: 100 - 100; min: 77.6 - max: 100)	100 (IR: 100 - 100; min: 100 - max: 100)	100 (IR: 100 - 100; min: 60.0 - max: 100)	100 (IR: 100 - 100; min: 60.0 - max: 100)	100 (IR: 100 - 100; min: 100 - max: 100)	100 (IR: 100 - 100; min: 100 - max: 100)	100 (IR: 100 - 100; min: 100 - max: 100)
p value	0.580	0.606	0.554	0.963	0.800	0.435	0.992

Table legend

IR: inter-quartile range; ISFE: lateral sinus floor elevation; min: minimum value; max: maximum value; tSFE: transcrestal sinus floor elevation.

* In tSFE group, DICOM files of three 12-month CT/CBCT exams could not be analyzed due to technical issues. Therefore, CON% measurements in tSFE group were performed on 23, and not 26, patients.

Figure 1. Flow chart of patient inclusion and follow-up.

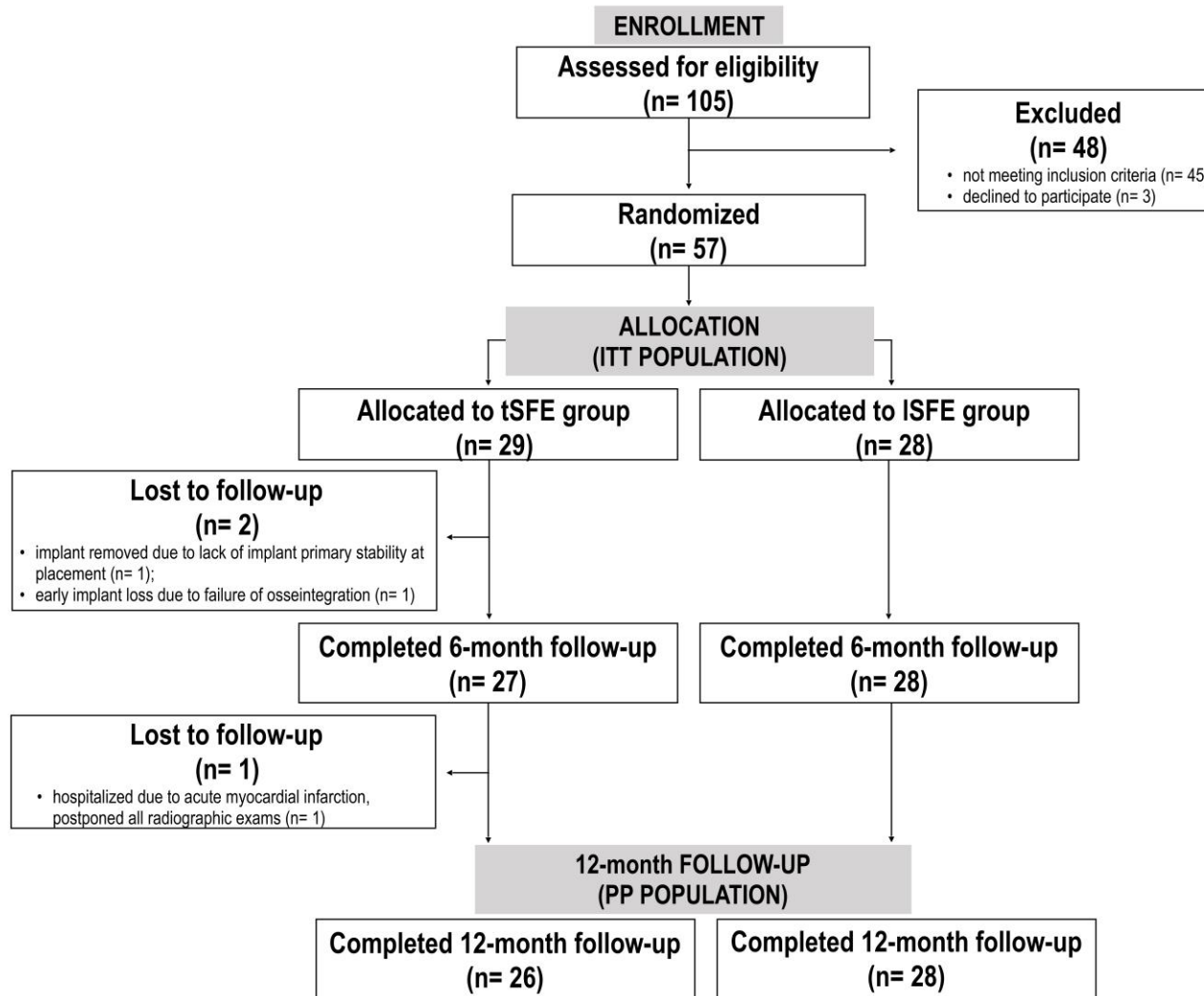


Figure 2. CON% (percentage proportion of the implant surface in direct contact with the radiopaque area) values as assessed on the 12-month CT/CBCT of each patient in tSFE and ISFE groups.

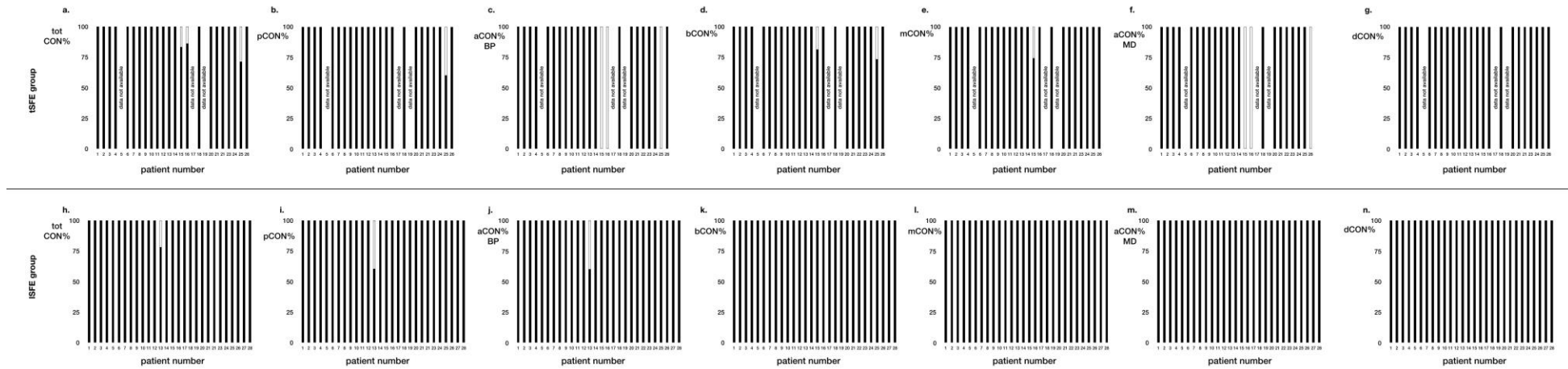


Figure 3. Height of the radiopaque area apical to the implant apex (aGH) as assessed in mm on the 12-month CT/CBCT of each patient in the tSFE group (a) and ISFE group (b).

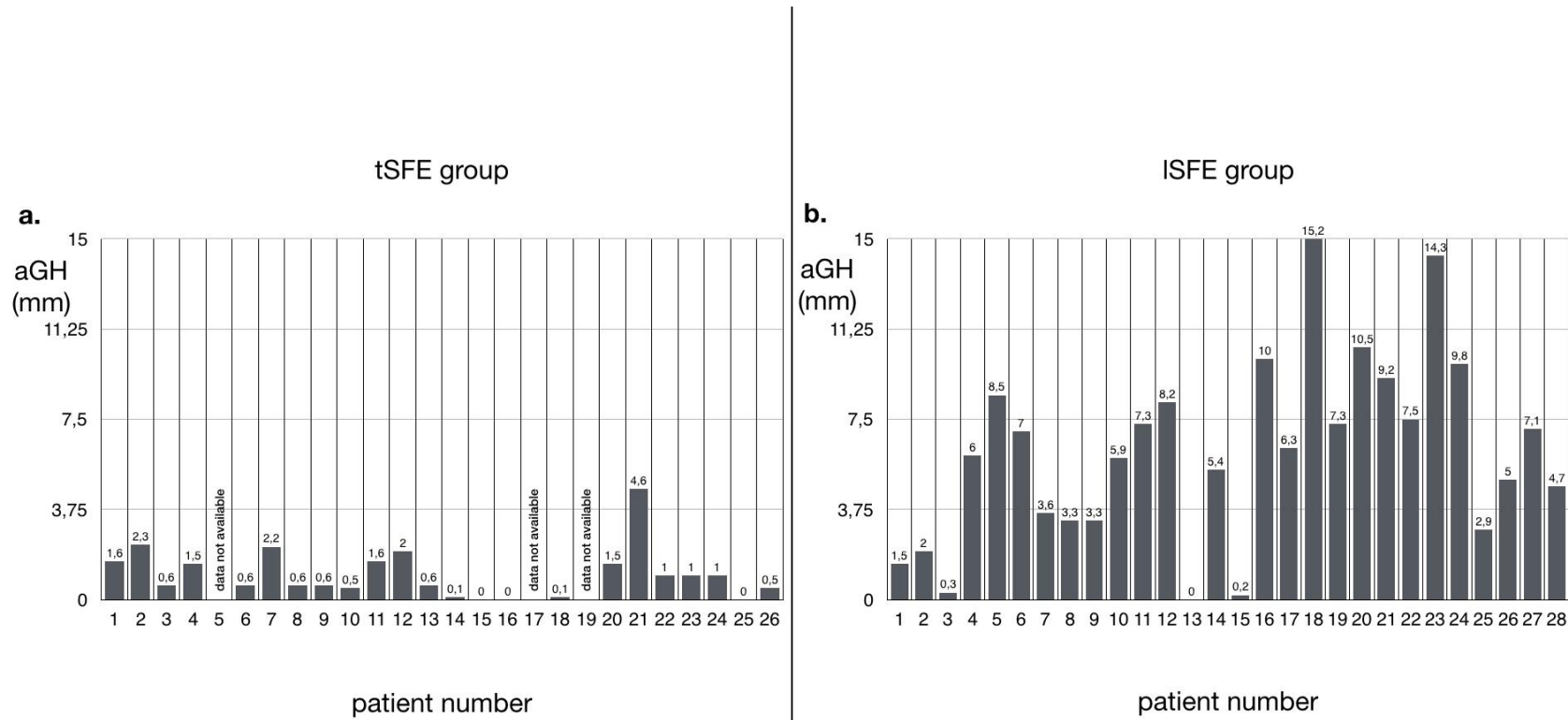


Figure 4. Peri-implant bone level (as assessed in mm on the 12-month periapical radiograph) at the mesial and distal aspects of the implant (mPBL and dPBL, respectively): **a)** mPBL in each patient of the tSFE group; **b)** dPBL in each patient of the tSFE group; **c)** mPBL in each patient of the lSFE group; **d)** dPBL in each patient of the lSFE group.

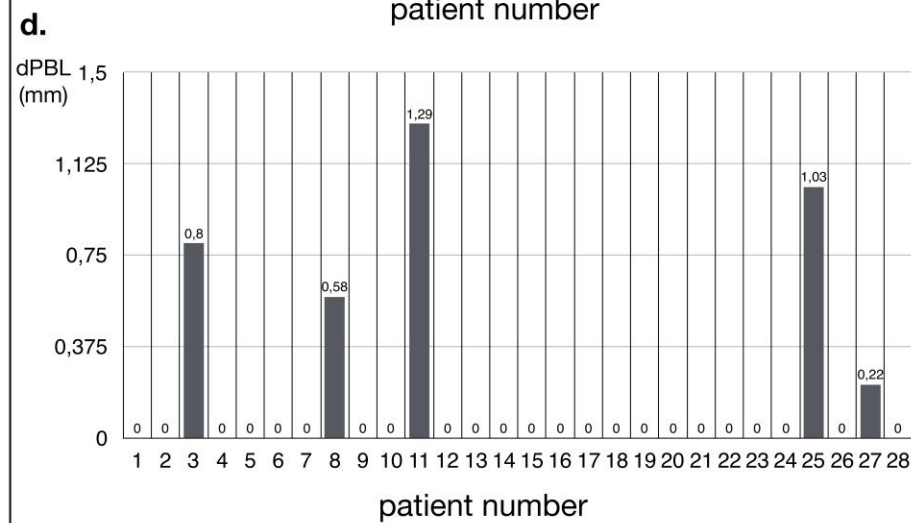
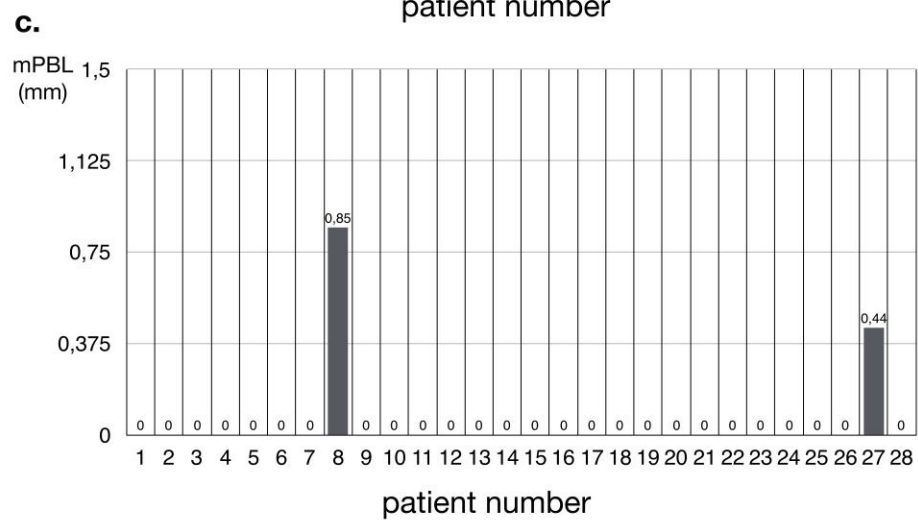
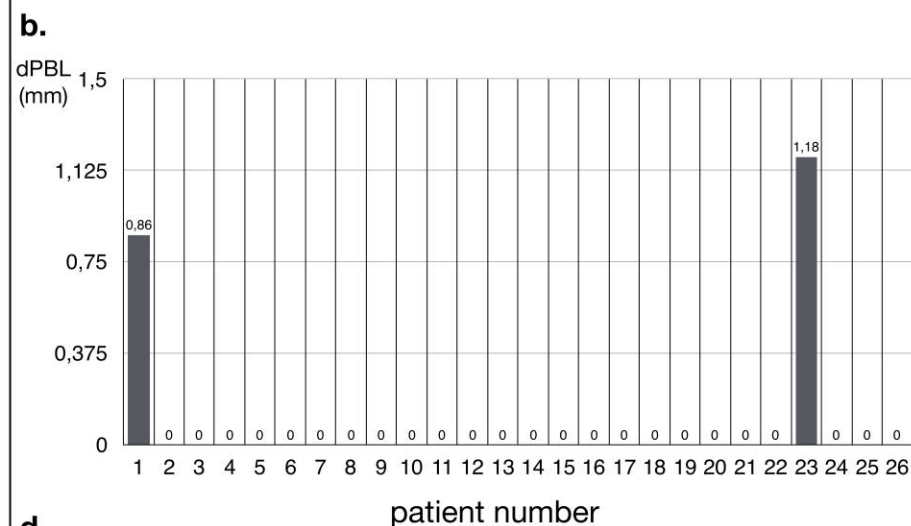
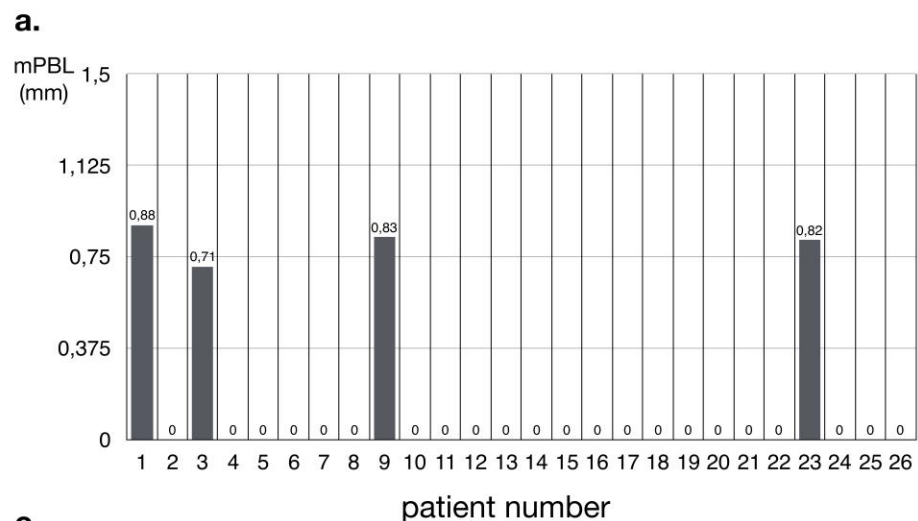
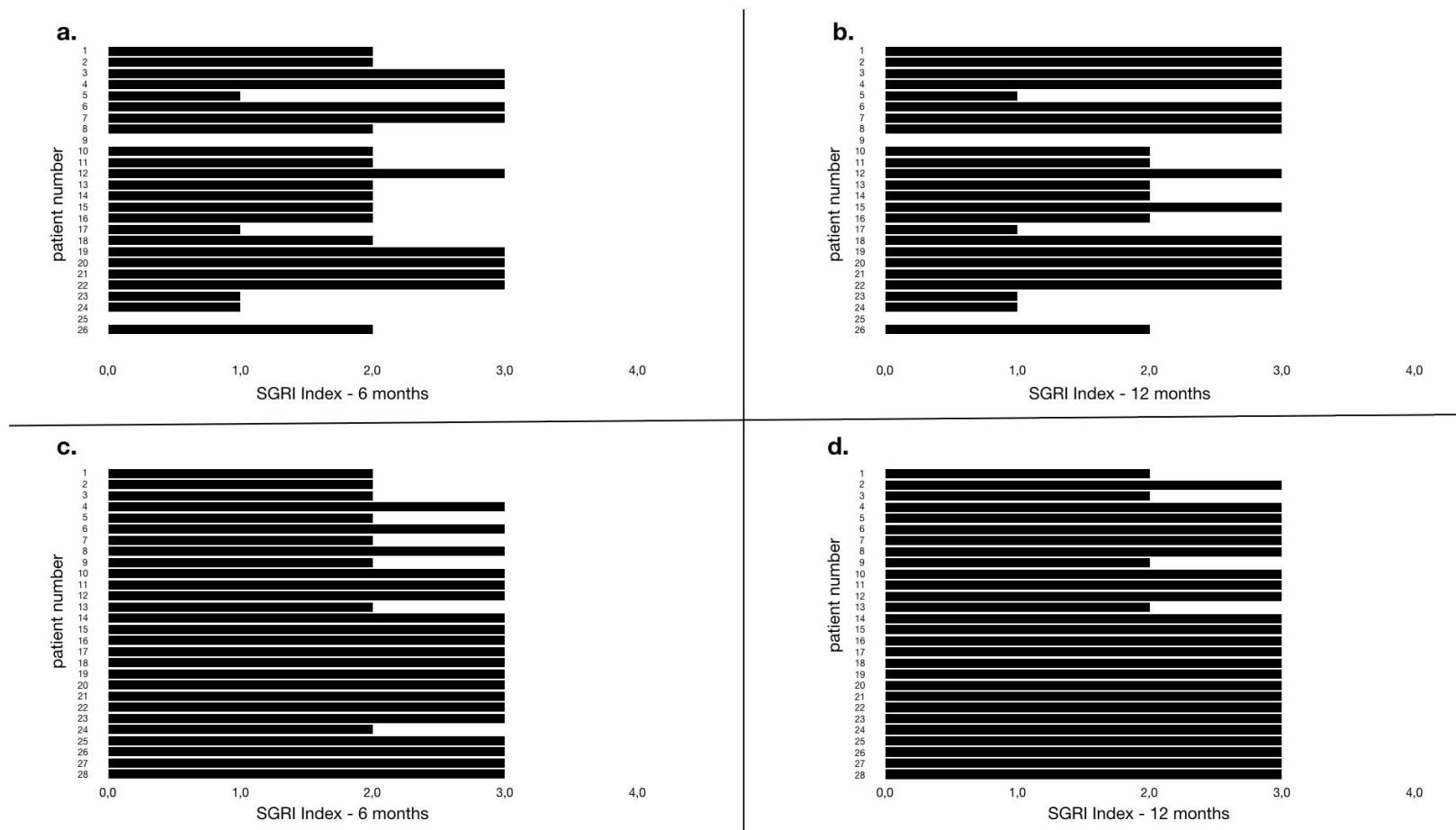


Figure 5. Sinus graft remodeling index (SGRI, Bragger et al. 2004) values as assessed on periapical radiograph in each patient of the tSFE group at **a)** 6 months and **b)** 12 months, and in each patient of the lSFE group at **c)** 6 months and **d)** 12 months.



SELECTIVE ADSORPTION OF IGG TO DEPROTEINIZED BOVINE BONE MINERAL ENHANCES IL-10 EXPRESSION IN HUMAN PRIMARY MACROPHAGES

Ludovica Parisi^{1,2,*}, Massimiliano G. Bianchi^{2,*}, Beatrice Mozzoni^{1,2,*}, Benedetta Ghezzi^{1,2}, Martina Chiu², Federico Rivara^{1,2}, Andrea Toffoli^{1,2}, Ovidio Bussolati², Guido M. Macaluso^{1,2}

¹ Centro Universitario di Odontoiatria, Università degli Studi di Parma, Parma, IT

² Dipartimento di Medicina e Chirurgia, Università degli Studi di Parma, Parma, IT

* Equally contribution of the Authors

Riassunto

L'osso bovino deproteinizzato (DBBM) è il sostituto osseo più comunemente utilizzato negli innesti ossei. Studi recenti hanno descritto la capacità del DBBM di influenzare il sistema immunitario dell'ospite inducendo i macrofagi a differenziare in senso antinfiammatorio (M2). Dopo aver confermato la capacità del DBBM di indurre il fenotipo macrofagico M2, l'obiettivo di questo studio è stato quello di identificarne un potenziale meccanismo regolatore. Abbiamo ipotizzato che la corona proteica che si forma attorno ai granuli di DBBM dopo il loro contatto con il sangue possa svolgere un ruolo importante nell'attivazione macrofagica. I risultati ottenuti con SDS-PAGE e Western Blot hanno evidenziato una selettività del DBBM per le immunoglobuline G (IgG). Pertanto, abbiamo analizzato la polarizzazione di macrofagi primari umani coltivati a contatto con il DBBM in presenza o in assenza di IgG. I risultati di espressione genica (RT-PCR) hanno rivelato un'attivazione macrofagica più marcata sul DBBM e indirizzata al fenotipo M2. Inoltre, l'induzione della citochina antinfiammatoria IL-10 è risultata significativamente più elevata di quella delle citochine pro-infiammatorie IL-8 ($p=0.00116$) e TNF α ($p=0.0091$). I risultati di questo studio indicano chiaramente che l'adsorbimento preferenziale di IgG al DBBM stimola i macrofagi a produrre IL-10 che, a sua volta, è plausibilmente implicata nella formazione di un microambiente favorevole all'osteogenesi.

Abstract

Deproteinized bovine bone mineral (DBBM) is the gold standard xenograft used in bone augmentation procedures. Recent findings have demonstrated that DBBM exerts an impact on host immune response by inducing macrophage polarization towards an alternative activation (M2). In this study, we confirmed the capacity of DBBM to induce the M2-phenotype and further identified a potential controlling mechanism. We hypothesized that the protein-corona formed around DBBM granules after their insertion plays an important role in the control of macrophage polarization. SDS-PAGE and Western Blot results identified a selectivity of DBBM for immunoglobulins-G (IgG). Therefore, we analyzed the polarization of primary human macrophages, derived from peripheral blood, on DBBM granules in the presence or in the absence of IgG. RT-PCR results demonstrated a higher activation of macrophages on DBBM and a tendency to shift their phenotype toward the M2 polarization. Furthermore, we detected a more marked induction of the anti-inflammatory interleukin IL-10 if compared to the pro-inflammatory IL-8 ($p=0.0116$) and TNF α ($p=0.0091$) expression. The results from this study indicate that the selective adsorption of IgG to DBBM preferentially stimulates the production of the anti-inflammatory IL-10 in human macrophages, which could be potentially involved in the creation of a microenvironment suitable for osteogenesis.

Introduction

Over the last decades, bone grafts have been widely used for bone augmentation procedures and the management of periodontal bone defects¹⁻³. Among them,

deproteinized bovine bone mineral (DBBM), which is basically hydroxyapatite obtained with the removal of any organic components from bone of bovine origin, is the gold standard xenograft. Even though DBBM lacks any intrinsic osteoinductive potential, large preclinical studies have confirmed its osteogenic and osteoconductive capacities, which prominently enhance the speed and the quality of new bone formation^{4, 5}. Interestingly, previous studies have also convincingly demonstrated the capacity of DBBM to induce the formation of large multinucleated giant cells (MNGCs) *in vivo*^{6, 7}. This evidence, together with the proof that cells from the monocytic lineage are among the first to come in contact with biomaterials^{8, 9}, suggests a potential important role of the host innate immunity in bone regeneration.

Macrophages are phagocytic cells involved in innate immunity that circulate in blood or reside in specialized tissues contributing in the maintenance of local homeostasis¹⁰. They are typically characterized by their plasticity in response to the exposure to different milieu signals, which leads to the switch of their metabolic and functional properties into a killing/inhibitory capacity (M1) or into a heal/promoting setting (M2)^{11, 12}. Therefore, it is conceivable that the role of these cells in bone tissue is highly influenced by the implantation of a foreign biomaterial, such as DBBM¹³. In this regard, *in vitro* studies on murine models have convincingly shown that osteoblasts differentiation on DBBM is not a direct consequence of the material contact¹⁴ but, rather, an effect of macrophage polarization towards an M2 phenotype¹⁵. However, the mechanism that controls macrophage phenotype upon interaction with DBBM has not been investigated yet.

During the surgical procedure DBBM is often used in combination with patient's own blood. It follows that plasma proteins are quickly adsorbed on material surface shortly after its insertion, and the formation of this so-called protein-corona is the first and decisive step to define cell-DBBM interaction¹⁶. Protein adsorption to biomaterials is a complex process, and when DBBM is exposed to blood plasma, certain molecules are preferentially deposited from the bulk. The most abundant protein species present in the bulk solution are adsorbed firstly. Subsequently, molecules endowed with greater affinity for the substrate may induce the detaching of the previously adsorbed and less affine ones^{17, 18}. Therefore, the characterization of blood plasma protein adsorption to DBBM is the first step to understand the mechanisms behind its clinical performance.

Immunoglobulins are among the most abundant proteins in blood (15-20mg/ml) and are capable to elicit a variety of cellular responses through their Fc portion. Immunoglobulins-G (IgG) represent the most abundant antibody class in blood (~12mg/ml) and are capable of binding various members of the Fc γ receptor family (Fc γ Rs), which are expressed on several immune cells^{19, 20}. Human macrophages express Fc γ RI and, interestingly, IgG4 binding to this receptor has been described to trigger the M2-like phenotype²¹.

Considering these premises, the aim of this work was to study the adsorption pattern of blood plasma protein to DBBM and, therefore, to determine potential mechanisms triggered by IgG in inducing the activation of macrophages towards M2-like phenotype.

Materials and Methods

This study has been conducted using BioOss® granules kindly provided by Geistlich Pharma AG (Wolhusen, CH) and primary macrophages isolated from whole human blood according to the approval by the local ethic committee (#3182/2018).

Protein adsorption studies

The adsorption pattern of blood plasma proteins to DBBM has been investigated by soaking DBBM granules (range size 0.25-1mm) in 2% human serum. The amount of protein adsorption has been monitored through Bradford assay, while the composition of

the protein-corona has been investigated through SDS-PAGE and Western Blot (WB) analysis.

Bradford assay – Seventy-mg of DBBM were weighed and soaked for 1h at room temperature (RT) on an orbital shaker with 500µl of PBS (Thermo Fisher, Waltham, MA – USA) supplemented with 2% of IgG-depleted human serum (IHPLA-SER-GF, Innovative Research, Novi, IT) in the presence or in the absence of a 2%-diluted physiological concentration (0.3mg/ml) of human IgG (I4506, Sigma-Aldrich, Saint-Louis, MI – USA). Ten-µl aliquots of supernatants were collected after 5, 15, 30, 45 and 60min and used for protein quantitation. Bradford assay (BIO-RAD Protein Assay, BIO-RAD, Hercules, CA – USA) was performed mixing serum aliquots with 200µl of Bradford Working Solution. Specimens were incubated at 37°C for 2min and their absorbance was assessed at 620nm with a Multiskan FC plate reader (Thermo Fisher).

SDS-PAGE – Seventy-mg of DBBM were weighed and soaked for 1h with 2% human serum in the presence or in the absence of IgG as described above. For total proteins recovering, samples were incubated with 100µl of Sample Buffer 1X (Tris-HCl 62.5mM pH 6.8, SDS 1.5%w/v, DTT 100mM and traces of Bromophenol Blue), cooled at -20°C overnight, sonicated for 10min and boiled at 95°C for 5min. Equal volumes of samples were thus loaded on a 12% polyacrylamide gel (Sigma-Aldrich) and separated at 110V for 1h and 30min. To reveal proteins, gel was exposed to the Silver Stain solution (Silver Stain solution kit, BIO-RAD) and images were acquired by Personal Densitometer SI (Molecular Dynamics, GE Healthcare, Little Chalfont, UK).

Western blot – After SDS-PAGE analysis, separated proteins were blotted on a PVDF membrane (Immobilon-P, Darmstadt, D) at 100V for 1h. Non-specific sites were blocked for 1h at RT in Tris-buffered saline (TBS, TrisHCl 50mM pH 7.5 and NaCl 150mM) containing 10% of blocking reagent (Roche S.p.A., Segrate, IT). Membrane was then incubated overnight with an anti-human HRP-conjugated IgG antibody (abcam, Cambridge, UK) diluted 1:10000 (Sigma-Aldrich). Immunoreactivity was visualized with enhanced chemiluminescence (Immobilon Western Chemiluminescent HRP, Sigma-Aldrich).

Samples preparation

To simplify the model and to better understand the effects of IgG on macrophage polarization, an albumin solution at serum concentration supplemented or not with human IgG was used for DBBM coating.

DBBM coating – Human albumin solution (Alburex®, CSL Behring, Bern, CH) was diluted at 2% in PBS (0.8mg/ml) and supplemented or not with IgG (Privigen®, CSL Behring) at a final 2%-diluted physiological concentration (0.3mg/ml). The 2 different solutions were then used to coat 70mg of DBBM granules or the bottom of 48-well tissue culture plates, which were used as controls, for 1h at RT on an orbital shaker. A WB analysis (see above) was then performed to confirm albumin and IgG adsorption on granules. Albumin detection was performed using an anti-albumin (Cell Signalling) primary antibody diluted 1:800 in 0.1% Tween20 in TBS supplemented with 5%BSA and revealed with an HRP-conjugated secondary antibody diluted 1:10000 (Cell Signalling).

In vitro assays

The polarization of human macrophages obtained after selection and differentiation of human monocytes isolated from whole blood plasma has been studied through RT-PCR.

Blood samples – Ten 5ml specimens of whole human plasma were collected. Eligible volunteers were identified from the members of the research team of the School of Dental Medicine of the University of Parma, Italy. The presence of hematological, immunological or diabetic diseases was an exclusion criterium. All the subjects gave written informed consent (#3182/2018), and full medical history was recorded. Blood samples were

collected in the morning and immediately transferred to the laboratory for monocyte isolation that was completed within 8h.

Macrophage isolation and culture – Ficoll-Paque Plus solution (Sigma-Aldrich) was used to separate peripheral blood mononuclear cells (PBMCs), followed by two rinses in PBS for better removal of platelets. After having determined the cell number, PBMCs were resuspended in RPMI-1640 (EuroClone, Pero, IT) supplemented with 5% of human serum (Innovative Research), L-Glutamine 2mM (Thermo Fisher) and 1% PenStrep (Thermo Fisher) and plated on a 6-well plate. Thirty minutes after seeding non-adhering cells were gently removed and the culturing media was further supplemented with M-CSF 50ng/ml (BioTechne, Minneapolis, MN – USA) for macrophage differentiation. After 7 days, macrophages were recovered and seeded on DBBM at a final concentration of 30000cells/sample in complete RPMI-1640 supplemented with 2% human albumin (CLS Behring), L-Glutamine 2mM and 1% PenStrep.

RT-PCR analysis – Total RNA from human macrophages was extracted 48h after seeding by TRIzol (Thermo Fisher) and further purified using the GeneJET RNA purification kit (Thermo Fisher). Five hundred-mg of RNA were used as a template for cDNA synthesis using a RevertAid RT Reverse Transcription kit (Thermo Fisher). The expression of cluster differentiation related genes CD68 (M0), CD86 (M1) and CD36 (M2), as well as the expression of the inflammatory-related interleukin-8 (IL-8) and tumor necrosis factor alpha (TNF α), and of the anti-inflammatory IL-10 was detected by RT-PCR. The specific primer sets are outlined in **Table 1**. RT-PCR was performed in a total volume of 20 μ l with the Power UP SYBR Green Master Mix (Thermo Fisher) and the target gene expressions were evaluated with a StepOne Plus Real-Time PCR System (Applied Biosystem, Foster City, CA – USA). Data analysis was made according to the relative standard curve method. Expression data were reported as the ratio between each investigated mRNA and RPL15 mRNA.

Gene	Forward (5'-end)	Reverse (3'-end)
CD68	GGAAATGCCACGGTTCATCCA	TGGGGTTCAGTACAGAGATGC
CD86	ACAAAAAGCCACAGGAATG	CAGGGAATGAAACAGACAAGC
CD36	CTGTCATTGGTGTCTCCTG	GCGTCCTGGGTACATTTTC
IL-8	ACTGAGAGTGATTGAGAGTGGAC	AACCCTCTGCACCCAGTTTTTC
IL-10	TCAAGGCGCATGTGAACTCC	GATGTCAAACCTCACTCATGGCT
TNFα	ATGAGCACTGAAAGCATGATCC	GAGGGCTGATTAGAGAGAGGTC

Table 1: Primer sequence used for RT-PCR

Statistical analysis

Data were analyzed using Prism8 (GraphPad, La Jolla, CA – USA) and are reported as the mean \pm SD of three repeated experiments performed in multiple replicates. Differences between groups were evaluated with either t-test or one-way ANOVA statistical test with Tukey multiple comparison post-hoc test and considered significant when $p < 0.05$.

Results

DBBM protein-corona formation

A Bradford assay was exploited to study the time-course of blood plasma protein adsorption to DBBM. Protein adsorption followed a hyperbolic trend ($R^2=0.9672$) showing a massive adsorption within 15min without any marked difference between IgG-depleted and IgG-supplemented sera (**Fig.1a**).

When the protein-corona composition was qualitatively analyzed by SDS-PAGE and WB, the patterning of DBBM adsorbed proteins was similar to that of complete human serum (**Fig.1b** lane3 vs. lane5). However, the intensity of revealed bands showed that some proteins were better adsorbed than others. Interestingly, the band around 70kDa, which is putatively that of serum albumin, was only moderately adsorbed on DBBM, while the one around 50kDa (putatively containing IgG heavy chains) and the one around 23.5kDa (putatively containing of IgG light chains) were more evident in the DBBM sample (lane5). Since electrophoresis data can only be considered semi-quantitative, to further characterize protein adsorption to DBBM, we performed an immunoblot. IgG heavy chains were massively present in the pool of DBBM-adsorbed proteins (**Fig.1c**). Noteworthy, DBBM showed a greater affinity for the IgG heavy chain, while no adsorption of other Ig isoforms, such as IgA or IgM was detectable as in the complete serum counterpart. Additionally, although roughly equal amounts of proteins were adsorbed to DBBM (**Fig.1a**), no evident pattern change, besides IgG-containing bands, was visible when IgG-depleted medium was used (**Fig.1b**).

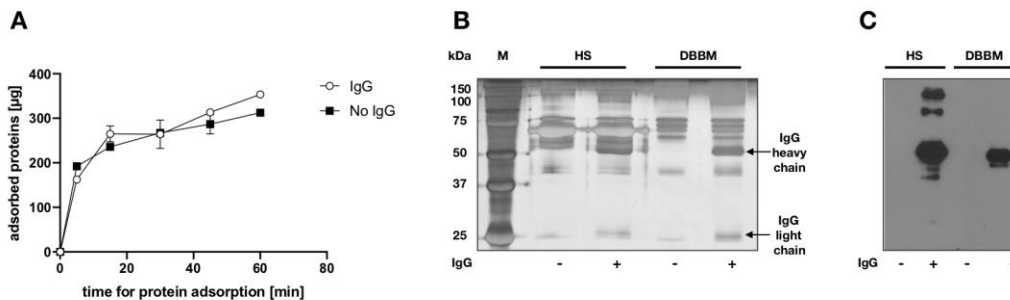


Figure 1: *Protein adsorption study*. (A) Time course of complete or IgG-depleted 2% human serum proteins to DBBM. (B) SDS-PAGE of complete or IgG-depleted 2% human serum proteins adsorbed for 1h to DBBM. (C) Western Blot analysis of IgG adsorbed to DBBM.

The affinity of DBBM for IgG was further confirmed when DBBM or controls were incubated with serum or albumin solution in the presence or in the absence of IgG. While DBBM evidently adsorbed IgG (**Fig.2b**), no IgG adsorption was detected for controls (bottom of culture wells). Moreover, controls showed a remarkable affinity for albumin, which, on the contrary, was less evidently adsorbed on DBBM (**Fig.2a**).

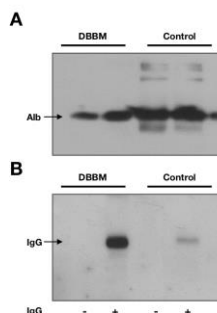


Figure 2: *Protein adsorption study*. (A) Western Blot analysis of albumin adsorbed to DBBM. (B) Western Blot analysis of IgG adsorbed to DBBM.

The effect of protein-corona on macrophage activation and differentiation

The study of macrophages activation was performed on DBBM and on controls previously exposed to a solution of albumin and IgG or of albumin at physiological concentrations. The expression of the CD68 was markedly enhanced when IgG were adsorbed on DBBM (**Fig.3a** – Control vs. DBBM + IgG $p=0.0016$; Control + IgG vs. DBBM + IgG $p=0.0014$; DBBM vs. DBBM + IgG $p=0.0029$). Furthermore, when the fold-change IgG vs. No IgG was considered, a higher expression of the macrophage marker dependent on the presence of IgG was evident for DBBM if compared to the control ($p=0.0130$). Noteworthy, the expression of the pro-inflammatory marker CD86 was greatly diminished on DBBM both in the presence or in the absence of IgG, showing statistically significant differences with the control pre-adsorbed with IgG (**Fig.3b** – Control + IgG vs. DBBM $p=0.0254$; Control + IgG vs. DBBM + IgG $p=0.0259$), while no significant differences were assessed on DBBM in the presence or in the absence of IgG ($p>0.9999$). Consistently, the analysis of the fold-change showed lack of induction on DBBM even though the difference with control was not significant ($p=0.0764$). On the contrary, the analysis of the fold-change for the expression of the scavenger receptor CD36 showed a positive effect of DBBM against the control even though without significant differences ($p=0.1445$). The levels of CD36 expression were indeed comparable among all the samples and statistically significant differences were detected only between DBBM and controls in the absence of IgG (**Fig.3c** – Control vs. DBBM $p=0.0434$).

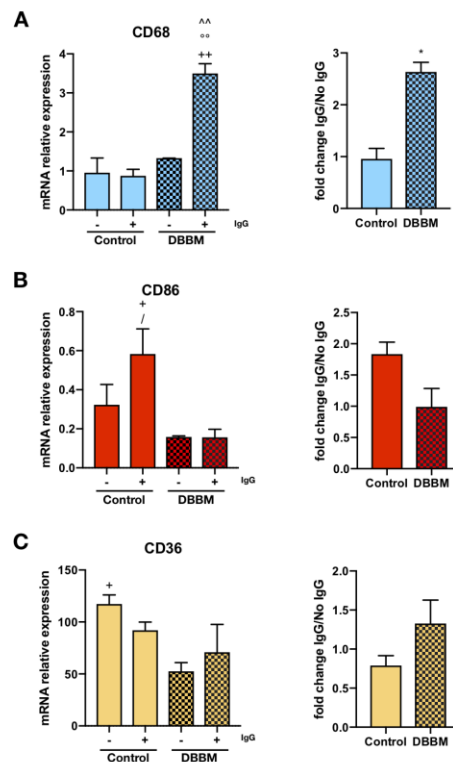


Figure 3: *CD expression analysis*. (A) Relative mRNA expression and IgG/No IgG fold change of CD68. (B) Relative mRNA expression and IgG/No IgG fold change of CD86. (C) Relative mRNA expression and IgG/No IgG fold change of CD36. [^] $p<0.05$ vs. Control + IgG; ^o $p<0.05$ vs. Control + IgG; ⁺ $p<0.05$ vs. DBBM; [/] $p<0.05$ vs. DBBM + IgG; ^{*} $p<0.05$ Control vs. DBBM.

The effect of protein-corona on cytokines expression

The influence of adsorbed proteins on macrophage polarization has been further investigated through the analysis of the expressed cytokines. Particularly, the transcription levels of IL-8, IL-10 and TNF α have been taken into consideration.

The expression of IL-8 was promoted on DBBM and further enhanced by the presence of IgG (**Fig.4a** – Control vs. DBBM $p=0.0041$; Control vs. DBBM + IgG $p=0.0006$; Control + IgG vs. DBBM $p=0.0289$; Control + IgG vs. DBBM + IgG $p=0.0017$; DBBM vs. DBBM + IgG $p=0.0177$). However, when the fold-change IgG vs. No IgG was considered, the production of IL-8 was more markedly enhanced by the antibodies on controls than on DBBM ($p=0.0046$), suggesting that the stimulatory effect of IL-8 production detected in macrophages exposed to DBBM is somewhat blunted by IgG. At variance with IL-8 expression, DBBM did not influence the expression of IL-10 (**Fig.4b** – Control vs. DBBM $p=0.2934$; Control + IgG vs. DBBM + IgG $p=0.1815$), which was instead markedly influenced by the presence of IgG (**Fig.4b** – Control vs. Control + IgG $p=0.0178$; Control + IgG vs. DBBM $p=0.0248$; DBBM vs. DBBM + IgG $p=0.0055$). The analysis of the fold-change indicated that IgG effect was significantly higher with DBBM than under control conditions ($p=0.0121$). Surprisingly, the expression of TNF α was comparable among all the groups and the fold-change did not reveal any significant difference (**Fig.4c** – $p=0.1335$).

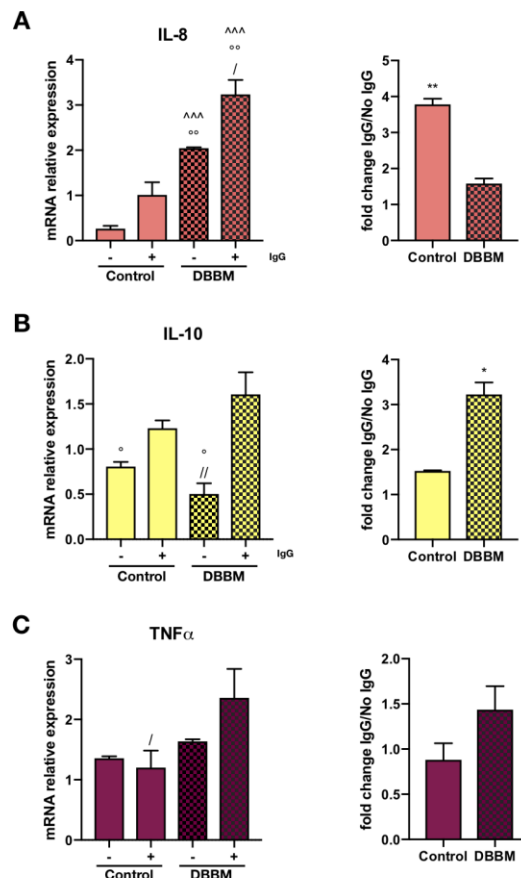


Figure 4: *Cytokine expression analysis.* (A) Relative mRNA expression and IgG/No IgG fold change of IL-8. (B) Relative mRNA expression and IgG/No IgG fold change of IL-10. (C) Relative mRNA expression and IgG/No IgG fold change of TNF α . $\wedge=p<0.05$ vs. Control + IgG; $\circ=p<0.05$ vs. Control + IgG; $+=p<0.05$ vs. DBBM; $/=p<0.05$ vs. DBBM + IgG; $*=p<0.05$ Control vs. DBBM.

The direct comparison of the fold-changes in cytokine expression induced by IgG in macrophages seeded on DBBM (**Fig.5**), highlighted a much higher induction of IL-10 compared to both IL-8 ($p=0.0116$) and $TNF\alpha$ ($p=0.0091$).

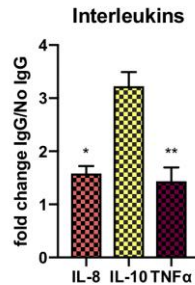


Figure 5: Cytokine expression analysis. Comparison of IgG/No IgG fold change of IL-8, IL-10 and $TNF\alpha$. $*=p<0.05$.

Discussion

Macrophages represent the driving force that coordinate the chronic inflammation at biomaterials interface after insertion²². Once activated, these cells interact with the foreign material showing most often features of a classically activated pro-inflammatory phenotype (M1). However, macrophages exhibit a functional plasticity that allows a more or less complete switch of their metabolism and functional properties towards an alternatively activated anti-inflammatory and pro-resolving phenotype (M2)¹². A debate on the mechanisms regulating macrophages commitment is still open and, together with the complexity of intermediate or mixed phenotypes, still renders difficult to understand the precise role played by macrophages during specific regenerative processes, such as the new-bone formation that occurs after augmentation procedures.

Recent findings have shown that DBBM, a typical bone xenograft commonly used in dentistry, promotes macrophage polarization toward an M2-pro-resolving phenotype, which further contributes to the creation of a microenvironment suitable for osteoblast maturation and new-bone deposition¹⁵. Nevertheless, the mechanisms that drive M2-polarization on DBBM remains to be characterized. In this study, we have analyzed the role of plasma protein adsorption at the interface of DBBM on macrophage activation and polarization.

When serum proteins were adsorbed on DBBM, a massive contribution of IgG in forming the protein-corona was evident (**Fig.1b-c**). Since, as a consequence of the Vroman effect¹⁸, albumin is the first molecule to be adsorbed on surfaces, we can presume that DBBM possesses a remarkable affinity for IgG. Therefore, we investigated if IgG could influence the response of macrophages when cultured on DBBM. The analysis of the CDs (cluster of differentiation) revealed that the expression of CD68, a general marker for macrophages activation, was promoted on DBBM when IgG were adsorbed (**Fig.3a**). Furthermore, the expression of CD86, which is expressed at low levels in monocytes and up-regulated on macrophages surface under inflammatory conditions²³, was stimulated by IgG adsorbed to culture plastic but not to DBBM (**Fig.3b**). Even though no significant differences were detected, the expression of the CD36, a scavenger receptor that is an important player in collagen-guided platelet adhesion²⁴, exhibited a positive trend in macrophages seeded on DBBM as an effect of IgG adsorption (**Fig.3c**). According to Shi et al., our findings confirm that DBBM elicited effects on the behavior of macrophages by shifting their phenotype toward the M2 extreme and suggest that IgG adsorption can influence this effect¹⁵.

Additional information has been obtained from the analysis of cytokine expression, which clearly identified a potential anti-inflammatory role of IgG when adsorbed on DBBM. Consistently with the literature, the expression of the gene for IL-8, which is a potent pro-inflammatory mediator, was promoted on DBBM and further enhanced by the presence of IgG both on DBBM and on controls²⁵. However, the effect of IgG was much smaller on macrophages seeded on DBBM and, interestingly, DBBM-dependent induction was laved in the presence of IgG, compared with samples treated with albumin alone, suggesting that IL-8 increase should be attributed to DBBM. Conversely, a 2-folds induction of IL-10 gene (**Fig.4a**), which is mainly expressed and secreted by immunocompetent cells to limit and control the inflammatory response, was observed when IgG were adsorbed on DBBM (**Fig.4b**). IL-10 is a potent anti-inflammatory cytokine that inhibits macrophage activation by suppressing the production of inflammatory cytokines²⁶. Consistently with this, the presence of adsorbed IgG seems to recover the expression levels of TNF α (**Fig.4c**), but this data should be confirmed with further analysis.

It should be stressed that our data have been obtained with primary human macrophages. To the best of our knowledge, previous efforts that aimed to study macrophage polarization on biomaterials *in vitro* were mostly conducted using murine cells or cell lines of human or murine origin. Since murine and human macrophage models are known to possess high discrepancies in their M1/M2 profiles, such as different capability of inducing NO synthase (NOS) activity, as well as of expressing in cytokines or chemokines receptors^{27, 28}, the use of primary macrophages isolated from whole blood plasma confers reliability to our results.

In conclusion, these data are consistent with the hypothesis that, while contact with DBBM promotes the acquisition of functional competence by blood-derived macrophages, preferential IgG adsorption to DBBM, due to a marked affinity of these proteins for the material, may promote anti-inflammatory and pro-repair responses of human macrophages through IL-10 expression. If expression data will be confirmed with determinations of secreted cytokines, we can furthermore speculate that macrophage-derived IL-10 could be involved in bone regeneration on two different levels. First, IL-10 is known to activate osteoblasts by stimulating the secretion of osteoprotegerin (OPG) and inhibiting that of the receptor activator of nuclear factor kappa-B ligand (RANKL), needed for osteoclast differentiation²⁹. On the other hand, IL-10 is an inhibitor of the TNF α production²⁶. High levels of TNF α enhance the secretion of the IL-6, a potent effector of the osteoclastogenesis, and further induces osteoclastogenesis by direct stimulation of macrophages when exposed to RANKL^{30, 31}. IL-10 could be involved in inhibiting this pathway. Further studies investigating the effects of macrophages conditioned medium on osteoblasts and osteoclasts activity are needed to validate these mechanisms.

Acknowledgements

This study has been supported by a 2017 research grant from the American Academy of Implant Dentistry Foundation. The authors would like to thank Geistlich Pharma AG (Wolhusen, CH) for kindly providing BioOss®, Dr. Birgit Schäfer (Geistlich Pharma AG) for her precious advice and Dr. Federica Bragantini (Geistlich Biomaterials Italia, Thiene, IT) for her technical support. The authors declare no conflicts of interests in relation to this work.

References

1. Donos, N.; Lang, N. P.; Karoussis, I. K.; Bosshardt, D.; Tonetti, M.; Kostopoulos, L., Effect of GBR in combination with deproteinized bovine bone mineral and/or enamel matrix proteins on the healing of critical-size defects. *Clinical Oral Implants Research* **2004**, *15* (1), 101-111.
2. Sartori, S.; Silvestri, M.; Forni, F.; Cornaglia, A. I.; Tesesi, P.; Cattaneo, V., Ten-year follow-up in a maxillary sinus augmentation using anorganic bovine bone (Bio-Oss). A case report with histomorphometric evaluation. *Clinical Oral Implants Research* **2003**, *14* (3), 369-372.
3. Hammerle, C. H. F.; Jung, R. E.; Yaman, D.; Lang, N. P., Ridge augmentation by applying bioresorbable membranes and deproteinized bovine bone mineral: a report of twelve consecutive cases. *Clinical Oral Implants Research* **2008**, *19* (1), 19-25.
4. De Santis, E.; Lang, N. P.; Ferreira, S.; Garcia, I. R.; Caneva, M.; Botticelli, D., Healing at implants installed concurrently to maxillary sinus floor elevation with Bio-Oss((R)) or autologous bone grafts. A histomorphometric study in rabbits. *Clinical Oral Implants Research* **2017**, *28* (5), 503-511.
5. Schwartz, Z.; Weesner, T.; van Dijk, S.; Cochran, D. L.; Mellonig, J. T.; Lohmann, C. H.; Carnes, D. L.; Goldstein, M.; Dean, D. D.; Boyan, B. D., Ability of deproteinized cancellous bovine bone to induce new bone formation. *Journal of Periodontology* **2000**, *71* (8), 1258-1269.
6. Chackartchi, T.; Iezzi, G.; Goldstein, M.; Klinger, A.; Soskolne, A.; Piattelli, A.; Shapira, L., Sinus floor augmentation using large (1-2 mm) or small (0.25-1 mm) bovine bone mineral particles: a prospective, intra-individual controlled clinical, micro-computerized tomography and histomorphometric study. *Clinical Oral Implants Research* **2011**, *22* (5), 473-480.
7. Jensen, S. S.; Gruber, R.; Buser, D.; Bosshardt, D. D., Osteoclast-like cells on deproteinized bovine bone mineral and biphasic calcium phosphate: light and transmission electron microscopical observations. *Clinical Oral Implants Research* **2015**, *26* (8), 859-864.
8. Chehroudi, B.; Ghrebi, S.; Murakami, H.; Waterfield, J. D.; Owen, G.; Brunette, D. M., Bone formation on rough, but not polished, subcutaneously implanted Ti surfaces is preceded by macrophage accumulation. *Journal of Biomedical Materials Research Part A* **2010**, *93A* (2), 724-737.
9. Pajarinen, J.; Kouri, V. P.; Jamsen, E.; Li, T. F.; Mandelin, J.; Konttinen, Y. T., The response of macrophages to titanium particles is determined by macrophage polarization. *Acta Biomaterialia* **2013**, *9* (11), 9229-9240.
10. Wong, K. L.; Yeap, W. H.; Tai, J. J. Y.; Ong, S. M.; Dang, T. M.; Wong, S. C., The three human monocyte subsets: implications for health and disease. *Immunologic research* **2012**, *53* (1-3), 41-57.
11. Mills, C. D., M1 and M2 Macrophages: Oracles of Health and Disease. *Critical reviews in immunology* **2012**, *32* (6), 463-88.
12. Italiani, P.; Boraschi, D., From Monocytes to M1/M2 Macrophages: Phenotypical vs. Functional Differentiation. *Frontiers in immunology* **2014**, *5*, 514.
13. Miron, R. J.; Bosshardt, D. D., OsteoMacs: Key players around bone biomaterials. *Biomaterials* **2016**, *82*, 1-19.
14. Miron, R. J.; Sculean, A.; Shuang, Y.; Bosshardt, D. D.; Gruber, R.; Buser, D.; Chandad, F.; Zhang, Y. F., Osteoinductive potential of a novel biphasic calcium phosphate bone graft in comparison with autographs, xenografts, and DFDBA. *Clinical Oral Implants Research* **2016**, *27* (6), 668-675.
15. Shi, M. S.; Wang, C.; Wang, Y. L.; Tang, C. Z.; Miron, R. J.; Zhang, Y. F., Deproteinized bovine bone matrix induces osteoblast differentiation via macrophage polarization. *Journal of Biomedical Materials Research Part A* **2018**, *106* (5), 1236-1246.
16. Vogler, E. A., Protein adsorption in three dimensions. *Biomaterials* **2012**, *33* (5), 1201-37.
17. Andrade, J.; Hlady, V., Protein adsorption and materials biocompatibility - a tutorial review and suggested hypotheses. *Advances in Polymer Science* **1986**, *79*, 1-63.
18. Hirsh, S. L.; McKenzie, D. R.; Nosworthy, N. J.; Denman, J. A.; Sezerman, O. U.; Bilek, M. M. M., The Vroman effect: Competitive protein exchange with dynamic multilayer protein aggregates. *Colloids and Surfaces B-Biointerfaces* **2013**, *103*, 395-404.
19. Takai, T., Fc receptors and their role in immune regulation and autoimmunity. *Journal of Clinical Immunology* **2005**, *25* (1), 1-18.
20. Nimmerjahn, F.; Ravetch, J. V., Fc gamma receptors as regulators of immune responses. *Nature Reviews Immunology* **2008**, *8* (1), 34-47.
21. Swisher, J. F. A.; Haddad, D. A.; McGrath, A. G.; Boekhoudt, G. H.; Feldman, G. M., IgG4 can induce an M2-like phenotype in human monocyte-derived macrophages through Fc gamma RI. *Mabs* **2014**, *6* (6), 1377-1384.
22. Davies, L. C.; Rosas, M.; Jenkins, S. J.; Liao, C. T.; Scurr, M. J.; Brombacher, F.; Fraser, D. J.; Allen, J. E.; Jones, S. A.; Taylor, P. R., Distinct bone marrow-derived and tissue-resident macrophage lineages proliferate at key stages during inflammation. *Nat Commun* **2013**, *4*, 1886.
23. Manzoor, A., Introduction to costimulation and costimulatory molecules. In *Developing costimulatory molecules for immunotherapy of disease*, Direct, S., Ed. 2015.

24. Tandon, N. N.; Kralisz, U.; Jamieson, G. A., Identification of glycoprotein IV (CD36) as a primary receptor for platelet-collagen adhesion. *J Biol Chem* **1989**, *264* (13), 7576-83.
25. Lange, T.; Schilling, A. F.; Peters, F.; Haag, F.; Morlock, M. M.; Rueger, J. M.; Amling, M., Proinflammatory and osteoclastogenic effects of beta-tricalciumphosphate and hydroxyapatite particles on human mononuclear cells in vitro. *Biomaterials* **2009**, *30* (29), 5312-8.
26. Hart, P. H.; Ahern, M. J.; Smith, M. D.; Finlay-Jones, J. J., Comparison of the suppressive effects of interleukin-10 and interleukin-4 on synovial fluid macrophages and blood monocytes from patients with inflammatory arthritis. *Immunology* **1995**, *84* (4), 536-42.
27. Mestas, J.; Hughes, C., Of mice and not men: differences between mouse and human immunology. **2004**, *172*, 2731-2738.
28. Schneemann, M.; Schoedon, G., Species differences in macrophage NO production are important. **2002**, *3*, 102.
29. Liu, D.; Yao, S.; Wise, G. E., Effect of interleukin-10 on gene expression of osteoclastogenic regulatory molecules in the rat dental follicle. *Eur J Oral Sci* **2006**, *114* (1), 42-9.
30. Kaneshiro, S.; Ebina, K.; Shi, K.; Higuchi, C.; Hirao, M.; Okamoto, M.; Koizumi, K.; Morimoto, T.; Yoshikawa, H.; Hashimoto, J., IL-6 negatively regulates osteoblast differentiation through the SHP2/MEK2 and SHP2/Akt2 pathways in vitro. *J Bone Miner Metab* **2014**, *32* (4), 378-92.
31. Lam, J.; Takeshit, S.; Barker, J.; Kanagawa, O.; Ross, F.; Teitelbaum, S., TNF-alpha induces osteoclastogenesis by direct stimulation of macrophages exposed to permissive levels of RANK ligand. *J Clin Invest* **2000**, *106* (12), 1481-1488.

Corresponding Author:

Dr. Ludovica Parisi

E-mail: ludovica.paris@gmail.com